Chapter One

Basic Concepts

1.1Introduction:

Laser has become a catch word for precision, quality, and speed. Desktop laser printers convert a colourful electronic image into a high quality permanent picture. The digital versatile disc (DVD) brings the experience of the cinema-high definition pictures and multi-channel sound-into the home. A laser scanner at the supermarket checkout translates a barcode into an item that appears on your receipt and disappears from the store's inventory .Lasers can be used to whiten your teeth, remove unwanted hair, and make your spectacles obsolete; the list grows every day(John C. Ion, 2005).

LASER is the acronym of Light Amplification by Stimulated Emission of Radiation. Although regarded as one of the nontraditional processes, laser material processing (LMP) is not in its infancy anymore.

Laser energy is flexible, accurate, easy to control, and has a very wide range of freedom in spatial, temporal, magnitude and frequency control. This unique energy source has found extraordinarily wide applications in material processing.

Many kinds of lasers have been developed in the past 50 years and an amazingly wide range of applications-such as laser surface treatment, laser machining, data storage and communication, measurement and sensing, laser assisted chemical reaction, laser nuclear fusion, isotope separation, and military weapons-have been found for lasers.

In fact, lasers have opened and continue to open doors to exciting worlds for both scientific research and engineering.

The successful application of laser material processing relies on proper choice of the laser system as well as on a good understanding of the physics behind the process (Wenwu Zhang, 2004).

Material processing refers to a variety of industrial operations in which the laser operates on a workpiece to modify it, for example, by melting it or removing material from it. Some of the possible applications include welding, hole drilling, cutting, trimming of electronic components, heat treating, and alloying.

Properties of laser light that enable material processing applications are its monochromaticity, collimation, radiance, and focusability. Because of these properties, laser light can be concentrated by a lens to achieve extremely high irradiance at the surface of a workpiece (John F. Ready, 1997).

The outstanding properties of ultrashort-pulsed laser have led to a huge amount of potential applications as a precise and flexible tool for materials processing. On the other hand, complex process parameter correlation paired with high investment costs require efficient process chains to ensure an economical use in production. Pulsar photonics presents a tool system that stands out by its integrated inspection routines and workflow management. Embedded sensors and networked actuators offer the industry 4.0 capability of machine data acquisition together with the benefits of and improved reliability. For competitive series applications Pulsar Photonics focuses on an increased efficiency by multiple beam processing. Hereby the laser beam is divided into up to 100 parallelized beams, thus enabling the efficient production of periodic

structure, large-scaled ablation or the parallel processing of multiple components (Jens Holtkamp, 2014).During the last years, the average power of ultrashort-pulsed laser sources increased significantly. Today, robust picosecond lasers with average powers of 50-150 W at medium to high pulse energies are available for industrial use (Jens Holtkamp, 2014).

1.2 The study objectives:

The main objective of this study is to micro-machine Polymethylemethacrylate, PMMA, sheets by laser to increase the thermal insulation of these sheets. X-Y electro-pneumatic platform was designed and implemented for this purpose.The idea is to engrave micro-channels alongside the sheets to resemble microcavities, into which when some solar light enters will undergo multiple reflections losing some of its power at each reflection. Some of the solar light will also undergo absorption and re-emission, thus increasing the emissivity of the sheets. By increasing the amount of reflected light, and by increasing the emissivity of the sheets the transmitted light will be diminished to the minimum, thus the thermal energy passing through the sheets will be reduced, and the thermal insulation of the sheets will be increased. The sheets could then be used as solar thermal insulators in buildings, to reduce the thermal loads and electricity consumption, specially in a hot weather countries like Sudan.

1.3 Thesis structure:

The thesis is consisting of four chapters. Chapter one goes through the basic principles of lasers, their types, application of lasers in material processing and basics of laser micromachining.

Chapter two is an overview of laser micromachining processes. The chapter covers the areas of mechanical micromachining, tool, techinques showing surface, bulk, and high aspect ratio micromachining. The chapter also covers the area of laser micromachining**,** light and colour and finally covered the area of solar reflectance index.

Chapter three demonstrated the experimental part, showing the design of the x-axis, pneumatic, direction of the table, and the y-axis, electrical, direction of the table. It showed also the final experimental setup and the experimental procedures.

Chapter four presented the experimental results tabulated and in a graphical format, showing the reduction in temperature of the micro-machined PMMA samples in comparison to those with standard surface. Parameters of sample colours, power variation, and number of laser passes were also presented. The results were discussed and conclusions were introduced.

1.4The laser-an innovative machine tool:

Traditional machine tools are normally designed for a particular purpose; modern lathes can be programmed to machine with high precision; carburizing furnaces automatically harden to predetermined requirements; and automated cutting and welding gantries part and join materials quickly and accurately. They all perform to the most exacting standards. But they only perform a particular task. The industrial laser is different .It is a flexible machine tool. It produces a beam of light with unique properties. Its light can be controlled accurately: it can be focused to a small spot, providing an intense source of energy that is ideal for penetrating materials; or spread into a diffuse heating pattern to treat

surfaces. As well as processing materials by thermal modes, the interaction between the photons of the laser beam and atoms in materials enables processes to be performed athermally (without heat): bonds can be made and broken. The beam can be manipulated with optical components to perform a variety of operations simultaneously, or switched between locations for sequential processing (John C. Ion, 2005).

The laser thus provides opportunities for innovation in material processing. Innovation: novel application of an existing idea; application of a novel process; or-in the most successful case-novel application of a novel process. In some applications, the laser can simply be used in place of an existing machine tool. For example, when the beam is used to cut sheets of materials, the cost of a laser can be recouped in months because productivity can be increased and product quality can be improved. Equally, the laser can be the tool around which a new manufacturing process is developed-laser-based rapid manufacturing enables products to be made in novel ways with their design governed by the function of the product rather than the limitations imposed by traditional fabrication techniques. Both approaches have been implemented successfully to meet the constant demand for increasing competitiveness in manufacturing industry (John C. Ion, 2005).

1.5Understanding of laser energy:

1.5.1Basic principles of lasers:

Lasers are photon energy sources with unique properties, these are: high degrees of monochromaticity, coherence, directionality and high intensity. As illustrated in figure 1.1a basic laser system includes the laser medium, the resonator optics, the pumping system, and sometimes the cooling system. The energy levels of the lasing medium, decides the basic

wavelength of the output beam, while nonlinear optics may be used to change the wavelength (Wenwu Zhang, 2004).

The output beam may pass through further optics to be adapted to specific applications such as polarizing, beam expansion, and focusing, and beam scanning.

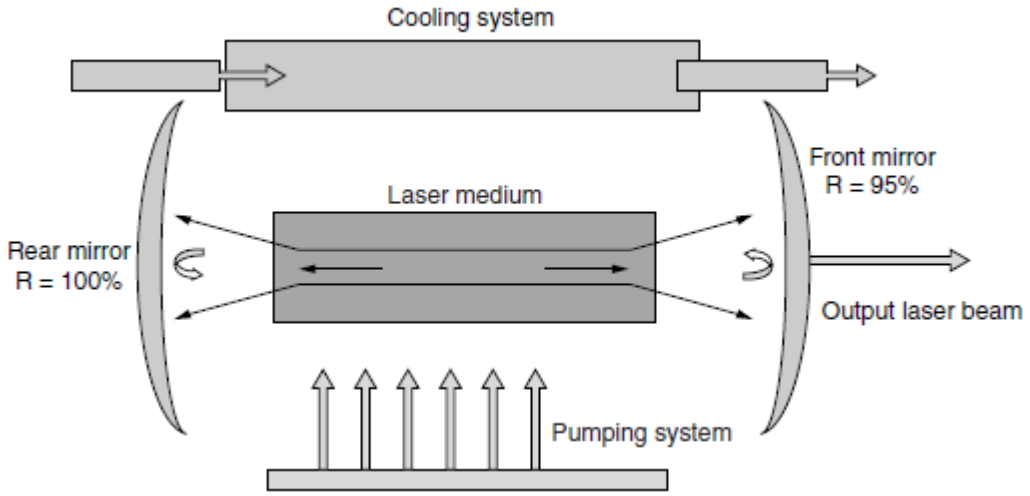

Figure1.1: Basic Structure of a Laser System

Understanding the physics of laser material interaction is important for understanding the capabilities and limitations for these processes (Wenwu Zhang, 2004).The basic structure for any laser system is shown in figure 1.1.

1.5.2 Types of lasers:

Depending of the nature of the active media, lasers are classified into three main categories, namely, solid, liquid, and gas. Scientists and researchers have investigated a wide variety of laser materials as active media in each category since 1958, when lasing action was observed in

ruby crystal. Here we will introduce one type of laser from each group as an example (Subbah Chandra Singh, 2012).

1.5.2.1 Nd:YAG laser : Is one of the solid state lasers that have active media obtained by embedding transition metals, rare earth ions, and actinides into insulating host lattice. Active media in solid state lasers are cylindrical and rod shaped with few millimeters diameter and few centimeters length. Several arrangements of cylindrical flash lamp and rod-shaped active media are used for optical pumping to get laser radiation. Various geometries for the arrangement of laser rod and flash lamps are illustrated in figure 1.2 (Subbah Chandra Singh, 2012).
Nd:YAG laser is widely used in the processing of materials and various characterizations. The properties of Nd:YAG are the most widely studied and best understood of all solid state laser media. The schematic diagram of Nd:YAG laser head is shown in figure 1.3.The head may have single or multiple chambers.

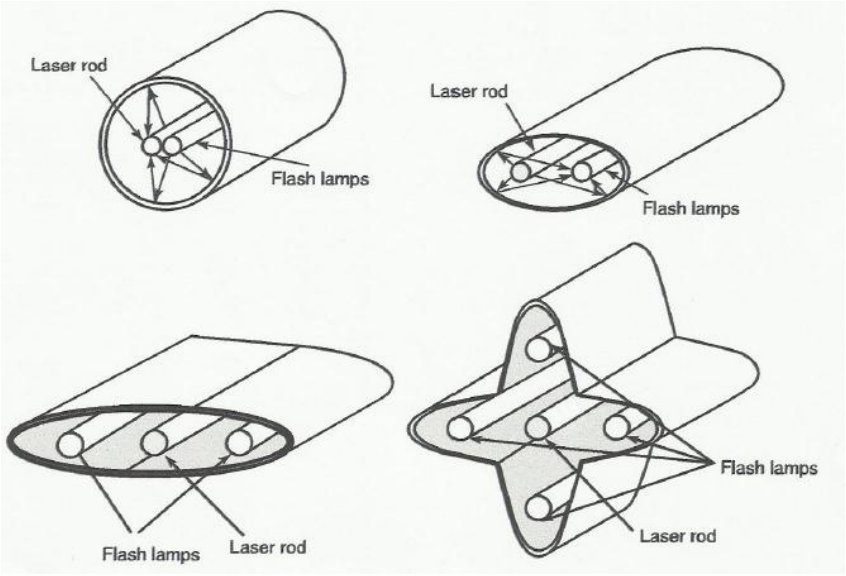

Figure 1.2: Different Geometries for the arrangement of flash lamp and laser rod in solid states lasers

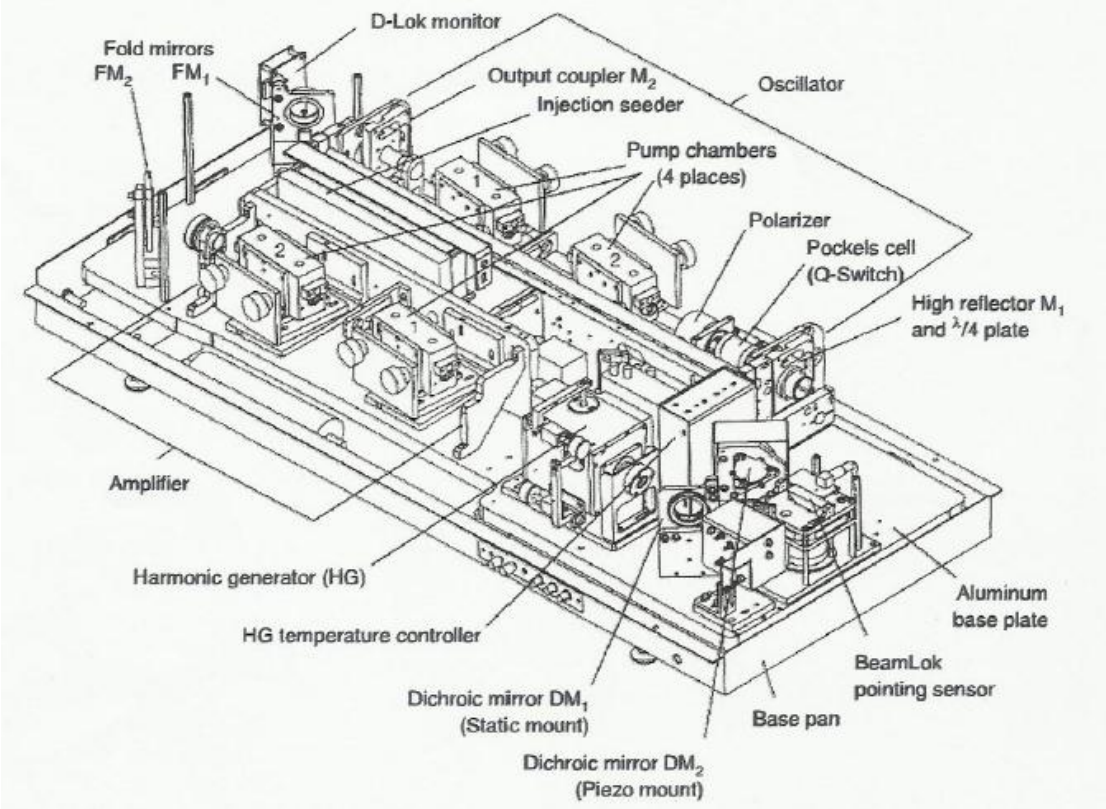

Figure 1.3: Assembly of various components in the head of an Nd:YAG laser system with four pump chambers

The harmonic generators, HGs, potassium di-hydrogen phosphate (KDP) and beta barium borate (BBO) crystals for frequency doubling and tripling, respectively.

It can be operated in long pulse and Q-switch modes. Long pulse mode has light pulses of almost 200μs duration and separation from each other by 2-4μs. The total energy of the pulse train is similar to that of a single Q-switched pulse. During Q-switched operation, the pulse width is less than 10ns and the peak optical power is tens of megawatts (Subbah Chandra Singh, 2012).

1.5.2.2 Carbon dioxide (CO_2) laser: Carbon dioxide is the most efficient molecular gas laser material that exhibits for a high power and high efficiency gas laser at infrared wavelength. It offers maximum

industrial applications including cutting, drilling, welding, and so on. It is widely used in the laser pyrolysis method of nanomaterial processing. Carbon dioxide is a symmetric molecule (O=C=O) having three (i) symmetric stretching [i00],(ii) bending [0j0], and (iii) antisymmetric stretching[00k] modes of vibrations (inset of Figure 1.4) , where I, j, and k are integers(Subbah Chandra Singh, 2012).

CO_2 lasers emit light with a wavelength of 10.6μm and have electrical efficiencies of approximately 10-15%.The laser gas mixture used in CO_2 lasers consists mainly of helium to ensure the dissipation of heat. It also contains carbon dioxide, the laser active medium, and nitrogen in which a gas discharge creates the energy necessary for excitation (C. Emmelman, 2000).

For the CO_2 lasers currently employed for material processing, the heat dissipation (approx.85-90% of the input electrical energy) is usually

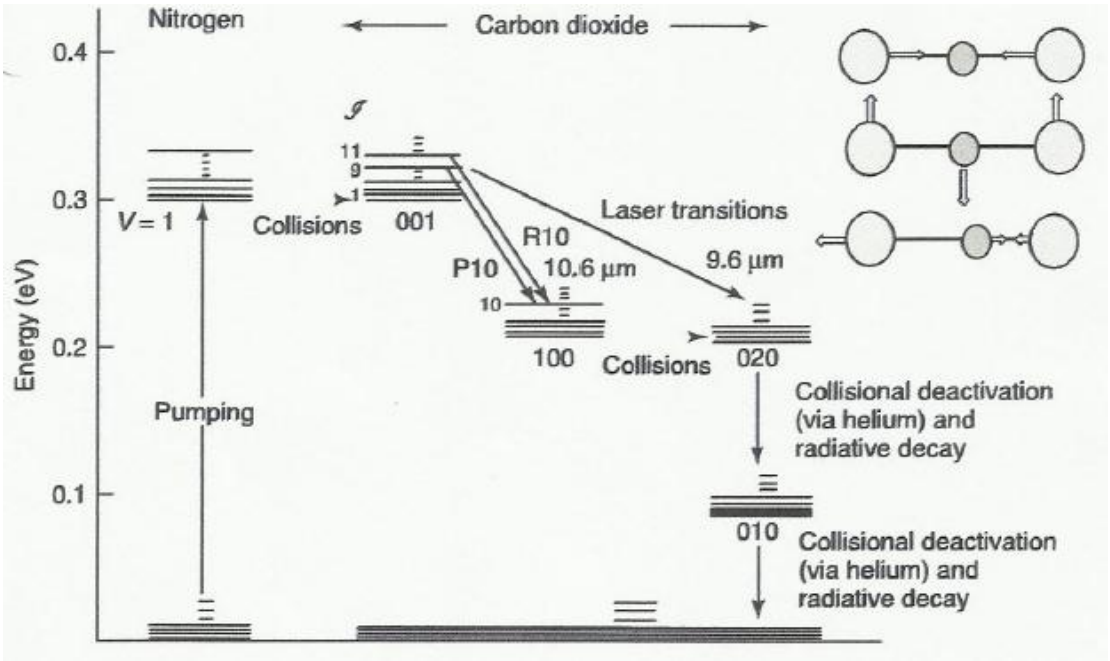

Figure 1.4: Modes of vibrations of CO_2 laser

achieved by using heat exchangers through which the gas is pumped via turbines, roots blowers or cross-flow fans. These lasers can be divided

into axial flow and cross flow types as shown in figures 1.5 and 1.6 respectively.

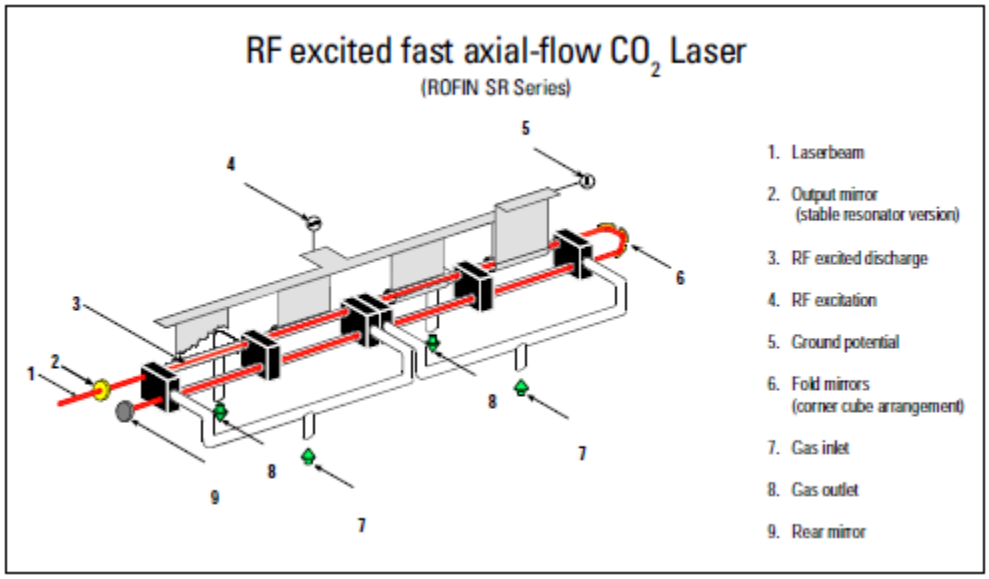

Figure 1.5: RF excited fast axial-flow CO_2 laser

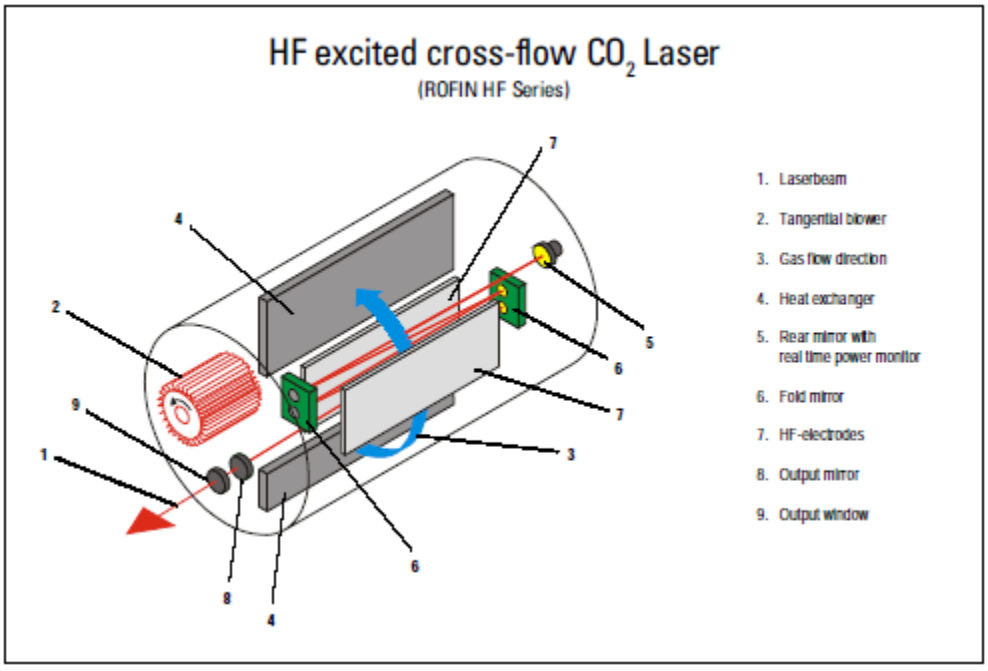

Figure 1.6:HF excited cross-flow CO_2 laser

For axial flow and cross-flow lasers, a continuous supply of fresh laser gas has to be connected to the gas circuit during operation to maintain the

efficiency necessary for optimum operation. Non-flow lasers, in which the laser gas mix in the discharge cavity is cooled only by heat conduction methods, have so far only been implemented with relatively low power beams. Diffusion cooled, high power CO_2 laser, which has meanwhile been developed to industrial maturity, the so-called CO_2 Slab laser, see figure 1.7, offers a number of advantages and already replaces flowing gas lasers in many application fields. The same design is used for low-power CO_2 Slab lasers, with the only difference of a sealed gas charge tube (C. Emmelman, 2000).

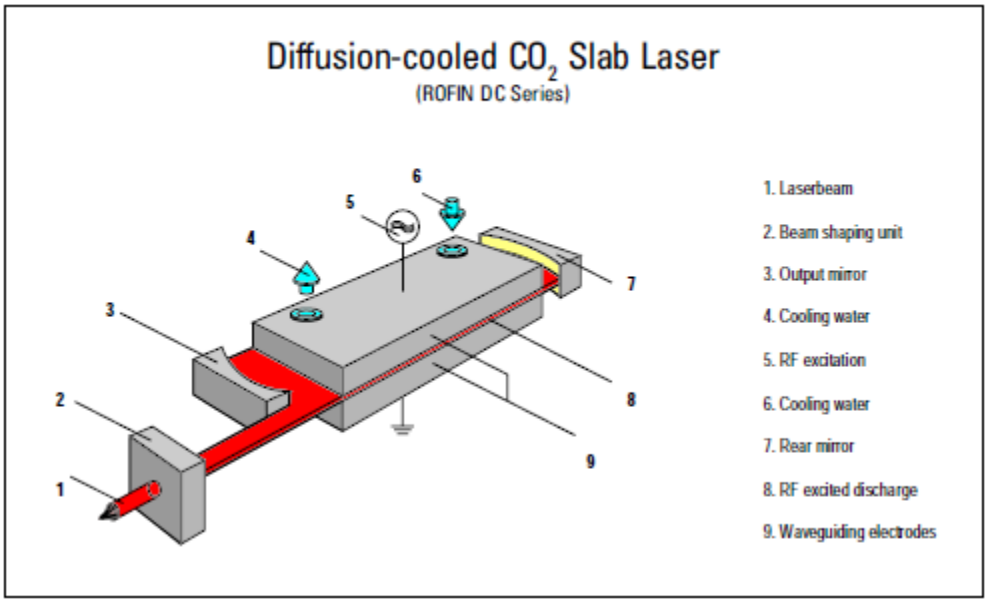

Figure 1.7: Basic principles of the CO_2 Slab laser

1.5.2.3 Semiconductor lasers: Practical semiconductor lasers are excited when current carriers in semiconductor recombine at the junction of regions doped with *n*- and *p*- type donor materials**.** This occurs when current is flowing through a forward-biased diode made from certain semiconductor materials. At low current densities, recombination at the diode junction generates excited states which spontaneously emit light, and the device operates as incoherent light-emitting diode (LED). If the

current density is high, and if the semiconductor device includes reflective facets to provide optical feedback, the diode can operate as a laser (McGraw-Hill, 2004).

1.5.2.4 Liquid lasers: The active medium in dye lasers is a fluorescent organic dye, dissolved in a liquid solvent. As in solid-state lasers, the only reasonable excitation technique is optical pumping with a flash lamp or (more often) with an external laser. The low efficiency of laser pumping is tolerable because it offers better quality output. The main attraction of the dye laser, is its tunable output wavelength and ability to produce ultrashort pulses or ultranarrow linewidth, are so important for many applications that its low overall efficiency is entirely acceptable. Laser action has been demonstrated from dyes in the vapor phase, of embedded in a solid host, but such lasers have not proved practical (McGraw-Hill, 2004).

1.5.3 Laser interaction with matter:

When electromagnetic radiation strikes a surface the wave travels as shown in figure1.8.Some radiation is reflected, some absorbed and some is transmitted (William M.Steen,2003).
The absorbed energy may heat up or dissociate the target materials (Wenwu Zhang, 2004).

From the microscopic point of view the laser energy is absorbed by free electrons first, the absorbed energy propagates through the electron system, and then is transferred to the lattice ions. In this way laser energy is transferred to the ambient target material, as shown in figure1.9. At high enough laser intensities the surface temperature of the target material quickly rises up beyond the melting and vaporization temperature, and at the same time heat is dissipated into the target through thermal

conduction. Thus the target is melted and vaporized. At even higher intensities, the vaporized materials lose their electrons and become a cloud of ions and electrons, and in this way plasma is formed. Accompanying the thermal effects, strong shock waves can be generated due to the fast expansion of the vapor/plasma above the target (Wenwu Zhang, 2004).

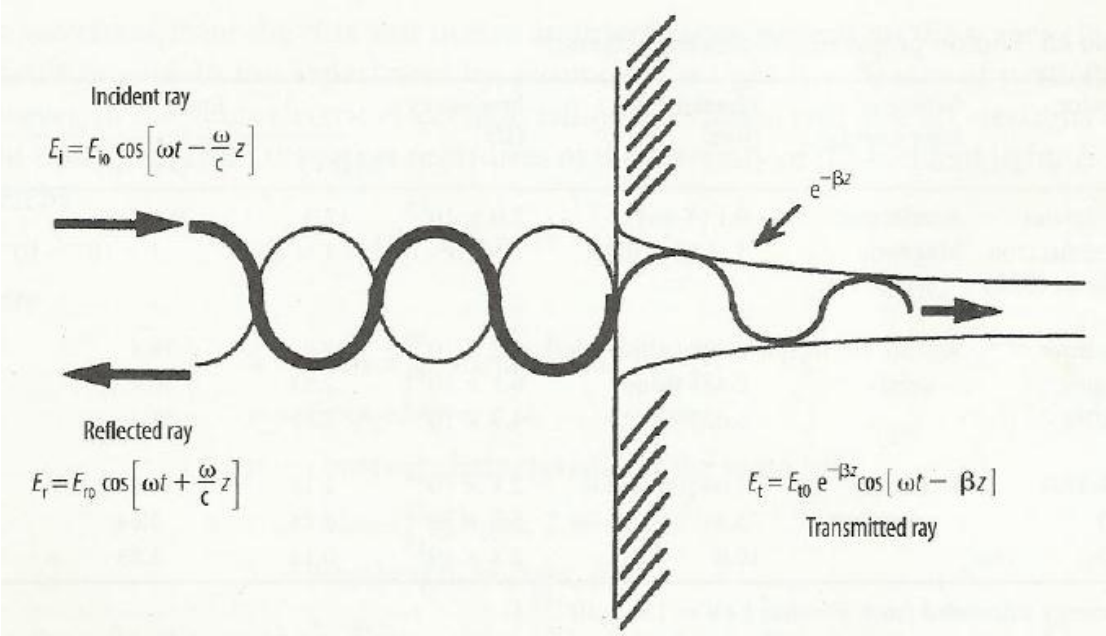

Figure 1.8: The phase and amplitude, E, of an electromagnetic ray of frequency, ω, travelling in the *z* direction striking an air/solid interface and undergoing reflection and transmission.

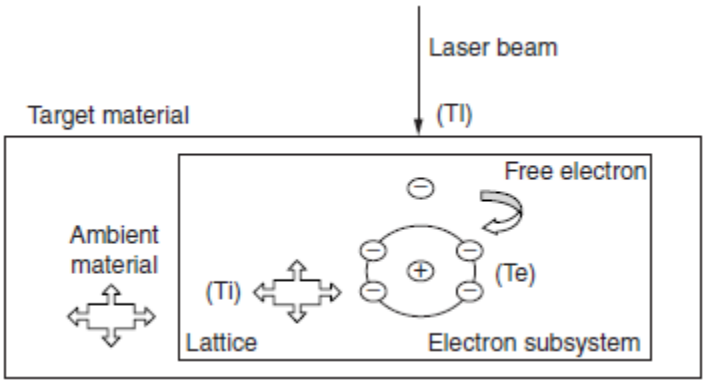

Figure1.9: Laser Energy Absorption by Target Material

Given the laser pulse duration, one can estimate the depth of heat penetration, which is the distance that heat can be transferred to during the laser pulse.

$$D=\sqrt{(4\alpha\, dT)} \qquad (1\text{-}1)$$

where, D is the depth of heat penetration, α is the diffusivity of materials, and dT is the pulse duration.

Laser energy transmission in target material is governed by Lambert's law:

$$I(z) = I_0 \exp.(-a\, z) \qquad (1\text{-}2)$$

Where I is laser intensity, I_0 is the laser intensity at the top surface, z is the distance from the surface, and a is the absorption coefficient that is wavelength dependent (Wenwu Zhang, 2004).

When considering the laser power in material processing, the effective energy is the portion of energy actually absorbed by the target. A simple relation for surface absorption of laser energy is:

$$As = 1-R-T \qquad (1\text{-}3)$$

where As is the surface absorptivity, R is reflection, and T is transmission. For opaque materials, T=0, then As =1-R.

It is important to understand that reflection and absorption are dependent on surface condition, wavelength, and temperature. For example, copper has an absorptivity of 2 percent for CO_2 lasers (wavelength10.64μm), but it has much higher absorptivity for UV lasers (about60 percent).

Absorption usually increases at elevated temperatures because there are more free electrons at higher temperatures (Wenwu Zhang, 2004).

1.6 Laser in material processing:

1.6.1 Laser applications in material processing:

1.6.1.1 Applications of laser welding: Continued laser development has now made laser welding economically competitive with other welding methods. Laser welding is chosen for production not only because it offers technical advantages, but because it costs less in many cases.

The parameters of the laser beam and the properties of the workpiece strongly influence the results of a laser welding application. The thermal diffusivity of the workpiece is important. High thermal diffusivity allows faster conduction of the heat energy through the workpiece and in general permit greater depth of welding. High surface reflectivity can reduce the energy absorbed by the surface. Surface finish can also influence light absorption and hence the weld penetration. The depth of penetration generally is decreased by polishing a metallic surface (John F. Ready, 1997).

Many properties of the laser must be properly chosen to optimize the interaction. These include the following:

1-The laser wavelength should be absorbed well by the workpiece.

2-The irradiance at the surface must be high enough to produce melting.

3-For pulsed lasers, the pulse duration must be long enough to permit penetration of the heat energy through the workpiece.

4-The pulse repetition rate must be high enough to weld a seam at a reasonably high rate.

5-The irradiance and pulse duration must fall into a regime where surface vaporization is not excessive (John F. Ready, 1997).

1.6.1.2 Applications in hole drilling: Hole drilling has developed as one of the most important laser applications in material processing. Laser drilling of holes in ceramic substrates has become widely used. Hole drilling in metals is useful in a variety of areas, such as production of tiny orifices for nozzles and controlled leaks, apertures for electron beam instruments, cooling holes in aircraft turbine blades, and pinholes for optical applications. Hole drilling typically employs pulses with shorter duration than those for welding. Pulse lengths in the region of several hundred microseconds, or even less, are generally used .The lasers most commonly used for hole drilling are the CO_2 laser and the Nd:YAG laser(John F.Ready,1997).

Practical hole drilling with lasers does suffer from some limitations. One limitation is associated with the limited depth of penetration, which arises from the limited amount of laser energy available in a short pulse. If one attempts hole drilling with longer pulses or with a continuous laser, the heat is conducted over a large volume of material, and much of the advantages of using lasers is lost. A second limitation is the quality of the hole. An example of the cross section of a typical hole in a massive sample appears in figure 1.10.

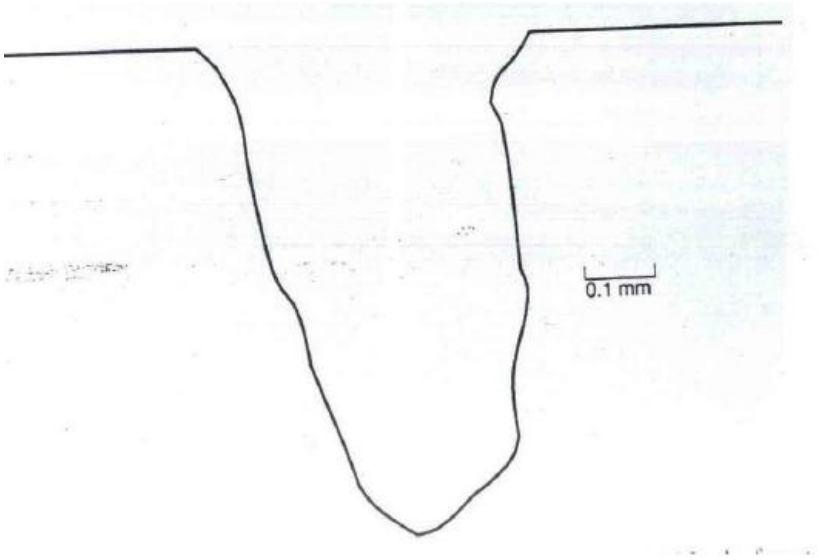

Figure1.10: Cross section of a hole produced in massive brass by a single 5J pulse from a Nd:glass laser focused on the target surface by a 31mm focal length lense.

This hole, drilled in brass by a single 5J pulse from an Nd:glass laser, shows a number of defects, including rough sides, lack of roundness, offset of the center line of the hole from the normal to the surface, and a general taper. These defects are difficult to eliminate completely and may disqualify the laser from some applications in which perfection of the hole is important. To reduce roughness of the sides of a hole drilled through a plate, one may blow gas through the hole as it is being formed. Another common limitation involves the re-condensation of material around the entrance of the hole, forming a crater-like lip for the hole, which could be removed mechanically, or by applying a coating to the sample that may easily be stripped after the drilling, taking the lip with it.

One significant application of laser hole drilling that reached production status very early, as early as 1960s, involved drilling of holes in gemstones. Holes in diamonds used as dies for extrusion of wire are

routinely produced by laser. This has proven a cost-effective application (John F. Ready, 1997).

1.6.1.3 Applications in cutting: Lasers may be used to cut or shape a wide variety of materials. By cutting, we mean vaporization of material along a line, so as to separate the workpiece into separate parts. Cutting at particular speeds often involves the use of a gas jet containing oxygen, in order to increase the cut rate. Materials with low thermal conductivity and low heat vaporization, like many organic materials, may be burned through directly by laser without expenditure of too much laser energy. This approach makes the greatest demands on laser power, and it is most applicable to easily vaporized materials.

Most cutting operations have used CO_2 lasers because of their capability for producing high values of average power. But the advent of multi-kilowatt Nd : YAG lasers has led to their application in cutting also. Cutting of nonmetallic materials proceeds easily in many cases .Because of higher reflectivity and higher thermal conductivity, cutting of metals usually requires more laser power than cutting of nonmetals (John F. Ready, 1997).

1.6.1.4 Applications in glazing: Laser glazing involves some surface melting. As the beam from a multi-kilowatt CO_2 laser is scanned over a surface, a thin melt layer is produced under proper conditions of irradiance and traverse speed. The interior of the workpiece remains cold. After the beam moves on, resolidification occurs very rapidly. The surface layer is quickly quenched. As a result of this process, one may produce surface microstructures with unusual and possibly useful characteristics. The grain size near the surface is very small, because of the high quench rate. The surface structure can appear glassy; hence, the

name laser glazing. This technique is applicable both to metals and ceramics. It appears to be controllable and reproducible.

Laser glazing can produce surfaces that are amorphous or that have a glassy, non-crystalline structure. Such surfaces can have increased resistance to corrosion (John F. Ready, 1997).

1.6.1.5 Applications in alloying: Surface alloying involves spreading of a powder containing alloying elements over the surface to be hardened. Then, the laser beam traverses the surface. The powder and a thin surface layer melt and intermix. After passage of the beam, the surface resolidifies rapidly. A thin layer containing the alloying elements remains, with hardness greater than that of the original material.

An alternative method of supplying the alloying elements uses a gas jet to blow the powder onto the melted surface. The laser typically is a multikilowatt CO_2 laser in order to achieve coverage of large areas .The treating rate is somewhat slower than for transformation hardening, because some surface melting is required.

Surface alloying can produce surfaces with desirable properties on relatively low cost substrate material (John F. Ready, 1997).

1.6.1.6 Applications in cladding: Laser cladding involves bonding of an overlay material to the surface to be hardened. The overlay material may be pre-positioned or it can be continuously fed. The laser beam melts a thin surface layer, similarly to the case of laser glazing. The overlay material is then metallurgically bonded to the surface. In contrast to glazing, the overlay material does not intermix with the surface. Only enough of the surface, melts to form the bond with the overlay material. The process is also called hard facing. Again, the laser would probably be multi-kilowatt CO_2 laser. Laser cladding usually involves covering a

relatively inexpensive substrate material with a more expensive alloy that will increase the resistance of the part to wear or corrosion. Cladding allows the bulk of the part to be made with inexpensive material, while providing the surface with desirable properties associated with the more expensive cladding material. Laser cladding has resulted in surfaces with very good finish, good homogeneity, and very low porosity. Common materials used for cladding include carbides, iron-based alloys, nickel base alloys, and cobalt base alloys (John F. Ready, 1997).

1.6.2Four-attributes analysis of the laser material processing systems:

Laser material interaction can be very complex, involving melting, vaporization, plasma and shock wave formation, thermal conduction, and fluid dynamics.

One can get a relatively complete picture of laser material processing system following the four- attributes analysis-time, spatial, magnitude, and frequency.

Time attribute: Laser output may be continuous (CW) or pulsed, and laser energy can be modulated or synchronized with motion. For a CW laser one should understand its capability of power modulations, focusing control, and energy-motion synchronization. The major purpose of pulsating the laser energy in laser material processing is to produce high peak laser power and to reduce thermal diffusion in processing (Wenwu Zhang, 2004).

Spatial attribute: Laser beam out of a cavity may have one or several modes, which are called transverse electromagnetic mode (TEM). For laser material processing, we are concerned with the spatial distribution

of the beam that affects the thermal field on the target. Laser intensity usually has a Gaussian beam distribution. For Gaussian beam with radius r and for a material with absorption A=1-R, where R is reflectivity and P (t) is the time dependent laser power, the spatial distribution of absorbed laser intensity on the target surface is:

$$I(x, y, t) = (1-R)\, I_0(t) \exp.\ (-(x^2+y^2)/r^2) \qquad (1\text{-}4)$$

where: $I_0(t)$ is the average laser intensity and equals to $P(t)/(\pi r^2)$. Laser energy distribution may take other shapes, such as flat-hat shape, in which the laser intensity at the center is uniform. In general, the formula for laser intensity transmitted to the material at depth z is:

$$I(x, y, z, t) = As^* I_0(t) \exp.\ (-a^*z)\, SP(x, y) \qquad (1\text{-}5)$$

where A*s* =fraction of laser energy absorbed by the material at the surface

$I_0(t)$ = temporal distribution of laser intensity

a = absorption coefficient

SP = spatial distribution of laser intensity

Special optics can be used to change the beam shape and spatial distribution.

Laser beam radius is normally defined as the distance from the center within which 86.4 percent or $(1-1/e^2)$ of total energy is included. Beam radius at the focus is called the focused spot size (Wenwu Zhang, 2004).

Magnitude attribute: Major magnitude parameters of laser energy are power (unit: watt), pulse energy (unit: joule), and intensity (unit: W/m^2 or W/cm^2). For pulsed laser, the laser intensity is equal to $E_0/ (t_p\ pi\ r^2)$, where E_0 is the pulse energy, t_p is pulse duration, and r is beam radius.

Many material properties such as thermal conductivity and reflectivity vary with material temperature and state, which are further decided by the magnitude of energy input. We tactically assume that only one photon is absorbed by one electron at a specific time at normal laser intensities, but when the laser intensity is extremely high as in the case of ultrafast lasers (pulse duration $< 10^{-12}s$), more than one photon can be absorbed by one electron simultaneously. This is termed as multi photon absorption. Material optical property is then highly nonlinear and is very different from single photon absorption. Materials can act as if it were irradiated by a frequency doubled or tripled laser source. In this meaning, we can say that extremely high magnitude of laser intensity can be equivalent to shorter wavelength.

Optical filters, polarizers, attenuators, and beam expanding and focusing systems can be used to modulate laser intensity and intensity spatial distribution so that one can match the laser output to a specific application without disturbing the internal laser source (Wenwu Zhang, 2004).

Frequency attribute: The characteristic frequency of energy field is important because materials may respond very differently to energy fields at different frequencies. The characteristic frequency of laser is its EM oscillation frequency, and more frequently we use its equivalence-wavelength. The frequency decides the individual photon energy of the laser beam. Lasers usually have very narrow spectral width, while other energy sources may have very broad and complex spectral distributions.

The diffraction limited spot size is proportional to wavelength. For circular beams, the focal spot size is: $D_{min.} = 2.44f\lambda/D$, where f is the focus length, λ is wavelength, and D is the unfocused beam diameter.

Thus for high-precision applications, shorter wavelength lasers are preferred. UV laser ablation of organic polymers can be very different in mechanism compared to infrared or visible laser ablation. The infrared and visible laser ablation is mainly photo-thermal degradation, while UV laser ablation may involve direct photo-chemical dissociation of the chemical bonds (Wenwu Zhang, 2004).

Materials show very different absorption properties at different wavelengths. Metals tend to have low absorption at mid infrared (CO_2 laser 10.6μm) while absorption increases with decreasing wavelength. Nonmetals such as ceramics and liquids have strong absorption at mid infrared, much decreased absorption at visible wavelength, and increased absorption at UV.

Keep in mind that absorption also depends on temperature, purity, and surface condition. Also keep in mind that at high enough laser intensity, multi photon absorption may occur, material reacts nonlinearly to the irradiation, and the beam acts as if its frequency is doubled or tripled. And once the surface temperature rises, absorption tends to increase, which forms a positive feedback. In this meaning, very high laser intensity may be regarded as wavelength-independent in material processing. Caution should be used when collecting the material properties from literature. In laser material processing, material properties are highly temperature-, wavelength-, geometry-, and intensity-dependent (Wenwu Zhang, 2004).

1.6.3Types of lasers used in material processing:

Lasers for material processing may be classified by: active medium (gas, liquid or solid); output power (m W, W or kW); wavelength (infrared, visible and ultraviolet); operating mode (CW, pulsed, or both); and

application (micromachining, macroprocessing etc.). Since the state of the active medium determines the principal characteristics of the laser beam for material processing, it is used here as a primary means of classification: gases (atoms, molecules, ions and excimers); liquids (principllay organic dyes); and solids (insulators and semiconductors).This categorization is shown in figure 1.11(John C. Ion, 2005).

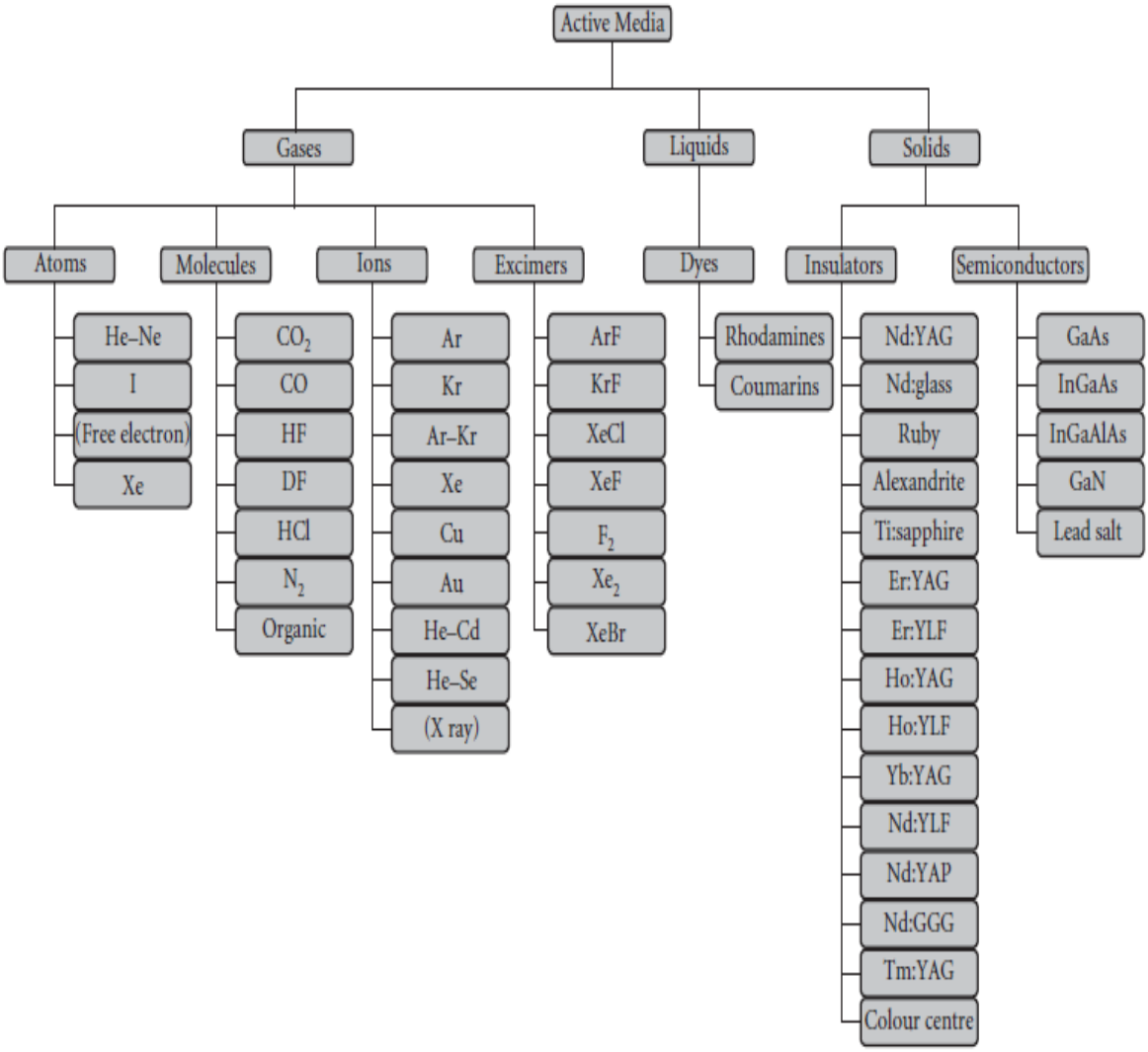

Figure 1.11 Types of Lasers used for material processing categorized by the type of active medium

1.6.4Types of laser processing handling systems:

The various combinations of laser processing handling systems are listed in Table1.1.

The most suitable laser processing system for a particular application, depends on a number of factors: the size of the part to be processed; the complexity of the part; the nature of the beam transmission; and the precision requirement (John C. Ion, 2005).

Table1.1: Combinations of laser beam and workpiece handling systems for two- and three-dimensional laser material processing

Processing geometry	**Workpiece**	**Laser beam**	**Handling System**
Two dimensional	Moving	Moving	x table, y optics
		Stationary	x-y table
	Stationary	Moving	Flying optics
		Stationary	_
Three dimensional	Moving	Moving	Robot-mounted workpiece and beam
		Stationary	Robot-mounted workpiece
	Stationary	Moving	Robot-mounted beam
		Stationary	-

1.6.5 Advantages and limitations of laser in material processing:

Compared with conventional processing technologies, laser processing offers a number of advantageous features:

1-Very high values of irradiance and very localized heating can be achieved. A laser can deliver higher irradiance than any other thermal source.

2-Heat-affected zones can be very small.

3-In many cases, fixturing is easy and fast.

4-The processing is easily compatible with automation.

5-No vacuum is required. This leads to a capability for rapid throughput. For some applications, a gas jet may be desirable.

6-There is no contact of any material with the workpiece, so that contamination problems are reduce.

7-Laser processing can work well with some "difficult" materials, such as refractory materials or hard, brittle materials.

8-Small hole- diameters can be achieved.

9-Extremely small welds may be accomplished on delicate objects.

10-Inaccessible areas or even encapsulated materials can be reached with laser beam.

There are some limitations to laser processing:

1-The initial capital cost is usually high.

2-The depth of penetration in laser welding is limited, except for multikilowatt lasers.

3-In laser welding, careful control of the process is required to avoid surface vaporization.

4-The depth of penetration of laser-drilled holes is limited, although repeated pulses can increase the depth.

5-The quality of laser-drilled holes is less than perfect. The walls of the holes are generally rough. Their cross sections are not completely round, and they taper somewhat from entrance to exit. There is often some recondensation of vaporized material on the walls of the holes and at the entrance to the holes. The control of size and tolerances is not perfect (John F. Ready, 1997).

1.7 Laser surface treatment:

It called that region of the solid where the symmetry and bonding between particles are intrinsically different from that in the bulk, a surface.

As a consequence , in many cases surfaces are characterized by a high reactivity (Somorjai, 1994).The diameter of a laser spot on a surface amounts to at least a few micrometers and the penetration depth of visible light is at least a few ten nanometers (H. G. Rubhan, 1999).

The laser has some unique properties for surface heating. The electromagnetic radiation of laser beam is absorbed within the first few atomic layers for opaque materials, such as metals, and there are no associated hot gas jets, eddy currents or even radiation spillage outside the optically defined beam area. In fact the applied energy can be placed precisely on the surface only where it is needed .Thus it is a true surface

heater and a unique tool for surface engineering. (William M. Steen, 2003).

Common advantages of laser surfacing compared to alternative

processes are :

1-chemical cleanliness;

2-controlled thermal penetration and therefore distortion;

3-controlled thermal profile and therefore shape and location of heat affected region;

4-less after machining, if any, is required;

5-remote non-contact processing is usually possible;

6- relatively easy to automate.

Surface treatment is a subject of considerable interest at present because it seems to offer the chance to save strategic materials or to allow improved components with idealized surfaces and bulk properties.

Currently the uses of lasers in surface treatment include:

1-surface heating for transformation hardening or annealing;

2-scabbling, the removal of the surface of concrete or stone;

3-surface melting for homogenization, microstructure refinement, generation of rapid solidification structures and surface sealing;

4-surface alloying for improvement of corrosion, wear or cosmetic properties;

5-surface cladding for similar reasons as well as changing thermal properties such as melting point or thermal conductivity ;this process has

progressed into direct laser casting for low -volume manufacture of three-dimensional components;

6-surface texturing for improved paint appearance;

7-surface roughening: for enhanced glue adhesion;

8-plating by Laser Chemical Vapour deposition (LCVD), Laser Physical Vapour Deposition (LPVD); enhanced plating for localized plating by electrolysis or cementation or improved deposition rates;

9-non-contact bending;

10-magnetic domain control;

11-stereolithography and other forms of layer manufacture;

12-paint stripping and cleaning;

13-laser marking;

14-micro-machining;

15-shock- hardening (William M.Steen, 2003).

From the point of view of mechanical engineers, the purpose of surface treatment is to obtain better performance of the workpiece whether it is submitted to wear and/or high temperature and/or corrosive media. Surface treatments enable to enhance the surface properties to answer any particular requirement, while the bulk of the workpiece keeps its structural properties. However for most applications the ideal surface is still being worked on. This is a contiuous search as it can contribute to a reduction in costs, either by diminishing repairs or replacement of components. In these contexts laser surface treatments have gained scientific and industrial interest (A. S. C. M. d'Oliveira, 2001)

Usually, laser irradiation is used e.g. for cleaning, structuring, chemical and morphological modification and curing of material surfaces. As a pre-treatment for adhesive bonding, laser radiation generates an oxide and grease free surface with a possible micro-structuring.

A wet chemical cleaning is unnecessary. Laser ablation works noise-and touch- free with small running costs. Precise control makes the integration in serial productions possible (Stefan Böhm).

The functional principle of removing coating layers e.g. dirt by laser irradiation is the following: The coating layer is removed by vaporization through absorbing the laser spot. The very short laser pulses cause a very little thermal influence on the base material. It is possible to treat the metal without damaging or melting of the base material.

Laser radiation offers the possibility to treat the material surfaces selectively(in contrast to blasting processes) with a high flexibility (fast and easy change of laser parameters) in order to improve the adhesion characteristics. This has the advantage in comparison to other procedures that only the required surfaces need to be processed (Stefan Böhm).

Chapter Two

Laser Micromachining, an Overview

2.1Fundamentals of micro-manufacturing:

During the last decade, there has been a continuing trend of compact, integrated and smaller products such as (i) consumer electronics-cell phones, PDAs(personal digital assistant), (ii) micro-and distributed power generators, turbines, fuel cells, heat exchangers; (iii) micro-components/features for medical screening and diagnostic chips, controlled drug delivery and cell therapy devices, biochemical sensors, Lab-on-chip systems, stents, etc.; (iv) micro-aerial vehicles (MAV) and micro-robots; and (v) sensors and actuators (See Figure 2.1) (Muammer Koç, 2011). This trend requires miniaturization of components from meso- to micro-levels. These issues lead the way for researchers to seek alternative ways of producing 3D micro-components with desired durability, strength, surface finish, and cost levels using metallic alloys and composites. Micro-machining processes have been widely used and researched for this purpose. For instance, the laser micromachining is used to fabricate micro-structures (channels, holes, patterns) as small as 5μm in plastics, metals, semiconductors, glasses, and ceramics. As a result, micro-scale heat exchangers, micro-membranes, micro-chemical-sensors and micro-scale molds can be fabricated with micro-machining. (Muammer Koç, 2011).

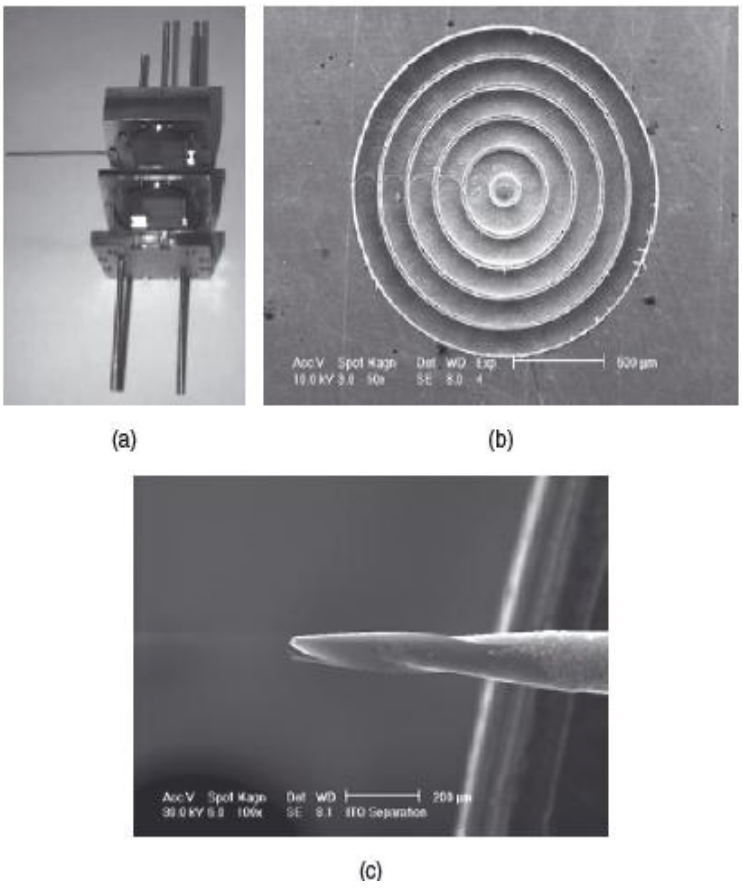

Figure 2.1 (a) Micro-channel chemical reactor, manufactured by laser micro-machining; (b) pattern of concentric 127μm channel of varying depth up to 125 μm cut into a brass workpiece; (c) SEM photograph of the front view of the 127 μm diameter two-flute end mill.

There is a growing need for fast, direct, and mass manufacturing of miniaturized functional products from metals, polymers, composites, and ceramics. The demand for miniaturized meso- (1-10mm)/micro-(1-1000μm) devices with high aspect ratios and superior surfaces has been rapidly increasing in aerospace, automotive, biomedical, optical, military, and micro-electronics packaging industries (Muammer Koç, 2011).

2.1.1 Mechanical micromachining:

Fabrication using miniaturized mechanical material removal processes has a unique advantage in creating 3D components using a variety of engineering materials.

Micro-mechanical machining is a fabrication method for creating miniature devices and components with features that range from tens of micrometers to a few millimeters in size (See Figure 2.2) (J.Chae, 2005).

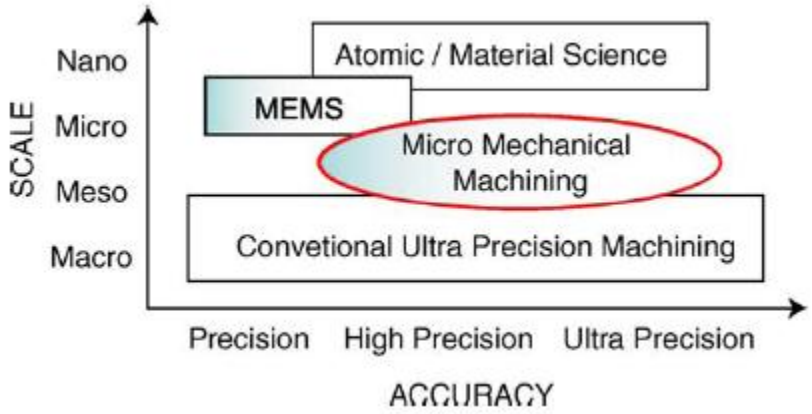

Figure 2.2 Dimensional size for the micro-mechanical machining

2.1.2 Micro-machine tools:

These are cost effective when compared with ultra-precision machine tools and require smaller amounts of materials when fabricated (J.Chae, 2005). Therefore, machining centers can be constructed with more expensive materials that exhibit better engineering properties. Micro-machine tools have higher natural frequencies compared with conventional macro-machines, due to substantially smaller mass. This translates into a wide range of spindle speeds to fabricate components without regenerative chatter instability. In addition, smaller machine tools have lower vibration amplitudes relative to the conventional machine loads. Figure 2.3 illustrates miniature micro-machine tools (J.Chae, 2005).

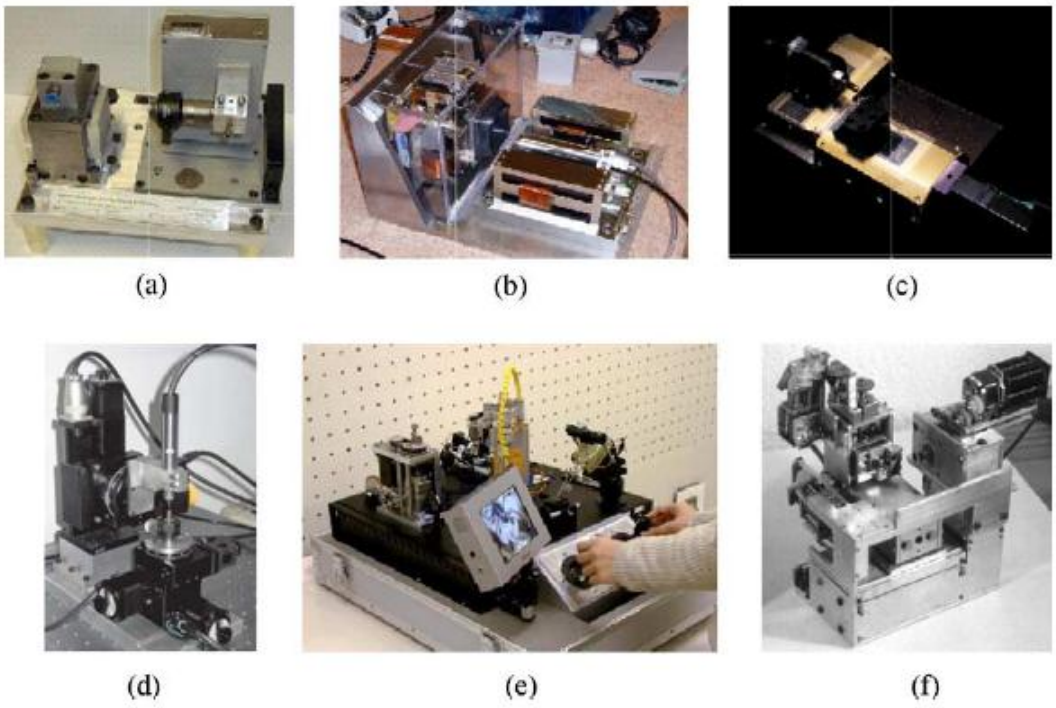

Figure 2.3Micro-machines (a) micro-factory; (b) 2nd.generation miniature machine; (c) commercial miniature machine; (d) miniature machine; (e) micro-factory; (f) micro-machine tool.

2.1.3 Micromachining techniques:

The microfabrication techniques employed contribute significantly towards the cost of the device. This has led to a struggle to find more efficient and cheaper fabrication technique without compromising performance and the ability to mass production (Sunil Ranganath Belligundu, 2005).

Most of the microfabrication or micromachining techniques can be classified into three categories:

i- Bulk micromachining,
ii- Surface micromachining, and
iii- High aspect ratio micromachining.

2.1.3.1 Bulk micromachining:

Bulk micromachining is a process that removes "bulk" substrate. It is a subtractive process that involves removing selective areas of the substrate material. Some of the features that can be fabricated using this type of process are reservoirs, channels, grooves, cantilevers, etc. Figure 2.4 shows a cavity fabricated using the bulk micromachining process (Sunil Ranganath Belligundu, 2005).

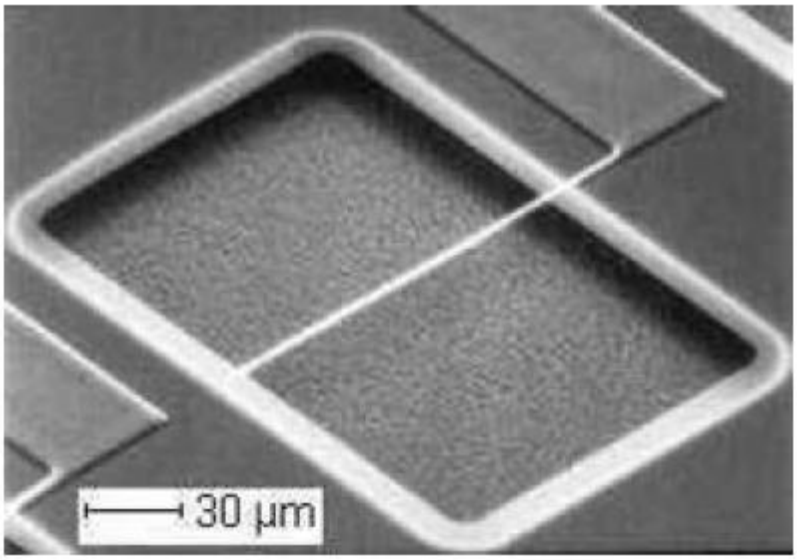

Figure 2.4: Deep cavity etched in Silicon

2.1.3.2 Surface micromachining

Surface machining is an additive process that refers to processing "above" the substrate. The microstructures are not fabricated in the substrate, instead the substrate is used as a base to build-up the microstructures. Released and movable microstructures are fabricated on a single substrate from thin layers of structural materials and sacrificial layers, deposited on the surface of the substrate. Some of the features using this technique are gears, comb fingers, cantilevers, and membranes. Figure 2.5 shows a micro-engine gear, that was fabricated using the surface micromachining process meshing with another gear (Sunil Ranganath Belligundu, 2005).

Figure 2.5: Micro-engine gear meshing with another gear

2.1.3.3 High aspect ratio micromachining

Aspect ratio is defined as the depth of the structure divided by its width. High Aspect Ratio Micromachining also called HARM, involves lithography techniques like LIGA (from German Lithographie, Galvanoformung, Abformung, meaning lithography, electroplating and molding). LIGA allows the use of materials other than silicon such as metals, ceramics and polymers, opening the door for many different types of structures and devices. LIGA structures typically have an aspect ratio of greater than 10:1, very precise geometries, and smooth, vertical sidewalls. Figure 2.6 Shows a microtrajectory sensing device manufactured at Sandia National Laboratories (Sunil Ranganath Belligundu, 2005).

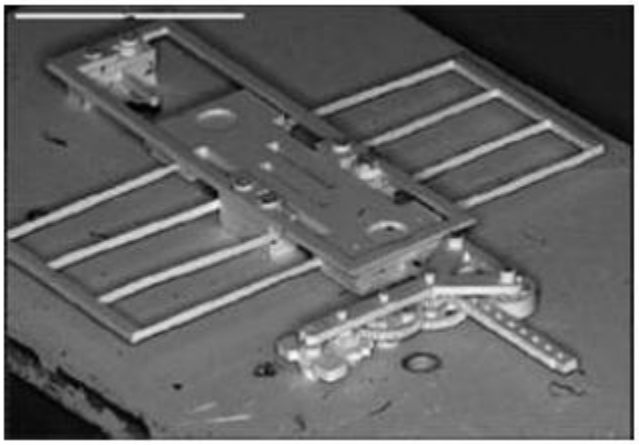

Figure 2.6: Micro-trajectory Sensing Device.

2.2 Laser micro-and nanofabrication:

Laser micro-and nanofabrication is based on the interaction of laser light with solid matter. As a result of the complex interaction between light and matter, small amounts of material can be removed from the surface. Two different phenomena are operating, namely: pyrolithic processing and photolithic processing. Pyrolithic processing is composed of heating, melting, and ablating the material at the surface, and photolithic processing is based on the direct breaking of chemical bonds in a wide range of materials (J. Chae, 2005).

Optical energy is transferred to the electrons by absorption, which essentially increases the energy of electrons by increasing the vibration of the electron that is sensed as heat (J.Chae, 2005).

2.2.1 Laser ablation for surface modification:

Laser treatment of materials offers advantages over both chemical and other physical methods. They enable precise modification of certain surfaces that are difficult to treat with conventional chemical methods. The resulting modified surfaces are free from contaminant. Most importantly, the bulk properties of the material remain intact. The

development of laser-assisted modification of polymer surfaces is rapidly growing and developing field that has gained considerable interest among scientist in the past decade (K. S. Tiaw, 2004).

2.2.1.1 Interaction of laser with polymers:

The interaction of laser with a polymer can result in a large variety of reactions which range from the modification of the polymer surface to the complete decomposition. The latter normally results in ablation and/or carbonization of the irradiated polymer area. Discussion relating to the ablation mechanism started very soon after the discovery of ablation, and up to now no general agreement exists whether the mechanism is photochemical or photothermal. Recent papers and reviews favor a photothermal mechanism, but these studies are based on modeling of data for one polymer, i.e.Kapton™.This approach may be reasonable, but we should also not forget that there exists a long standing research topic ,i.e., organic polymer photochemistry, that has proven that irradiation of organic molecules or polymers with UV photons leads to in photochemical reactions. Therefore, it is also very likely that under ablation conditions, i.e., much higher fluences, photochemical reactions take place. Polymers may be classified for photon-induced reactions into polymers that can depolymerize upon irradiation and into polymers that decompose into fragments (Thomas Lippert, 2005).

2.2.1.2 Polymers surface modification:

Laser ablation as means of polymer surface treatment offers modification of the morphology, chemistry, and texture of the surface material. The influence laser exposure on a polymeric surface depends on the mechanism of ablation of that particular material.

For strongly absorbing polymers, a phenomenological etch rate can be determined which is directly related to the laser fluence and pulse duration. However, in weakly absorbing polymers, there is a different phenomenon associated with ablation. Prior to ablation, there is an incubation period in which the polymer absorbs energy that is followed by side-chain scission resulting in a less saturated backbone and strong UV absorber (Allison Suggs, 2002).

Polymethyl methacrylate, PMMA, demonstrates an entirely different surface topography following ablation. PMMA ablates through surface superheating, meaning that the material heats above its softening point below the surface, degrades and releases dissolved gases that create subsurface explosions. This mechanism of ablation results in the overall destruction of the surface material into a cratered structure with significant debris formation. The modification of the surface in this way should promote biological attachment (Allison Suggs, 2002).

2.2.2 Laser beam characteristics:

Ideally the laser beam is Gaussian in shape. The cross section shows the intensity of the beam. The beam is defined when the hot spot may be shifted slightly to the right as shown in figure 2.7 (Mark J. Jackson, 2007).This means that the laser cavity needs adjusting to correct the beam profile. The beam may be affected by the optics and apertures it travels through; for example if it passes through a small hole it could become diffracted, as shown in figure 2.8. Eventually the propagating beam will naturally spread out but stays parallel better than any other light source. The laser light spreads out owing to diffraction; the waist being the minimum diameter of the beam denoted W_0. It is at this point that it

becomes sensible to focus the beam on the surface. However, all is not lost if this is not achieved.

Either-side of W_0 is the Rayleigh length, this is a length where the beam is still highly focused and though not ideal, laser ablation can still be achieved (Mark J. Jackson, 2007).

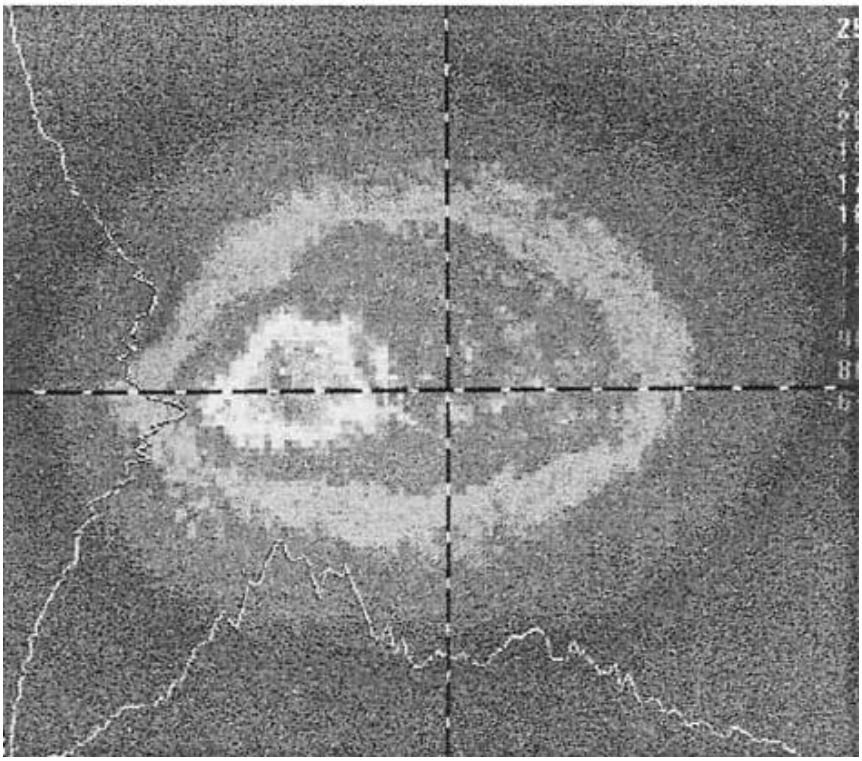

Figure 2.7: Eccentric laser beam profile

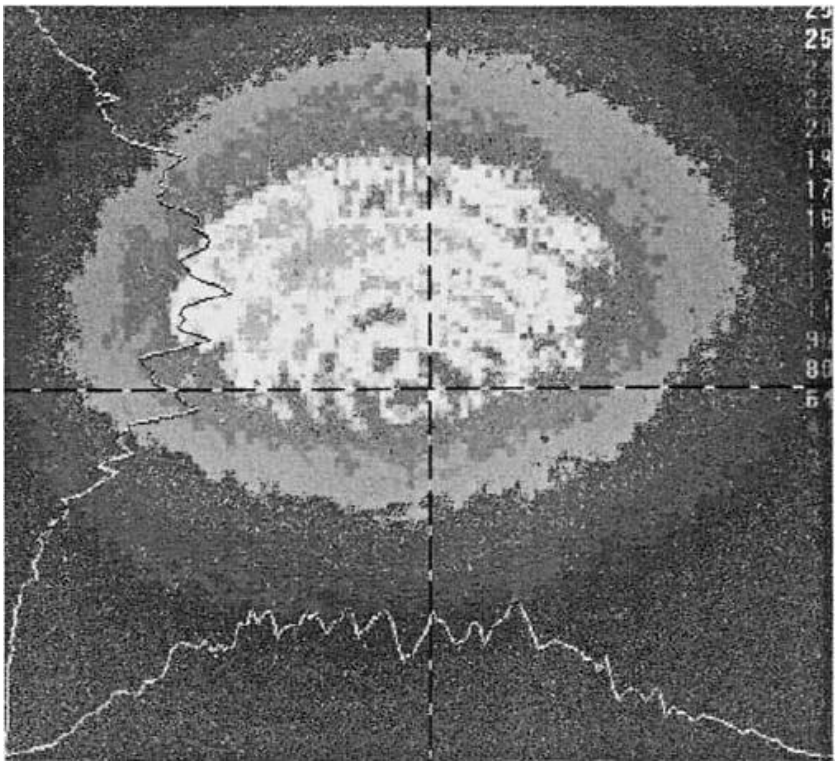

Figure 2.8: Effects of diffraction on the laser beam

Optics are used to change the diameter of the beam or its intensity and direction. For an ideal beam,

$$\theta W = \pi/\lambda \qquad (2.1)$$

The realistic laser beam equation is:

$$\theta W = M^2\pi/\lambda \qquad (2.2)$$

Where, θ= half the divergence angle, W=beam waist size, and λ= wavelength. As everything is ideal here this expression is true over the whole length of the beam. However, in reality perfect conditions never exist. M^2 is a beam quality number, which is one for a perfect beam. The minimum spot size can be found in the following way;

$$\theta_f = D/2f \qquad (2.3)$$

Resulting in a minimum spot size,

$$\delta = 4/\pi \, M^2 \lambda \, f/D \qquad (2.4)$$

Where, *f* is the focal distance, D is the lens diameter, and δ is the minimum spot size diameter. Minimum spot size governs the minimum feature size. Remember that in conventional machining small features can be created with relatively large cutting tools. Clearly M^2 is an important parameter to control as it one of the major influences of the minimum spot size. Hence, a high-quality beam is desirable for micromachining. For micromachining, a small spot size is required. This is obtained when $M^2 = 1$, with a short wavelength, and a short focal length. Examples of beam properties are shown in table 2.1 (Mark J. Jackson, 2007).

Table 2.1 Properties of laser beams

Laser	Wavelength λ (μm)	Power, P (W)	W.θ (mm.rad)	Beam quality, M^2	Spot diameter with f/4 lens δ(μm)
HeNe	0.63	0.002	0.2	0.98	3
Fine drilling Nd:YAG	1.06	100	6	10	50
Nd:YAG	1.06	1000	25	80	500
Q-switched Nd:YAG	1.06	10	2	3	15
Q-switched Nd:YAG	1.06	100	6	10	50
CO_2	10.6	1000	10	1.5	80
Copper va-por	0.51	20	0.5	3	8
Ti:Sapphire	0.78	1			
Excimer	0.193-0.351	100	20	200	

2.3 Laser micromachining:

2.3.1Principles of laser material removal:

The mechanism of laser beam interaction and material removal is shown in figure 2.9(a). Laser energy is focused on the material surface and partly absorbed. The absorptivity depends on the material, the surface structure, the power density, and the wavelength. Absorption occurs in a very thin surface layer, where the optical energy is converted into heat. The optical penetration depth is defined as the depth for which the power density is reduced to 1/e of the initial power density. The absorbed energy diffuses into the bulk material by conduction. For short pulses the heat flow is approximately one-dimensional (Joseph Mc. Geough, 2002).

The high vaporization rate (vapor speed have been reported in the range of 3 to 10 km/s) causes a shock wave and a high vapor pressure at the liquid surface considerably increases the boiling temperature. Finally the material is removed as a vapor by the expulsion of melt, as a result of the high pressure and by an explosive-like boiling of the superheated liquid after the end of the laser pulse (Joseph Mc. Geough, 2002).

In metals a rim of resolidified material caused by laser micromachining is clearly evident.In plastics, however, the process is quite different; here the material is removed by breaking the chemical bonds of the macromolecules, and is dispersed as gas or small particles. No melt is found (Joseph Mc. Geough, 2002).

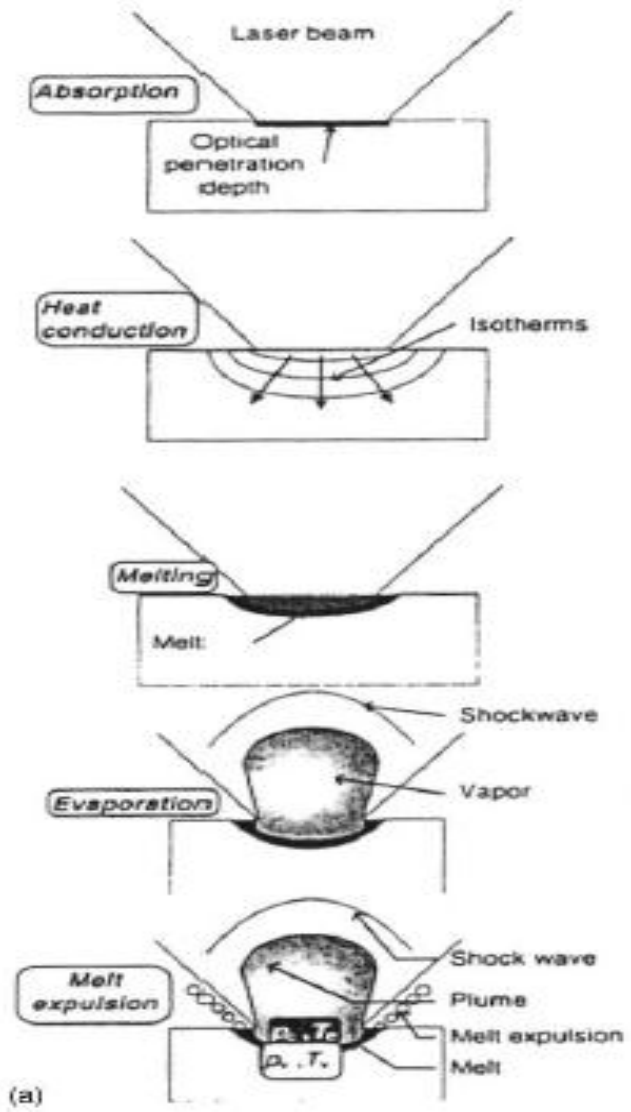

Figure 2.9(a): Laser beam interaction and material removal

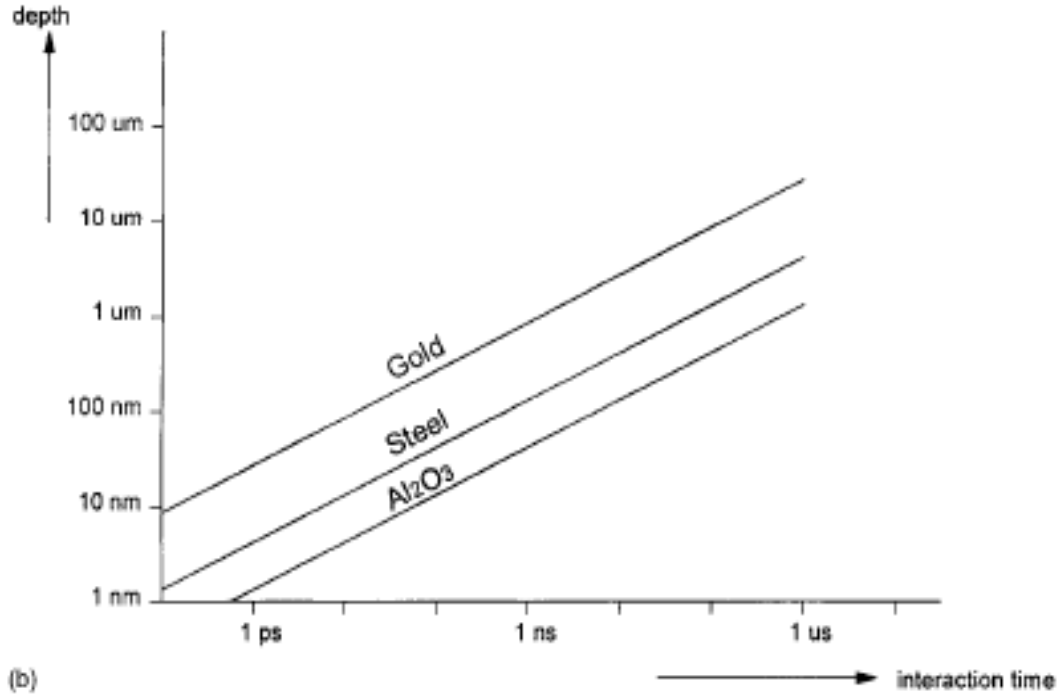

Figure 2.9(b) For short pulses the penetration depth is at micron or submicron level. The heat penetration in micromachining can therefore be considered as one-dimensional.

2.3.2 Laser micromachining mechanisms:

The two important mechanisms of material removal with micron and submicron precision during laser micromachining are ablation and laser-assisted chemical etching (Narendra B. dahotre, 2008).

2.3.2.1 Laser ablation:

The ablation during laser processing refers to the material removal due to thermal and/or photochemical (nonthermal) interactions. The laser-material interactions during ablation are complex and may involve the interplay between thermal and photochemical processes often referred to as photophysical processes. Figure 2.10 presents the various mechanisms of laser ablation (Bäuerle 2000; Narendra B. Dahotre, 2008).

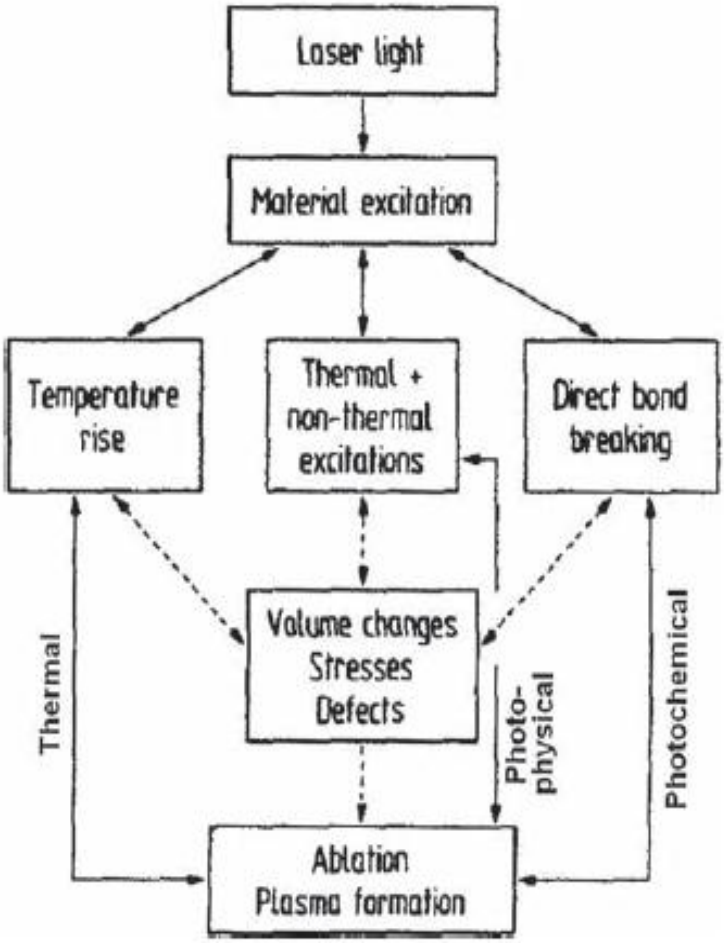

Figure 2.10Various mechanisms of laser ablation

In nonthermal ablation, the energy of the incident photon causes the direct bond breaking of the molecular chains in the organic materials resulting in material removal by molecular fragmentation without significant thermal damage. This suggests that for the ablation process, the photon energy ($h\nu$) must be greater than the bond energy (Narendra B. Dahotre, 2008).

In multiphoton mechanism, even though the energy associated with each photon is less than the dissociation energy of bond, the bond breaking is achieved by simultaneous absorption of two or more photons. Figure 2.11 presents the photon energies associated with various laser radiations and

the dissociation energies of various molecular bonds (Narendra B. Dahotre, 2008).

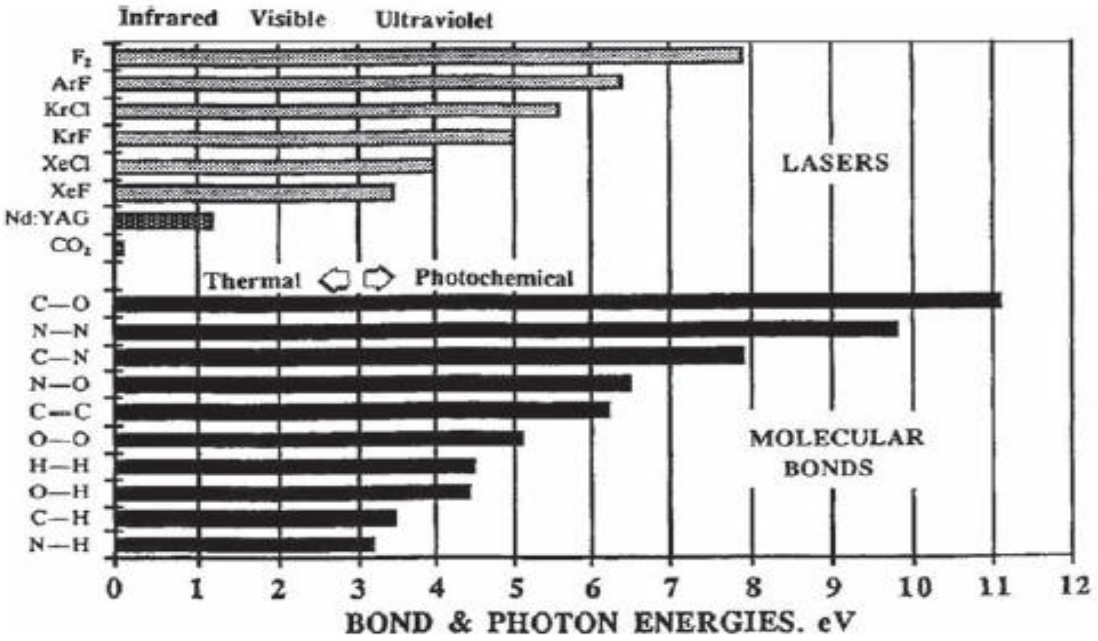

Figure 2.11 Dissociation energies of some common molecular bonds and photon energies of some common lasers.

One of the important considerations during the laser-material interaction during ablation is the thermal relaxation time (τ), which is related with the dissipation of heat during laser pulse irradiation and is expressed as (Vogel et al.1999):

$$\tau = d^2/4k$$

where d is the absorption depth and k is the thermal diffusivity. Thus the two important parameters that determine the ease with which the ablation can be initiated are absorption coefficient (α) and thermal diffusivity (k).

The large value of absorption coefficient and small value of thermal diffusivity generally provide the high ablation efficiency of material (Narendra B. Dahotre, 2008).

2.3.3 Advantages of precision laser micromachining:

Precision laser micromachining provides a unique solution to fabricate micromoulds and dies for mass production, e.g. using injection moulding and/or hot embossing processes. The laser micromachining process offers four major advantages over conventional technologies. First of all, a laser beam can be used as a sharp material removal tool, which can be focused down to 1µm in diameter. Secondly, a wide range of materials can be machined, e.g. from glass and plastics to difficult-to-machine materials such as tool steels and ceramics. Also, combined with a high precision motion system a tightly focused beam can remove precise amounts of material with high accuracy and precision. Finally, laser micromachining is an environmentally friendly process compared to chemical etching processes (Evgueni Bordatchev, 2008).

Laser micromachining is a contactless process. It will not damage material surface except the pile-up effects for metallic materials, debris redeposition for polymers and cracks due to additional heating stress. But those effects can be avoided by some pre-process, post-process and deliberately setting machining conditions. The laser micromachining can be operated under atmospheric conditions and at room temperature. Due to the contactless characteristics, there is no tool wear in laser micromachining like conventional machining methods.

Laser micromachining is suitable for rapid prototyping even with complex geometric patterns because of its flexibility (Deyao Ren, 2009).

2.3.4 Laser micromachining of polymers:

Polymers as substrates have advantages over their glass counterparts as their properties are more easily tailored for specific applications and are cheaper and easier to manufacture. One of the advantages of polymers is their lower threshold for optical breakdown, which can be reached using

non-amplified nanojoule femtosecond pulses. Considerable researches have also been conducted into the different applications involving fabrication by femtosecond pulses in polymers, such as three-dimensional data storage and fabrication of photonic band gap structures (Narendra B. Dahotre, 2008).

2.3.4.1 Laser ablation of polymers:

During the last decade, processing of polymers has become an important field of applied and fundamental research. One of the most important fields is laser ablation involving various techniques and applications. Laser ablation is used as an analytical tool for MALDI (matrix-assisted laser deposition/ionization) and LIBS (laser induced breakdown spectroscopy) or as a preparative tool for PLD (pulsed laser deposition) of inorganic materials and of synthetic polymer films.

Another application is surface modification of polymers; if low fluences are applied, the polymer surface can be either chemically modified to improve adhesion, or it can be changed physically. This can be either a random increase of the surface area or it can result in LIPMS (laser-induced periodic microstructures in the nm range) which have been suggested to be used for the alignment of liquid crystals (Thomas Lippert, 2004).

Excimer laser ablation of polymers is demonstrated to be a well suited technology for cost effective fabrication of prototypes of polymer microstructures in relatively short times. Prototyping is realized by ArF excimer laser ablation (193nm) using mask projection techniques in combination with high precision sample movement as well as mask movement (Thomas KLOTZBÜCHER, 2001).

For micromachining of polymers excimer lasers are commonly used. Excimer lasers are well established in industrial applications and exhibit relatively high pulse energies in the order of several 100mJ (pulse duration=20ns) as well as high life cycle times with at the same time high stability of operation. The wavelength of excimer lasers, depending on the choice of gas fill, can be set to λ=157nm (F_2), λ=193nm (ArF), λ248nm (KrF), λ=308nm (XeCl) or λ=351nm(XeF).

The high photon energy of the excimer laser radiation allow a photon-induced breaking of C-H(3.5eV) and O-H(4.4eV)as well as C-C(6.2eV) bonds in polymers. This together with the relatively low thermal heat conduction coefficients and low optical absorption coefficients of polymers, allows the well-defined ablation of polymers with almost no thermal damage (Thomas Klotzbücher, 2001).

2.3.4.2 PMMA micromachining with CO_2 laser:

Machining with the CO_2 laser involves removing material by a thermal process. The infrared radiation excites vibrational and rotational levels in the irradiated sample, which heats up and evaporates or burns. The exact nature of the process depends on the absorption characteristics of the sample material. Thus, it is crucial to select a material which responds in a useful manner to CO_2 laser irradiation. Otherwise the resulting structures will show effects due to the thermal nature of the material removal process, such as scorching or boiling up, on a length scale comparable to the structures themselves. This is shown in Figure 2.12, where a test structure has been machined in poly-methyl-methacrylate (PMMA), polycarbonate (PC), polystyrene (PS), and poly-ether-ether-ketone (PEEK), respectively. It is seen, that PC and PEEK look burned with a lot of soot deposited on the surfaces, whereas PS and PMMA look

clean. However, only PMMA machines well, since the structure in PS is molten, and has poor edge definition (Martin F. Jensen, 2004).

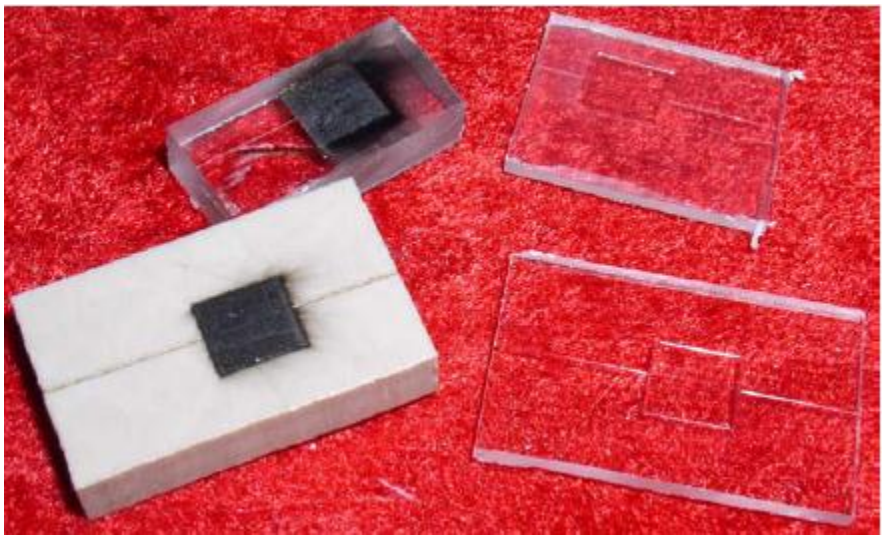

Figure 2.12: Photo of a simple test structure machined in PC, PS, PEEK and PMMA from top left to bottom right respectively.

It is generally accepted that PMMA is the only polymer and only some specific grades thereof, that machine really well. Others machine acceptably, others again are acceptable only when thin films are machined (Martin F. Jensen, 2004).

2.3.4.3 Interdependence of channel depth and length:

On account of conductive and capacitive heat loss terms, there is always a certain amount of heat that is not available to evaporate PMMA. Instead, the heat disperses into the adjacent material. Depending on the relative amount of the heat loss terms and the available time for dispersing heat into the surrounding material, the affected area will be larger or smaller. These results in two observable effects: the channel width is dependent on the cutting sequence and the channel depth might become dependent on the length of the channel.

If a channel is cut with more than one pass, the cooling time between the passes becomes relevant. If the time is short, the needed energy for

subsequent ablation is lower and therefore the channels are expected to become deeper. The available cooling time depends on the channel length, which consequently means that shorter channels will be deeper at the same laser settings. Figure 2.13 shows the influence of the cooling time on the channel depth (Detlef Snakenborg, 2004).

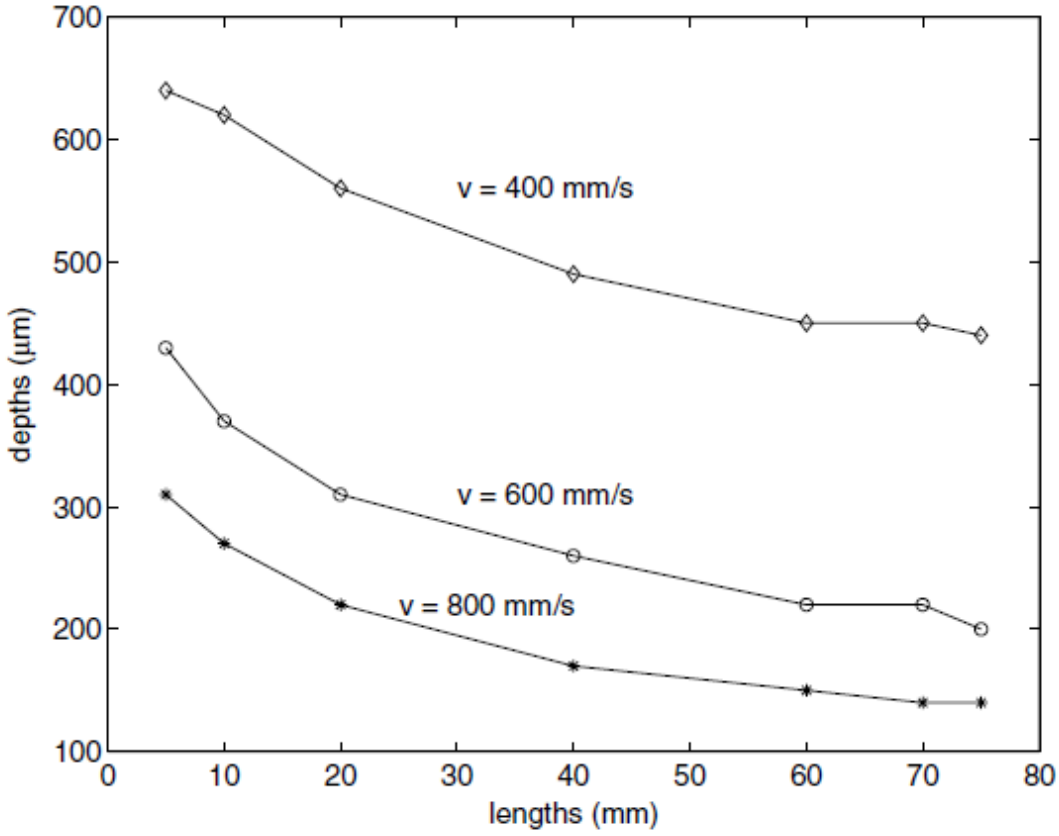

Figure 2.13: Heat loss examination. Channels were cut using a power of 8W at velocities of 400, 600 and 800 mms^{-1}.

Twenty passes were used to cut the channels. As a result, the depths of the channels depend on the cooling time available between the passes so that shorter channels are deeper than longer ones. For channel lengths over 70mm, the effect becomes negligible.

2.3.4.4 Varying the Channel Width:

The heat required to warm up the substrate retards the evaporation process, since a certain amount of heat is not available for evaporation. This fact can be used to generate channels of narrower or broader width depending on the number of passes and the amount of power applied. Earlier investigations have shown that the channel depth is linearly proportional to the number of passes at a fixed velocity.

The channel width depends on the spot size of the laser beam as defined by the diameter of the spot where the irradiance is larger than the threshold value for ablation. The spot size defined in this way is thus time-dependent, since the irradiance of the laser beam has a Gaussian distribution. As a result, a slow moving laser beam produces broader channels than a fast moving beam (Detlef Snakenborg, 2004).

2.3.5 The Interaction of light with a transparent material:

Light can interact with a transparent material in several ways, shown in figure 2.14.The incident light can be reflected at any surface. The light passing through the material can be scattered or absorbed. If some of the absorbed light is re-emitted, usually at a lower energy, it is called fluorescence. The light which leaves the material is the transmitted light. Ignoring fluorescence, these interactions can be expressed thus:

Incident intensity(I_0) = amount of light reflected(I_r)
+ amount scattered(I_s) + amount absorbed(I_a)
+ amount transmitted(I_t)

$$I_0 = I_r + I_s + I_a + I_t$$

$$\text{or } 1 = R + S + A + T \qquad (2.1)$$

where R is the fraction of light reflected, S is the fraction of light scattered, A is the fraction of light absorbed and T is the fraction of light

transmitted. In good quality optical materials the amount of light scattered and absorbed is small and it is often adequate to write:

$$I_0 = I_r + I_t$$

$$1 = R+T$$

The appearance of a solid is often dominated by reflection. If the surface is smooth the reflection is said to be specular while if the surface is rough it is diffuse, as depicted in figure 2.15.

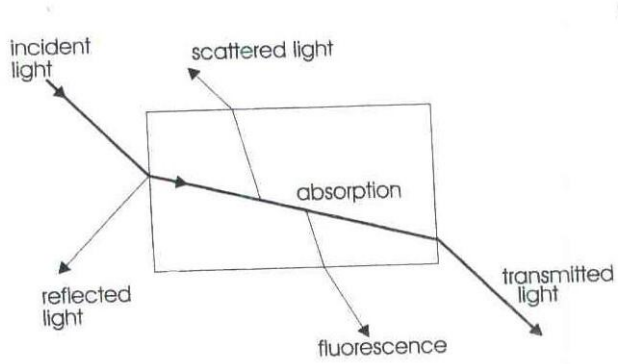

Figure 2.14: The interaction of light with a transparent material.The "bending "of the light ray on entering and leaving the material is called refraction. All of the processes labelled (reflection, absorption, scattering and fluorescence), can lead to colour production

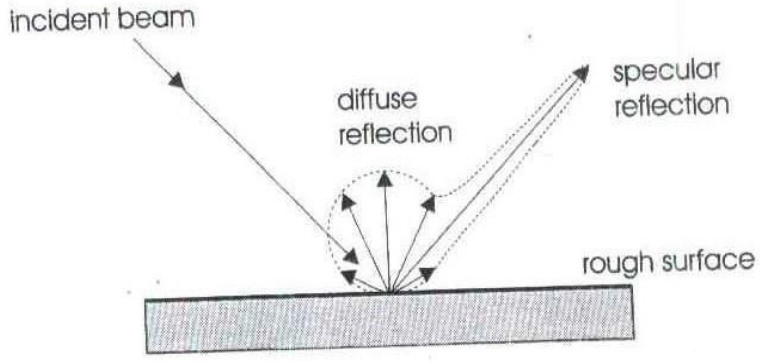

Figure 2.15 Reflection of light from a rough surface consists of two components, diffuse reflection and specular reflection.As the surface roughness increases the amount of diffuse reflection relative to the specular reflection increases. The ratio is an indication of surface gloss.

2.4 Heat islands, SRI and cavity radiators:

Through micromachining process of PMMA, it is the desire to reduce the effect of heat island and to increase the solar reflectance index, by increasing the reflectivity and the absorptivity of the samples. This consequently will reduce thermal loads in buildings and electricity consumption. It is first of interest to understand these terms and their effects.

2.4.1 Heat islands:

A significant impact of the built environment is the generation of a heat island, an area of increased ambient air temperature due to absorption and release of the sun's energy by buildings and other manmade structures. Heat islands are most common in urban areas where surfaces are comprised of synthetic materials. In particular, roofing and pavement absorb heat from the sun, especially when their capability to reflect solar radiation is poor (Duke Pointer, 2009).

Heat islands usually occur in urban areas; hence they are sometimes called urban heat islands. Urban heat islands occur when built-up areas are warmer than the surrounding environment. Figure 2.16 is a schematic depiction of a heat island (Medgar L. Marceau, 2007).

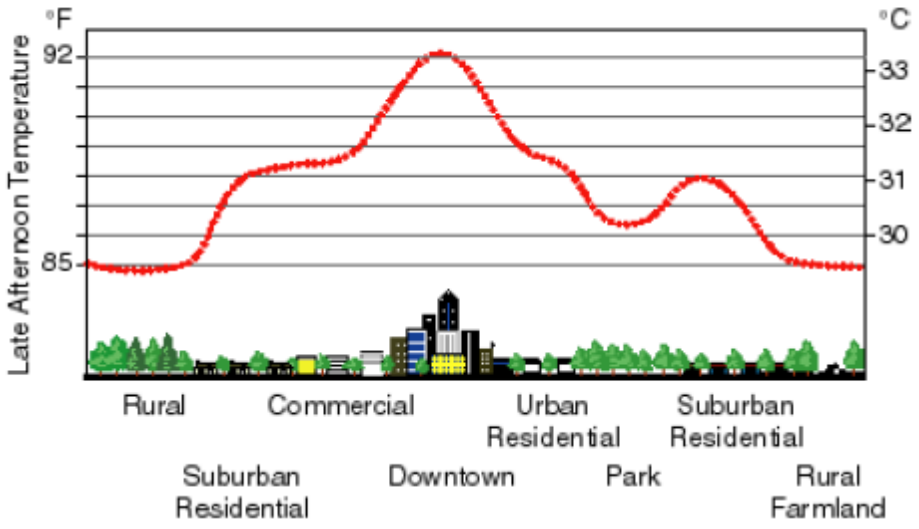

Figure 2.16: Schematic depiction of a heat island shows that air temperature is higher in the city center relative to the surrounding countryside.

When the absorbed heat is returned to the air (through convection), the resultant rise in temperature can be quite burdensome on air quality, natural resources, and ecosystem. For instance, one of the main ingredients of smog is heat. The amount of heat absorbed by a building determines the quantity of energy expended by the building's cooling system. As such, increased absorption results in greater consumption of energy, which requires further energy production and the generation of additional pollutants (Duke Pointer, 2009).

2.4.2 Fundamentals of solar reflectance index (SRI):

The metric associated with the heat island concept is known as Solar Reflectance Index (SRI). Defined by the Cool Roof Rating Council (CRRC), SRI is calculated as "the ratio of the reflected flux to the incident flux". Essentially, it is the ability of a material to reject solar energy. As such, a material's contribution to a heat island decreases with increasing SRI. Relatively high SRI products are referred to as cool materials, such as cool roofs and cool pavements.

Heat islands (and SRI) are often thought to correlate with color of a material, since lighter colors reflect more of the visual spectrum than darker colors. While color may provide a relative estimate of a material's ability to generate a heat island, it is not the only determining factor. Two pieces of information are needed to compute the SRI of a material: solar reflectance and thermal emittance (Duke Pointer, 2009).

2.4.3 Blackbody cavities:

All objects emit infrared radiation characterized by intensity and wavelength, which are both temperature dependent. Most handled low temperature radiation thermometers operate over a single band, typically near 4µm, or in the range 8-14µm; the temperature of an object is found by measuring the intensity of the radiation emitted by the object.

Emissivity and reflectivity are complementary properties. Surfaces with a low emissivity are good reflectors of radiation, and vice versa. For opaque objects (non-transparent), the emissivity plus the reflectivity equals 1.0. An object with an emissivity of 0.9 has a reflectivity of 0.1, and therefore reflects 0.1 (10%) of all of the radiation that falls on the surface.

We can improve the emissivity of objects by making so-called blackbody cavities, as shown in Figure 2.17.The principle is to make sure that any radiation entering the cavity is absorbed; then, since there are no reflections, the emissivity of the cavity must be 1.0. The ideal black body cavity is a perfect emitter and absorber of radiation (M. Bart, 2004).

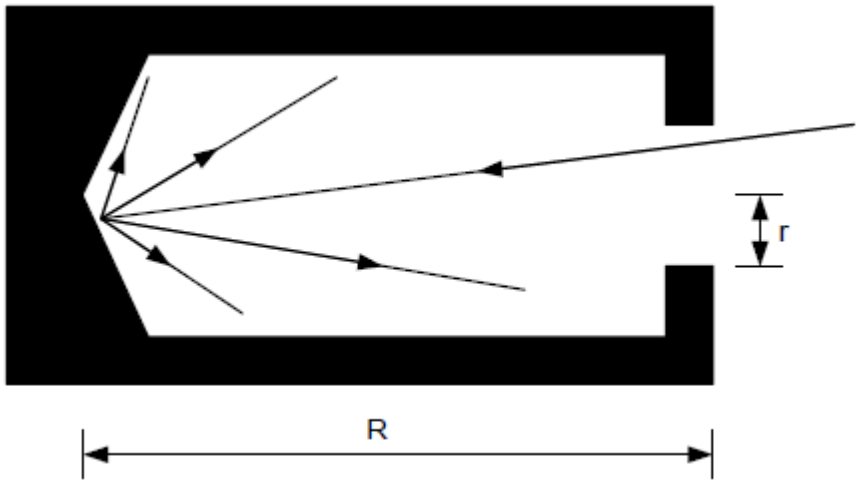

Figure 2.17: A simple representation of a blackbody cavity .The greater the ratio of the cavity size, R, to the aperture, r, the greater the emissivity of the cavity.

2.4.3.1 Design of blackbody cavities

A blackbody cavity is a total emitter for infrared radiation as it is an artificial body and designed for that purpose. If we could assure that the total emitter of infrared radiation is also total absorber for it, according to Kirchhoff's Law which states that for a body in thermal equilibrium then its absorptivity equals its emissivity:

$$A = \varepsilon \qquad (2\text{-}2)$$

If we could proof that an object is a total absorber, we could proof that it is also a total emitter (Anis Malik Al-Rawi, 1992).

Figure 2.20 shows a cross sectional view of an object with a conical opening. If the infrared radiation is allowed to enter the opening several internal reflections will occur before it reflects to the outside of the opening, we could imagine what will happen to that radiation.

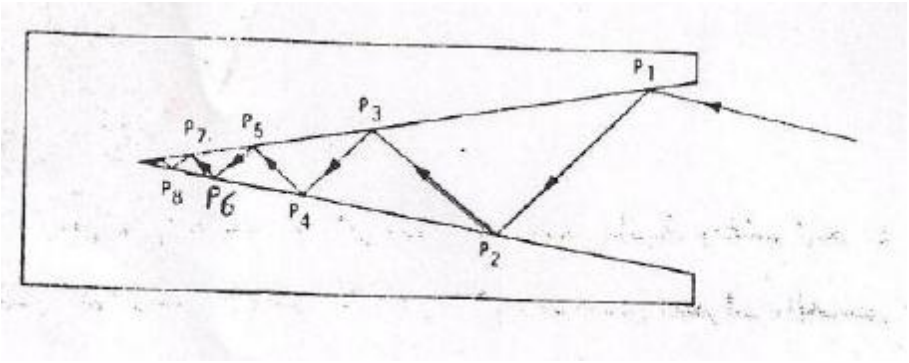

Figure 2.18: Reflection of incident rays in cross sectional view of a cone

For figure 2.18, let us assume that the material of the cavity is opaque having an emissivity of 0.5. Also we can assume that the angle of the conical opening allows the entering radiation to reflect internally ten times. Another assumption to make is that power entering is 100 Watts, then when it strikes point P_1, 50 Watt will be absorbed and 50 will be reflected .In point P_2 50% (25 Watt) will be absorbed and 25 will be reflected. At P_{10}, 99.9 Watt will be absorbed and only 0.0976 Watt will reflect to the outside (Anis Malik Al-Rawi, 1992).

2.5 Literature review:

Lasers have been widely used in micromachining processes for different purposes. In this section some of the work done , using laser micromachining techniques for different purposes are reviewed.

In laser ablation of polymers, a study by Efthimipoulos *et al*, (2000), showed that with weakly absorbing polymers, the incubation period can lead to superheating of the surface by volumetric bubble creation.

The laser used in the study was KrF excimer laser at 248 nm. At this wavelength, PMMA, poly methyl methacrylate, was a known weak absorber, while PET, poly ethyl terephthalate, is a strong absorber and the absorption characteristic PTFE, poly tera fluoroethylene, were unknown.

Several studies however, have revealed that the characteristic rolling structure associated with ablation can be achieved in low absorption index polymers by simply applying a higher radiation dose (Allison Suggs, 2002).

Laser ablation has been shown to produce a characteristic rolling texture effect in a number of polymers including PET, poly(ether ether ketone), polyimide, poly(acrylamide), polyethylene, bisphenol-A polycarbonate/PMMA blends, and poly(butyl terephthalate).

All of these polymers displayed the same repeated rolling surface structure following ablation .Theories behind the source of this rolling structure are varied.

One study assumes that the rolling structure is due to thermal shock waves that are travelling through the surface material due to the immense energy introduced. An example of this type of rolling structure is shown in figure 2.19 below (Allison Suggs, 2002).

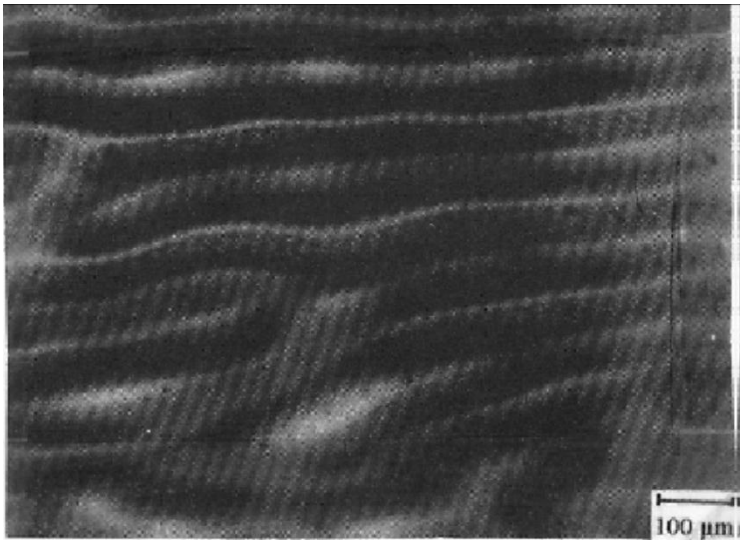

Figure 2.19: Characteristic rolling structure generated on polymeric surface by laser ablation (polarized light micrograph of polypropylene foil irradiated at 193 nm and 0.1 J/cm^2).

In 2002, Klank et al. found that there is a linear relationship between the channel depth and the laser power as well as the number of scanning passes. Beside these two parameters, Nam- Trung *et al.* have investigated the influence of the beam speed on the cross-section geometry. Channel widths and channel depths were measured using SEM system and the obtained the results shown in Figure 2.20 (Nam-Trung nguyen, 2002).

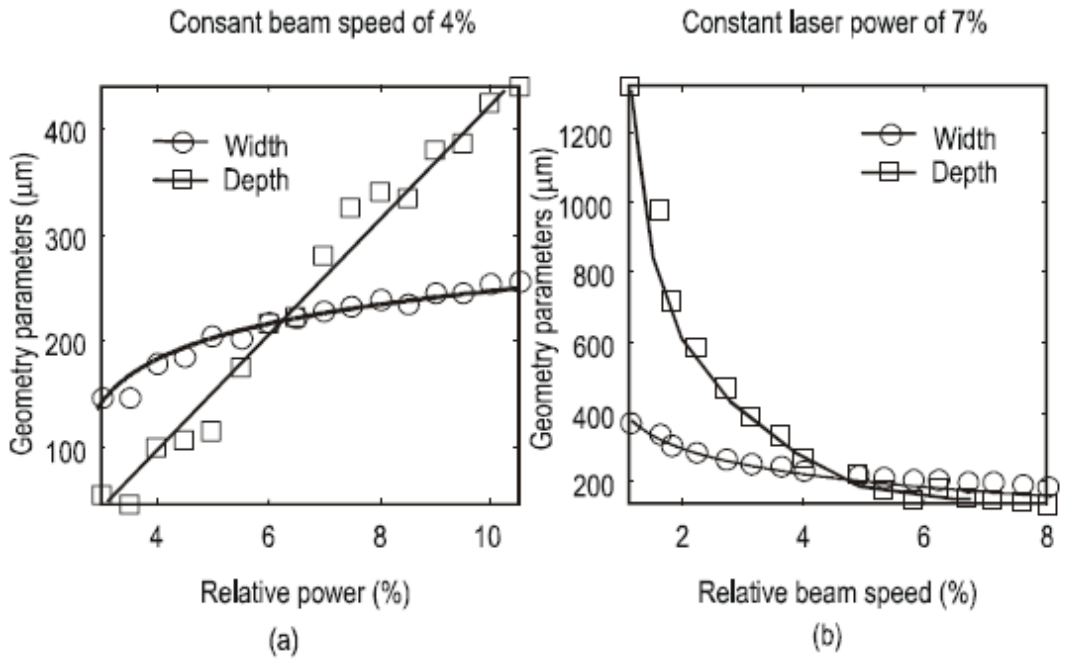

Figure2.20: Influence of laser power (a) and beam speed (b) on geometric parameters. The relative values are based on maximum laser power of 25W and a maximum beam speed of 640mm/s.

Other study done by Daniel Day and min Gu, concluded that when using femtosecond pulses with energy of 0.9 nJ per pulse and a 80MHz repetition rate at a wavelength of 750 nm to fabricate straight micro-channels in a PMMA substrate, the size and shape of the micro-channels can be controlled by changing the fabrication parameters of speed, the number of fabrication repeats and delay in-between fabrication repeats. It has been proposed that the absorption of energy in the focal region modifies the density of the polymer matrix which after annealing the

sample above the glass transition temperature results in formation of the micro-channels. Diffusion of heat through the substrate is a uniform process which has the effect of creating symmetrically shaped channels. This fabrication method is expected to have applications in the fabrication of microstructures or microfluidic devices in polymer substrate (Daniel Day, 2005).

In a work done by Y. Zhang *et al.* in 2002, high aspect ratio holes have been produced using a Gaussian beam with large Numerical Aperture (e.g.0.25) from an ultrafast ,100 fs,800 nm laser. These microstructures are limited to aspect ratios of around 10. When deeper structures are machined, tapering and sometimes bending of the holes can occur. In the case of projection patterning with transparent polymers, highly regular arrays of micro-strings have diameters as small as 2μm and length greater than 10 mm can be formed deep within the bulk of the material. The micro-string arrays may find possible application in high-density optical data storage or waveguide formation in photorefractive polymers. However, the resolution with mask projection is much worse than that with an incoherent homogenized beam from an excimer laser and it appears that the projection patterning may not be a useful method for micromachining with an ultrafast solid-state laser (Y. Zhang *et al.*, 2002).

M. M. Noor *et al.*in a paper for developing the artificial intelligent model for surface roughness, using partial swarm optimization (PSO),have used crystal clear acrylic sheets irradiated by 30 Watt pulsed Nd:YAG laser. They concluded that, the surface roughness is significantly affected by the tip distance followed by the power requirement, cutting speed and material thickness. Surface roughness becomes larger when using low power, tip distance and material thickness. They also concluded that, for the optimized parameters by PSO of cutting speed of 2600 pulse/s, tip

distance of 9.7 mm, 95% of the power and 9mm material thickness produced roughness of 0.0129μm. The error of roughness obtained by optimized roughness model was 0.085%. When using 6mm material thickness, 9.5 mm tip distance, cutting speed of 3000 pulse/s and 95% of the laser power there is melting and burning area. (M. M. Noor *et al*, 2011).

Chapter Three

The Experimental Part

3.1Introduction:

In this chapter the experimental setup is described, which is composed of the x-y work station for workpiece movement, beside the laser system and other accessories. Components and design of the pneumatically operated x-stage is presented in details. The laser was used to make parallel grooves in samples of coloured acrylic sheets using the x-y work station to control the micromachining speed, number of laser passes and the width of each channel. The acrylic sheet samples after micromachining were used to reduce the temperature inside wooden boxes. The wooden boxes and the data loggers, used for measuring the temperature difference, are also described in this chapter.

Experimental procedure and the way of deducing the temperature difference between the micro-machined and the standard samples are also presented in this chapter.

3.2 The samples of Polymethylmethacrylate (PMMA):

The first step in designing the x-y laser micromachining platform is to know the properties of Polymethylmethacrylate (PMMA) in order to calculate the required forces for pulling/pushing the sheet and consequently chose the suitable acting pneumatic cylinder.

Polymethyl methacrylates represent a group of thermoplastic polymers obtained from methyl methacrylate ($C_5H_8O_2$). Commercially it is available in the form of sheets, rods, tubes, powders, granules, solutions, and emulsions. They have a density of 1.2g/cm^3 (0.04lb/in^3), a refractive index of 1.49, high transparency (above 90%), excellent optical

properties, moderate hardness and strength, good resistance to ultraviolet radiation, good dielectric properties, low heat resistance, poor flame resistance, an upper service temperature of 90°C(194°F), low water absorption, good weatherability, good machinability and moldability, good resistance to dilute acids and alkalies, fair resistance to concentrated acids, and poor resistance to aromatic hydrocarbons, greases, oils, halogens and ketones. Often sold under trade names and trademarks, such as *Altuglas, Baycryl, Degulan, Elvacite, Lucite, Lucryl, Perspex, Plexiglas* or *Vedril,* they are used for lenses, optical instruments, transparent enclosures, furniture components, outdoor signs, lighting fixtures, light diffusers, nameplates, decorations, display items, dials, bottles, industrial and architectural glazing, aircraft canopies and windows, windshields for boats, etc., aircraft parts, ornaments, drafting equipment, surgical appliances, and as facing materials for composites. Abbreviation: PMMA (Haral Keller, 2004).

Mass and force calculation are required to design and choose the suitable velocity and the size of the pneumatic double acting cylinder. Table 3.1 lists the forces required for acrylic sheets of different length, width and thickness.

Table3.1: Mass and forces for different sizes of Acrylic sheets.

Length (mm)	**Width (mm)**	**Thickness (mm)**	**Volume (mm^3)**	**Density (g/cm^3)**	**Mass (Gram)**	**Force (N)**
100	100	2	20000	1.2	24	0.23544
150	150	2	45000	1.2	54	0.52974
200	200	2	80000	1.2	96	0.94176
100	100	3	30000	1.2	36	0.35316
150	150	3	67500	1.2	81	0.79461
200	200	3	120000	1.2	144	1.41264
100	100	4	40000	1.2	48	0.47088

150	150	4	90000	1.2	108	1.05948
200	200	4	160000	1.2	192	1.88352
100	100	5	50000	1.2	60	0.5886
150	150	5	112500	1.2	135	1.32435
200	200	5	200000	1.2	240	2.3544
100	100	6	60000	1.2	72	0.70632
150	150	6	13500	1.2	162	1.58922
200	200	6	24000	1.2	288	2.82528
100	100	7	70000	1.2	84	0.82404
150	150	7	157500	1.2	189	1.85409
200	200	7	280000	1.2	336	3.29616
100	100	8	80000	1.2	96	0.94176
150	150	8	180000	1.2	216	2.11896
200	200	8	320000	1.2	384	3.76704
100	100	9	90000	1.2	108	1.05948
150	150	9	202500	1.2	243	2.38383
200	200	9	360000	1.2	432	4.23792
100	100	10	100000	1.2	120	1.1772
150	150	10	225000	1.2	270	2.6487
200	200	10	400000	1.2	480	4.7088

Acrylic sheets of 2 millimeters thickness, with different colours; red, green, blue, black and white were used in this study, in sizes of 100 x 100 millimeters.

3.3Tinytag data loggers:

3.3.1 Loggers description:

Data loggers are electronic temperature measuring units capable of measuring temperature in the range of -40 to +70°C with accuracy of 0.001°C, see Figure 3.1.They can be programmed using either Centigrade or Fehranhite temperature recording. The time interval between every two readings can be programmed together with the required number of readings be recorded. The recorded temperature can be get either in the form of individual temperature measures, graphical representation, and

summary of the readings including the maximum, minimum, average temperature together with the mean kinetic temperature.

The loggers were used in this work to measure the ambient temperature, out of a wooden box, the temperature inside an open-top box, the temperature inside a box with its top closed by un-machined standard acrylic sheet and the temperature inside a box with its top closed with micro-machined sheets. The recorded temperature will tell how much temperature reduction is happened by micromachining the sheets compared with the standard sheets.

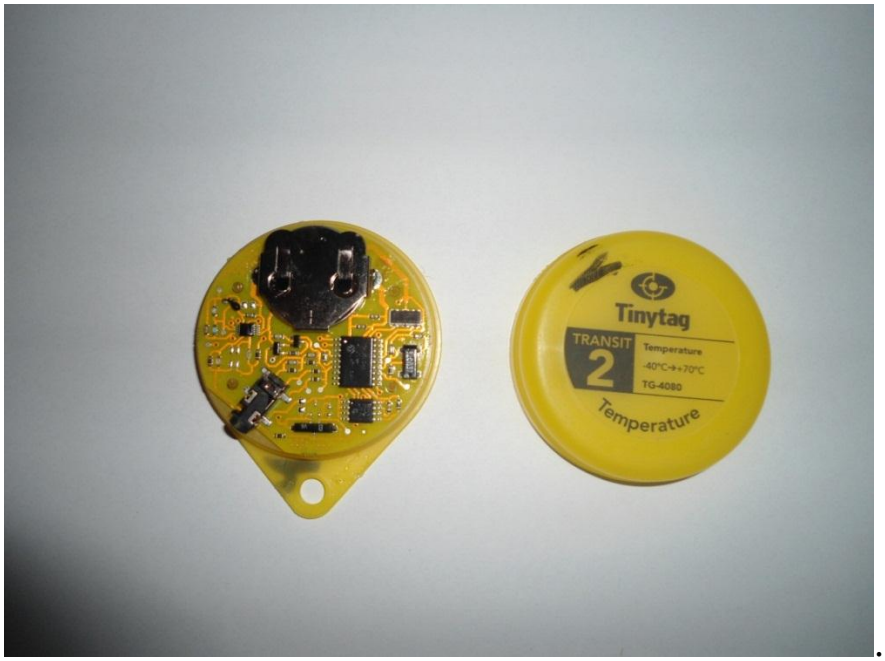

Figure 3.1: Uncovered Logger (left) and the logger's cover (right)

3.3.2. Software requirements:

The data loggers are supported by computer software, which is the application software for all Tinytag data loggers. Installing the software will enable the user to launch the loggers, enter data, reset the data and get data from the computer, either in tables or in graphical form. To run Tinytag Explorer, a personal computer with the specifications shown in table 3.2, or above, is required.

Table 3.2: Personal computer specification requirement for running data loggers (Tinytag Explorer).

	Specification
Operating System	Windows Vista, 7 or8/8.1(x86 & 64 versions
Browser	Internet Explorer version 7 or above, Firefox version 2 or above
Processor	200MHz Pentium III processor or better
Memory	512 Mb
Hard Disk Space	At least 30Mb available hard disk space
Monitor	Minimum 256 colours, resolution 800 x 600

The loggers are supplied with computer software and logger inductive pad for launching, stopping and getting the recorded data out of the loggers, see Figure 3.2.

Figure 3.2 Inductive pad in connection with personal computer

3.3.3 Launching of data loggers:

By getting to the launch menu, several setting tools will appear in the screen, which include description of the process, logging interval, start

options, measurements, step options and the alarm. To enter and set each one the user need to click on the (+) button and choose the required data.

After selecting the required options and launching the logger, temperature can be recorded. To get the required recorded readings one should choose the" get data" tool from the main menu of the loggers. They have the capability of recording temperature using either' minutes' mode or 'seconds' mode. It is also possible when programming the software to schedule the date, starting time, stopping time and time interval between every two recorded readings on the data loggers.

3.4The wooden boxes:

Three wooden boxes were designed and manufactured according to the size of the acrylic sheets. The sheets were inserted into a longitudinal slots engraved alongside every one of the boxes. To measure the temperature inside the box, data loggers were put into these boxes and two of them were covered with the sheets.

Five sides of each box were closed with wooden sheets, see Figure3.3, while the top side of each of them was left unclosed in order to slide the acrylic sheet into the top groove of the box.

Figure 3.3: Wooden Boxes with Loggers inside

3.5 Pneumatic system for the longitudinal x- direction motion:

3.5.1 Background:

The word pneumatics is defined as working and controlling devices using compressed air. Today, pneumatic devices are used more frequently in industry because of their advantages including low cost, ease of maintenance, cleanliness, and low power requirements (Hao Liu, 2007). Due to their high power-to-weight ratio and low cost, pneumatic actuators are attractive for robotics and automation applications
(M. G.Papoutsidakis, 2005).

Fluid, electric and solar powers are some of the energy technologies used for driving modern automated systems.

The technology of 'degree of mechanization' is decided upon the principles of minimization of cost, improved productivity both qualitative

and quantitative, improved accuracy, better safety etc., which again is posed with higher initial investments, higher maintenance costs etc.. Automation is a higher degree mechanization in which human participation is replaced by mechanical, electrical, fluid power technologies capable of doing physical and even mental work as in the case of CNC machines. In some situations automation also demands accurate sensing, recall, memory storage physical efforts or movements requires special sensors for controlling the technological process (M. Muthukarruppan, 2007).

3.5.2 Pneumatic circuit design:

The first requirement in circuit design is a thorough understanding of the symbols to be used. The most important and frequently used symbols are the five port and three port valves. They are also the most frequently misunderstood symbols. The buildup of a typical five port valve is shown in Figure 3.4, in which a double acting cylinder is shown connected to a five port valve .The square envelope represents the valve body and there are three ports on the bottom edge and two on the top edge. A compressed air supply is connected to the centre port 1. Air exhausts to atmosphere at ports 3 and 5.Air outlets to power the cylinder at port 2 and 4. The lines within the envelope show the passages the valve for the current valve state.

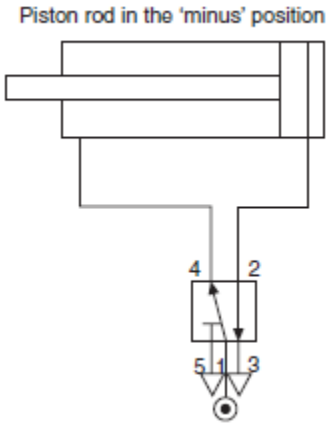

Figure 3.4: Type 3/5-way valve directly connected to a Double Acting Pneumatic Cylider in Minus Position

The air supply 1 is connected to the outlet 4 and outlet 2 is connected to exhaust 3. Exhaust 5 is sealed .This means that the cylinder has air pressure pushing the piston to the in stroke or 'minus' position .The other side of the piston is connected to exhaust. To the cylinder move to the outstroke or 'plus' position the valve has to be operated to change to its new state. This is shown in Figure 3.5. Note that the envelope and the port connections are exactly the same and it is only the connection path inside the valve that has changed (Colin H. Simmons, 2004).

The full symbol of a 5/2 way valve (five ports, two positions) are these two diagrams drawn alongside each other. Only one half will have the ports connected .Which half, will depend on whether the cylinder is to be drawn in the in-stroked or out-stroked state. The method by which the valve is operated, i.e. push button, lever, foot pedal, etc. is shown against the diagram of the state that it produces. Figure3.6 shows a 5/2 way push button operated valve with spring return. It is operating a double acting cylinder. In addition pair of one way flow regulators is included to control the speed of piston rod movement. The symbol for this type of flow regulator consists of a restrictor, an 'arrow' which indicates it is

adjustable and a non- return valve in parallel, to cause restriction in one direction only. The conventional way to control the speed of a cylinder is restrict the exhaust air. This allows full power to be developed on the

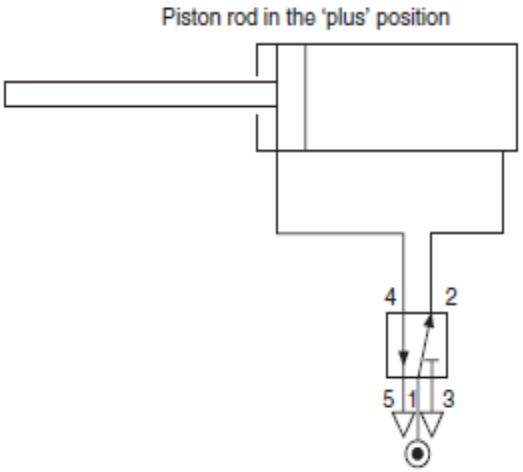

Figure 3.5: Type 3/5-way valve directly connected to a Double Acting Pneumatic Cylider in Plus Position

driving side of the piston which can then work against the back pressure and any load presented to the piston rod (Colin H. Simmons, 2004).

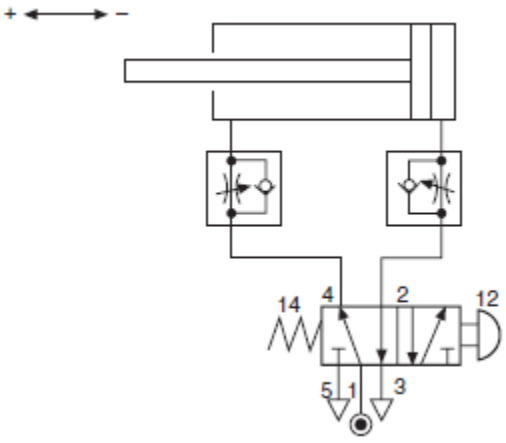

Figure 3.6: Type 5/2 way push button operated valve with spring return, operating a double acting cylinder

3.5.2.1 Logic Functions:

Designers of pneumatic circuits are not usually consciously thinking in pure logic terms, but more likely designing intuitively from experience and knowledge of the result that is to be achieved. Any circuit can be analysed however, to show that it is made up of a combination of logic functions. The four most commonly used are illustrated in Figures 3.7 to 3.9.

The AND Function: The solenoid valve A (AND) the plunger operated valve B must both be operated before an output is given at port 2 of valve B. See Figure 3.7.

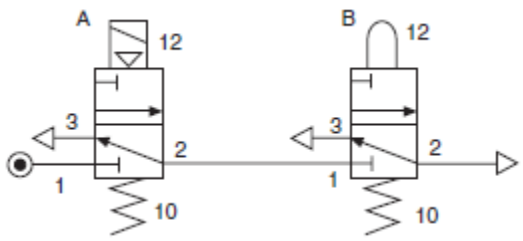

Figure 3.7: "AND" Function

The OR Function: For this a shuttle valve is required so that either of two push-button valves A (OR) B can provide a signal that is directed to the same destination. The shuttle valve contains a sealing element that is blown by an incoming signal to block off the pass back through the other valve's exhaust port. See Figure 3.8, (Colin H. Simmons, 2004).

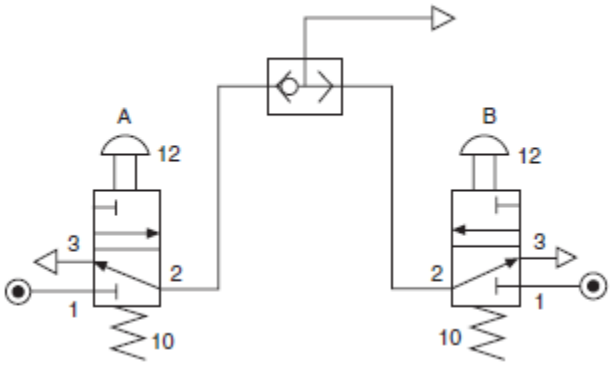

Figure 3.8: "OR" Function

The NOT Function: This is a simply a normally open valve. When it is operated by a pilot signal on port 12, it will NOT give an output. The outlet will be given when the valve re-sets to its normal state by removing the signal. See Figure 3.9.

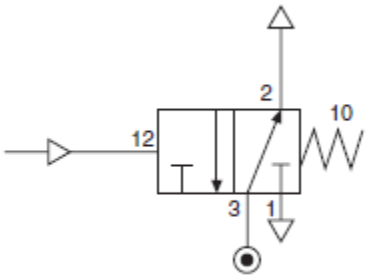

Figure 3.9: "NOT" Function

The TIME DELAY Function: By using a flow regulator and a 3/2 way pilot operated pressure switch, a signal can be slowed down to provide a time delay. Figure 3.10 shows that when a signal is fed through the flow regulator, it will slowly build up pressure in an air reservoir (R) and on the signal port 12 of the pressure switch. This will continue until the pressure is high enough to operate the pressure switch. Then, a strong unrestricted signal will be sent to operate a control valve or other device. The delay can be adjusted by changing the setting on the flow regulator. A reservoir, of approximately 100 cc in volume, would allow a delay

range between 2 to 30 seconds. Without the reservoir, the range will be reduced to approximately 3 seconds maximum (Colin H. Simmons, 2004).

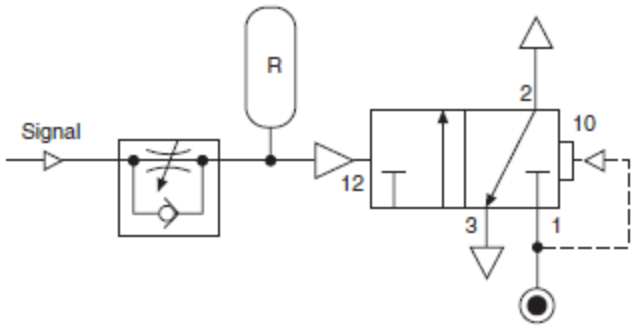

Figure 3.10: "TIME DELAY" Function

3.5.3 Design of the pneumatic x-stage using Fluidsim®:

3.5.3.1 Design characteristic requirements:

The key characteristics of the design in this work are as follows:

1-The work station should be portable to be used with as much laser sources as possible.

2-The laser source is fixed.

3-The work-piece is movable in the longitudinal direction.

4-The pneumatic cylinder should be able to push/pull the acrylic work piece of dimensions 100 x 100 x 2mm.

5- The movement of the pneumatic cylinder, and consequently the work-piece, should be with adjustable and with variable speeds to allow for different laser exposure times.

6-There should be an adjustable delay time between the in-stroke and outstroke of the pneumatic cylinder to allow for the feeding of the lateral-y direction movement of the stepper motor.

7-The pulling force and the pushing force of the pneumatic cylinder should be almost the same.

3.5.3.2 Drawing of Pneumatic Circuit using FluidSIM®:

To meet the above mentioned characteristics, the design of the pneumatic system was first drawn and tested using FluidSIM® 3.5software (FluidSim®, 3.5, 2001).

The final schematic design of the pneumatic circuit is shown in Figure 3.11.

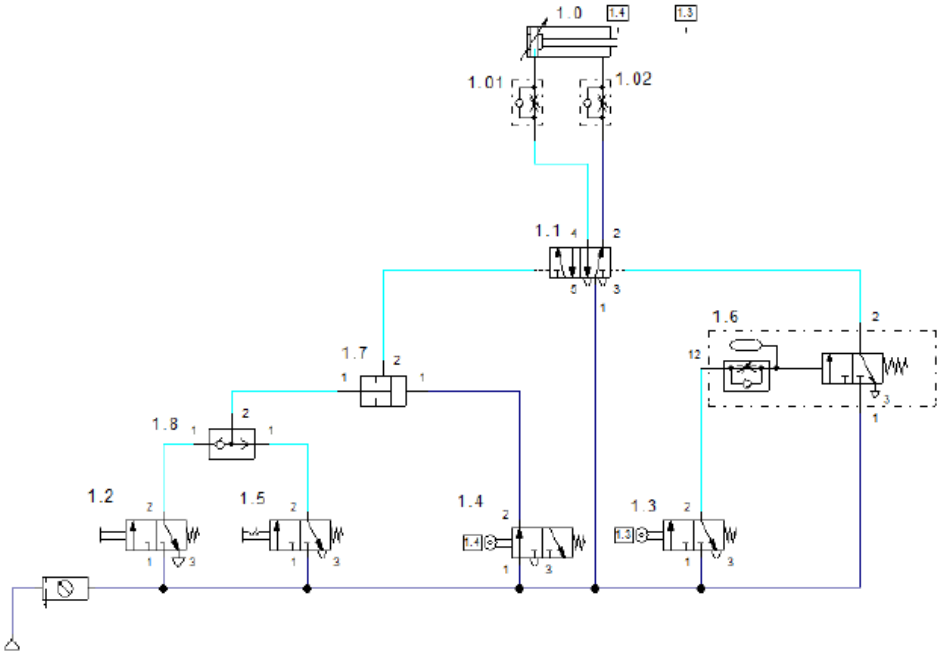

Figure 3.11: Final schematic design of the pneumatic circuit

3.5.4 Description of the system components:

The x-direction work station (or platform) components built in this work, except the air compressor, were manufactured by FESTO, Germany in 2011-2012, composed of the followings:

3.5.4.1 Compressed air supply: The compressed air supply provides the needed compressed air. It contains a pressure control valve that can be adjusted to output the desired operating pressure, see figure 3.12.

Figure 3.12: The Air Compressor used in This Work

3.5.4.2 Air service unit: Is made up of a compressed air filter with water separator and a pressure control valve, see figure 3.13.

Figure 3.13: Air Service Unit Used Here

3.5.4.3 Type 3/2-way valve with pushbutton, normally closed:

Pressing the push button operates the valve. The flow passes freely from 1 to 2. Releasing the pushbutton allows the valve to return to its starting position through the use of a return spring. Connection 1 is shut. See figure 3.14.

Figure 3.14: Type 3/2-way valve with pushbutton, normally closed

3.5.4.4 Type 3/2-way valve with selection switch or striking button:

Press the red striking button operates the valve. The flow passes freely from 1 to2. Releasing the button has no effect; the valve remains in its operating position. Turning the button to the right, sets the striking back to its original position and the valve returns to its starting position through the use of a return spring. Connection 1 is shut (FluidSim®, 3.5, 2001). See Figure 3.15.

Figure 3.15: Type 3/2-way valve with selection switch

3.5.4.5 Shuttle valve: The shuttle valve is switched based on the compressed air entering into either input connection1and leaving output connection 2. Both input connections should be receiving compressed air, the connection with the higher pressure takes precedence and is putout (OR Function). See Figure 3.16.

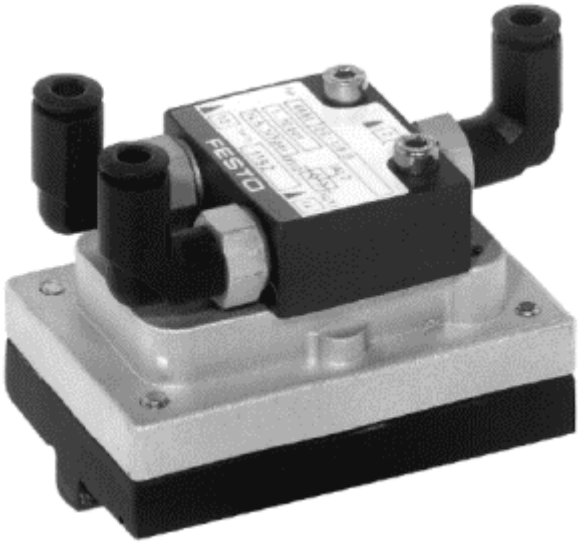

Figure 3.16: Shuttle Valve (OR Function)

3.5.4.6 Two pressure valve: The two pressure valve is switched based on the compressed air entering into both input connection 1 and leaving via

an output connection 2. Both input connections should be receiving compressed air, the connection with the lower pressure takes precedence and is put out (AND Function) (FESTO, Learning Systems, 2012). See Figure 3.17.

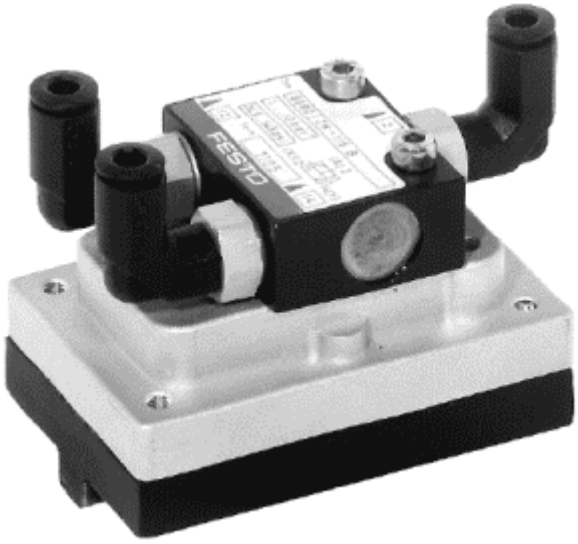

Figure 3.17: Two Pressure Valve (AND Function)

3.5.4.7 Type 3/2-way roller lever valve, normally open: The roller lever valve is operated by pressing on the lever, for example through the use of a switching cam or a cylinder. The flow passes through from 1 to 2.See Figure 3.18.

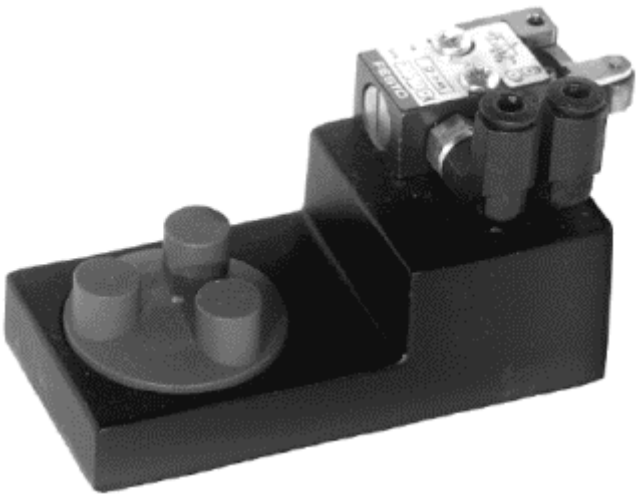

Figure 3.18: Type 3/2-way roller lever valve, normally open

3.5.4.8 Type 3/2-way roller lever valve, normally closed: The roller lever valve is operated by pressing on the lever, for example through the use of a switching cam or a cylinder. The flow passes through from 1 to 2. After releasing the lever, the valve returns to its initial position through the use of a return spring. Connection 1 is shut. See Figure 3.19.

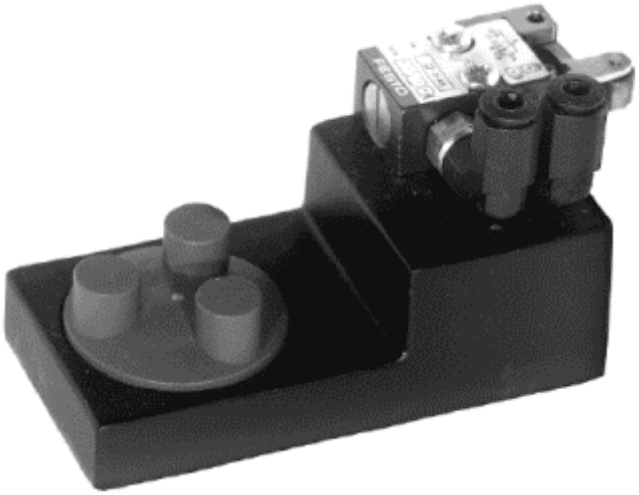

Figure 3.19: Type 3/2-way roller lever valve, normally closed

3.5.4.9 Time delay valve, normally closed: The time delay valve is made up of a pneumatically operated 3/2-way valve, a one-way flow control valve, and small air accumulator. When the necessary pressure is reached at the control connection 12 of the unit, the 3/2-way valve switches and the flow passes freely from 1to 2.See figure 3.20.It is necessary to mention here that this valve in experimental work is replaced by a mechanical time delay one.

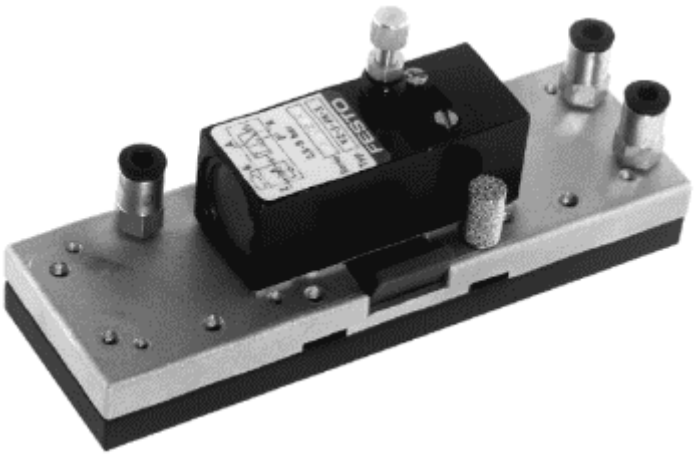

Figure 3.20: Time Delay Valve, Normally Closed

3.5.4.10 5/2-way Impulsive valve, pneumatically operated: The pneumatic valve is controlled by applying reciprocal pilot pressure at connection 14 (flow passes from 1 to 4) and connection 12 (flow passes from 1 to 2). The valve's operating position remains until an opposite signal is received by the valve shut (FluidSim®, 3.5, 2001). See Figure 3.21.

Figure 3.21: Type 5/2-way Impulsive Valve, Pneumatically Operated

3.5.4.11 One-way flow control valve: the one way flow control valve is made up of a throttle valve and a check valve. The check valve stops the flow from passing in a certain direction. The flow then passes through the

throttle valve. The cross-section of the throttle is adjustable via a regular screw. In the opposite direction the flow can pass through the check valve. See figure 3.22.

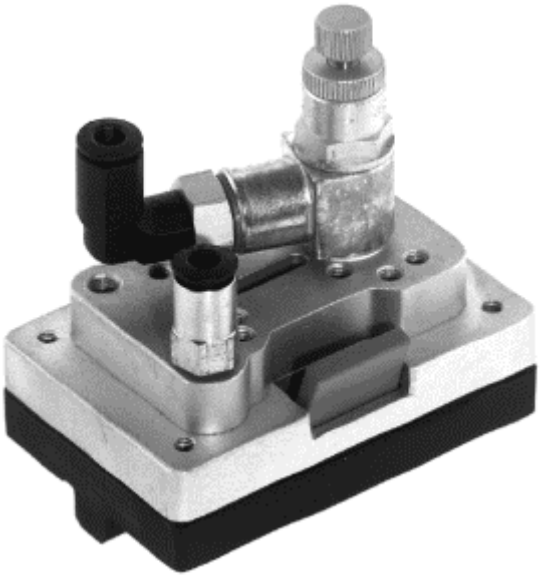

Figure 3.22: One-way Flow Control Valve

3.5.4.12 Double acting cylinder: The piston rod compressed air of a double acting cylinder is operated by the reciprocal input at the front and back of the cylinder. The position damping is adjustable via two regular screws as shown in figure 3.23. The piston of the cylinder contains a permanent solenoid which can be used to operate a proximity switch.

Figure 3.23: Double Acting Cylinder

3.5.4.13 Distance rule: The distance rule is a device for attaching switches at the cylinder. The lables at the distance rule define links to the actual proximity switches or limit switches in electrical the circuit (FluidSim®, 3.5, 2001).

3.5.5 Installing System Components:

To meet the characteristics mentioned above, the system components were chosen from Festo catalogue installed according to their functions (FESTO, Learning Systems, 2012).

These components are shown in Figure 3.24, and listed in Table 3.3.

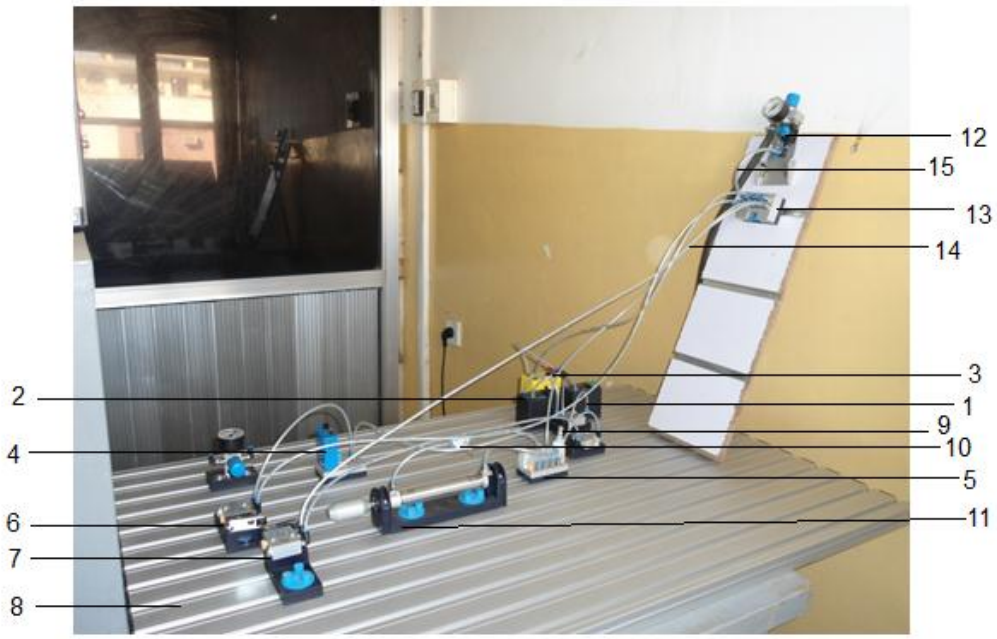

Figure 3.24: Pneumatic System Components Installed

Table 3.3: Description and part numbers of Pneumatic Components

No.	Item Description	Part Number
1	3/2- way valve with pushbutton actuator, normally closed	152860
2	3/2-way valve with selector switch, normally closed	152863
3	3/2-way valve with mushroom-head emergency switch, normally open	152864
4	Pneumatic timer, normally closed	540694

5	5/2-way valve, pneumatically actuated, one side	538694
6	3/2-way roller lever valve, normally closed	152866
7	3/2-way roller lever valve, normally open	162267
8	700 x 1100 mm Aluminium profile plate	159511
9	One way flow control valve	193967
10	One way flow control valve	193967
11	Double acting cylinder	152888
12	Start-up valve with filter control valve	540691
13	Manifold	152896
14	Plastic tubing 4x0.75 silver	151496
15	Plastic tubing 6 x 1silver	152963

3.5.6: System modification:

The system was modified to allow for attachment with the lateral movement stage(y-direction).This was made by drilling a hole in the front centre of the head of the pneumatic cylinder, and internally thread the hole. A threaded shaft was fixed in on and to the cylinder and the other end to the stepper motor y-direction unit.

3.6 The Lateral, y-direction, Motion of the Table:

The lateral motion in our system, was carried out using a stepper motor, made in Japan, to give Lateral steps ranging from 47μm up to 1000μm.The table was controlled using special computer software and electronic circuit, by which the time delay between every two steps and motor speed were adjusted to be synchronized with the time-delay of the pneumatic cylinder in order to achieve the required number of laser passes for engraving the acrylic sheets. The lateral component used in this work is shown in figure 3.25 and listed in table 3.4.

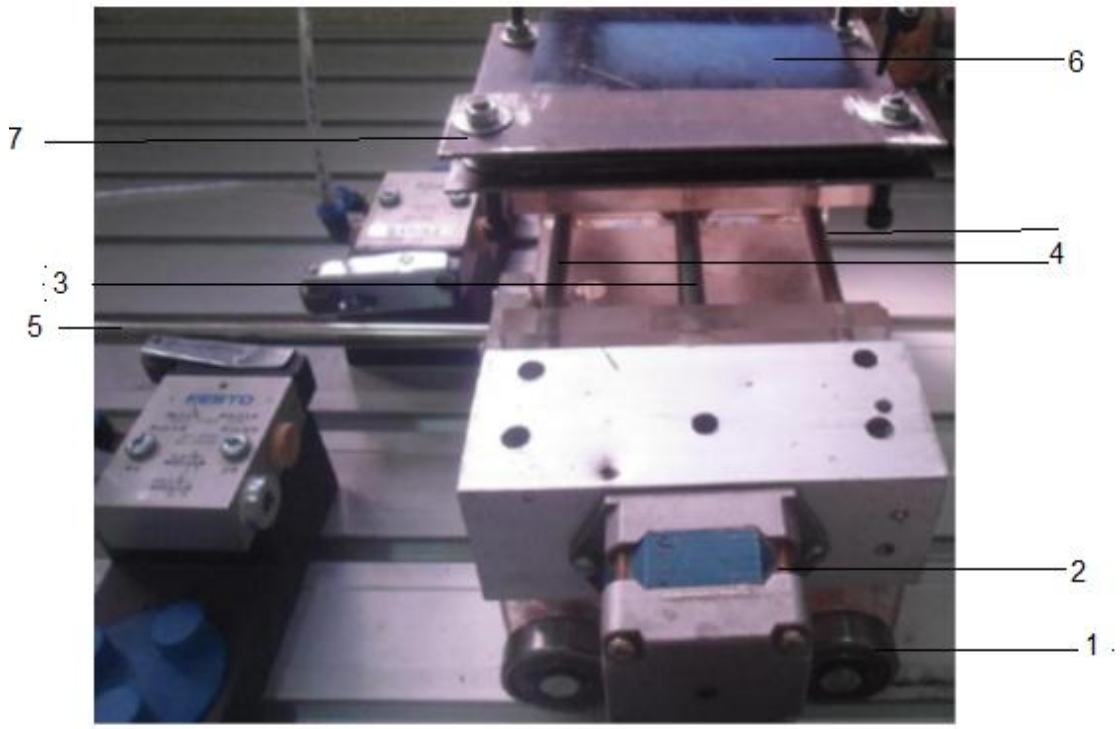

Figure 3.25 Lateral Components of the x-y table

Table 3.4: Description of Lateral Components of the x-y Table

No.	Item Description
1	Sliding Bearings
2	Electrical Stepper Motor
3	Electrically Operated, Movement Transmission Shaft (y-direction)
4	Guide Ways
5	Pneumatically Operated ,Push-Pull Shaft(x-direction)
6	PMMA Workpiece
7	Fixing Plate of PMMA Workpiece

3.7 The laser system:

The Laser system used in this study to micromachining the PMMA samples was 30WCO_2 LASER SURGICAL SYSTEM Model IB-601B (Beijing Innobri Technology,China).

The IB-601B is a CO_2 laser, with a specific wavelength of 10.6 μm, and is the latest microprocessor-controlled instrument based on a sealed-off

CO_2 laser providing up to 30W output power. It is easy and safe to operate.

The laser system is composed of CO_2 laser source, switch, main control panel, cooling system, foot switch and articulated arm. See figures 3.26 and 3.27.

The compound light consists of sealed-off CO_2 laser tube, light intensity detector, diode laser and beam combiner. The beam combiner combines CO_2 laser beam and diode laser beam coaxially and guides them into the articulated arm beam delivery system.

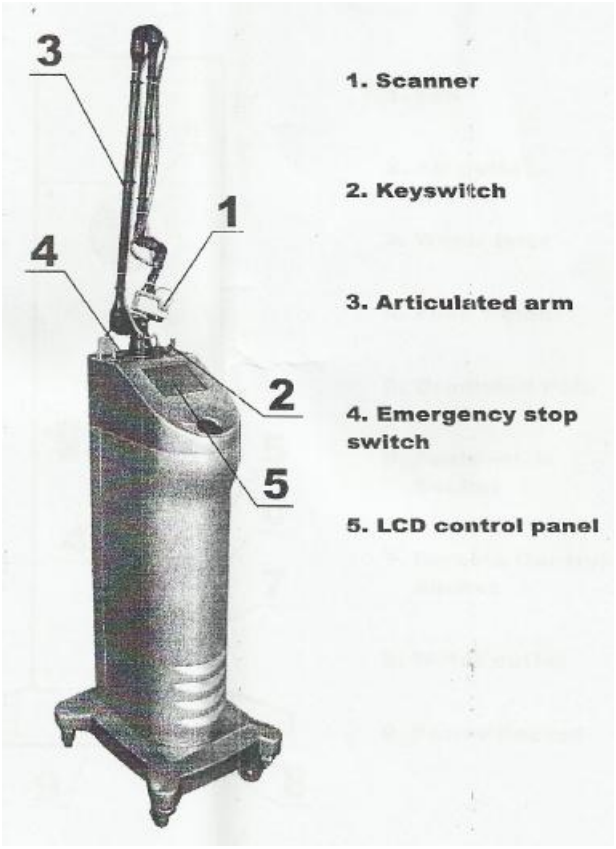

Figure 3.26: Front View of the Laser System

The microprocessor-based main panel is used to control all functions by touching the thin film switch. Time and power are displayed digitally, which is clear and accurate.

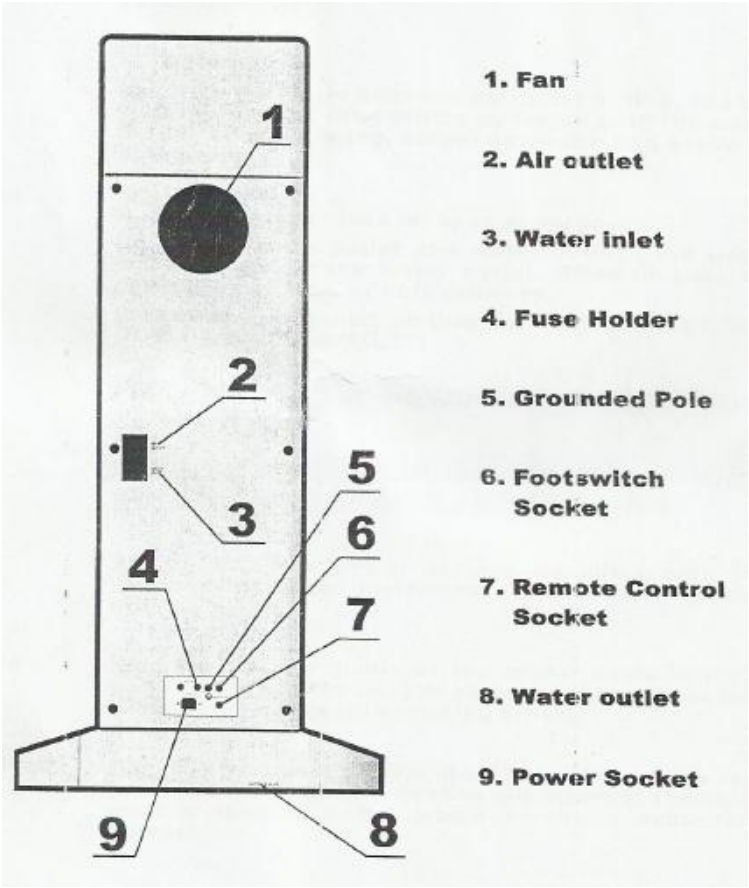

Figure 3.27: Back View of the Laser System

The laser cooling system is a closed circulating loop. The cool (distilled water or ion water) is circulated by a pump.

A foot switch is used to control laser output. When the foot switch is pressed, the shutter opens and laser emits from the articulated arm.

The laser beam delivery system consists of light-weight, spring-balanced, 7-joints articulated arm. The working radius of the articulated arm at full extension is 110 cm (Beijing Innobri Technology).

3.8 Final experimental setup: The final experimental setup is a combination of the previously mentioned systems in synchronization. The overall system is provided with a longitudinal pneumatic system capable of pulling or pushing the table with different velocities. The lateral

system together with the longitudinal system, subjected to laser radiation are capable of apply micromachining process to the 100 x100 x2 mm acrylic sheets. See Figure 2.28.

Figure 2.28 Final Experimental Setup for laser micromachining of PMMA

3.9 Experimental Procedure:

The experimental work was done in the following steps:

1- Acrylic sheets with colours of: red, green, blue, black and white were chosen to represent the RGB model of colours, together with the white to represent additive colouration of the RGB. Black was chosen to represent the addition of the subtractive colouration.
2- Samples were cut to the dimensions of 100 x 100 x 2mm, and coded according to colour, laser power, and number of passes.

Samples and their codes are listed in table 3.5.The code indicates the colour of the sheet, power used, and number of passes, e.g., code number R30W3P, means that the colour is red, power is 30 Watt and passes are 3. Samples marked STD means standard samples without micromachining process, e.g. RSTD means standard red sample.

3- Wooden boxes were designed and fabricated according to the size of acrylic samples. Inside the boxes the data loggers were put to record the solar temperature with four situations, namely the ambient temperature outside the box, the temperature inside an open-top box, inside a box closed with standard un-machined, standard, sheet , and the temperature of the logger inside a box closed with micro-machined acrylic sheet.
4- Number of temperature readings were chosen to be 61 reading, with an interval of 5 minutes to get the total time of 5 hours, from12PM to5PM to represent the peak solar load, for each single test.
5- The parameters used for temperature comparison between the machined and standard samples were chosen to be colour, laser power of 30, 25, 20, and 15 Watt, and the number of laser passes per fixed laser power of 30 Watt to be 1, 2, 3, and 4 passes .The repeated pulse mode of the laser was chosen for the micromachining process.
6- Speed of the pneumatic cylinder was fixed by throttling the throttle valve to give 21% of the maximum speed of the cylinder rod.
7- Time delay between the in-stroke and out-stroke of the double acting cylinder rod was chosen to be 3 seconds.
8- Micro-channels were engraved by moving the x-stage pneumatically to the out-stroke direction with the laser in operation

to ablate the sheet and make the channel. The sheet was placed at a distance of 2mm away from the focal point of the laser due to practical consideration, of not allowing the laser pointer which indicate the focal distance to be broken by the station movement. The focal distance of the laser was 50mm. The laser was stopped in the back- stroke, so ablation is done in one direction.

9- When the laser is in the off-position, the stepper motor moved the workpiece in the y-direction a distance of 1 millimeter, to allow for engraving of the next channel. By synchronization of the motion in the lateral and longitudinal directions, the entire width of the sheet was micro-machined.

10-Micromachined sheet was then placed and fixed to the wooden box through the groove designed for this purpose, and the temperature was measured. The temperature difference was deduced from the reading before and after micromachining.

11-Data from the loggers were graphically presented and summaries were tabulated.

3.5: Codes of PMMA Samples Used in the Experimental Work

Serial Number	Sample Code	Sample Colour	Laser Power (W)	No. of Laser Passes	Idle Time (s)	Duty Time (s)	Energy per Pulse (mJ)
1	RSTD	RED	0	0	0	0	0
2	R30W1P	RED	30	1	0.01	0.99	29700
3	R30W2P	RED	30	2	0.01	0.99	29700
4	R30W3P	RED	30	3	0.01	0.99	29700
5	R30W4P	RED	30	4	0.01	0.99	29700
6	R25W1P	RED	25	1	0.01	0.99	24750
7	R20W1P	RED	20	1	0.01	0.99	19800
8	R15W1P	RED	15	1	0.01	0.99	14850
9	GSTD	GREEN	0	0	0	0	0

10	G30W1P	GREEN	30	1	0.01	0.99	29700
11	G30W2P	GREEN	30	2	0.01	0.99	29700
12	G30W3P	GREEN	30	3	0.01	0.99	29700
13	G30W4P	GREEN	30	4	0.01	0.99	29700
14	G25W1P	GREEN	25	1	0.01	0.99	24750
15	G20W1P	GREEN	20	1	0.01	0.99	19800
16	G15W1P	GREEN	15	1	0.01	0.99	14850
17	BSTD	BLUE	0	0	0	0	0
18	B30W1P	BLUE	30	1	0.01	0.99	29700
19	B30W2P	BLUE	30	2	0.01	0.99	29700
20	B30W3P	BLUE	30	3	0.01	0.99	29700
21	B30W4P	BLUE	30	4	0.01	0.99	29700
22	B25W1P	BLUE	25	1	0.01	0.99	24750
23	B20W1P	BLUE	20	1	0.01	0.99	19800
24	B15W1P	BLUE	15	1	0.01	0.99	14850
25	WSTD	WHITE	0	0	0	0	0
26	W30W1P	WHITE	30	1	0.01	0.99	29700
27	W30W2P	WHITE	30	2	0.01	0.99	29700
28	W30W3P	WHITE	30	3	0.01	0.99	29700
29	W30W4P	WHITE	30	4	0.01	0.99	29700
30	W25W1P	WHITE	25	1	0.01	0.99	24750
31	W20W1P	WHITE	20	1	0.01	0.99	19800
32	W15W1P	WHITE	15	1	0.01	0.99	14850
33	KSTD	BLACK	0	0	0	0	0
34	K30W1P	BLACK	30	1	0.01	0.99	29700
35	K30W2P	BLACK	30	2	0.01	0.99	29700
36	K30W3P	BLACK	30	3	0.01	0.99	29700
37	K30W4P	BLACK	30	4	0.01	0.99	29700
38	K25W1P	BLACK	25	1	0.01	0.99	24750
39	K20W1P	BLACK	20	1	0.01	0.99	19800
40	K15W1P	BLACK	15	1	0.01	0.99	14850

CHAPTER FOUR

Results and Discussion

4.1Introduction:

In this chapter, the results of the temperature difference between micro-machined PMMA sheets, and standard sheets are presented in tables and graphs. The effects of the sheets colour, laser power and number of laser passes are presented also. All these results are discussed and several conclusions are listed in the end of this chapter, in addition to the suggested future work.

4.2The effect of sheets colour on the temperature difference:

To determine the effect of sheets colour on the temperature difference, red, green, blue, black and white samples were irradiated with power of 30 Watts and single pass for each sample.

4.2.1 Temperature difference for red PMMA samples:

Four data loggers were used to record temperature out of the wooden box, inside an open top wooden box without acrylic sample, inside a box covered by a standard red sample, and finally logger inside a wooden box covered by micro-machined red sample. The readings were recorded every 5 minutes of standard and micro-machined samples. Results are shown in figure 4.1.The temperature data for the loggers are shown in Appendix A.

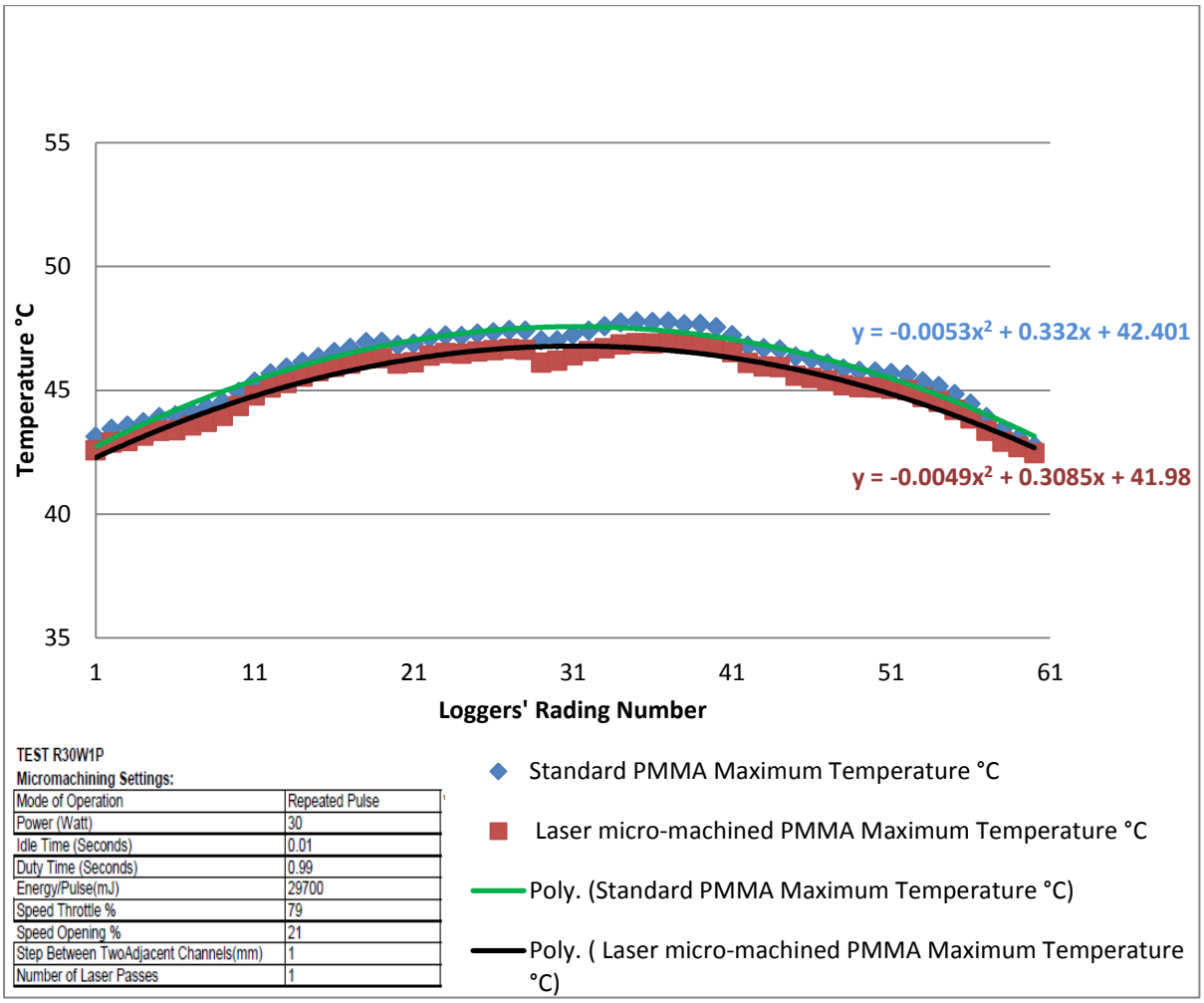

Figure 4.1: Recorded Temperature of Standard and Micro-machined Red PMMA Samples (30W, 1 laser pass)

4.2.2 Temperature difference for green PMMA samples:

To obtain the results of the green PMMA, the four data loggers used for the red samples were used here together with the same wooden boxes. The results are shown in figure 4.2, while the drawn data for the loggers are shown in Appendix B.

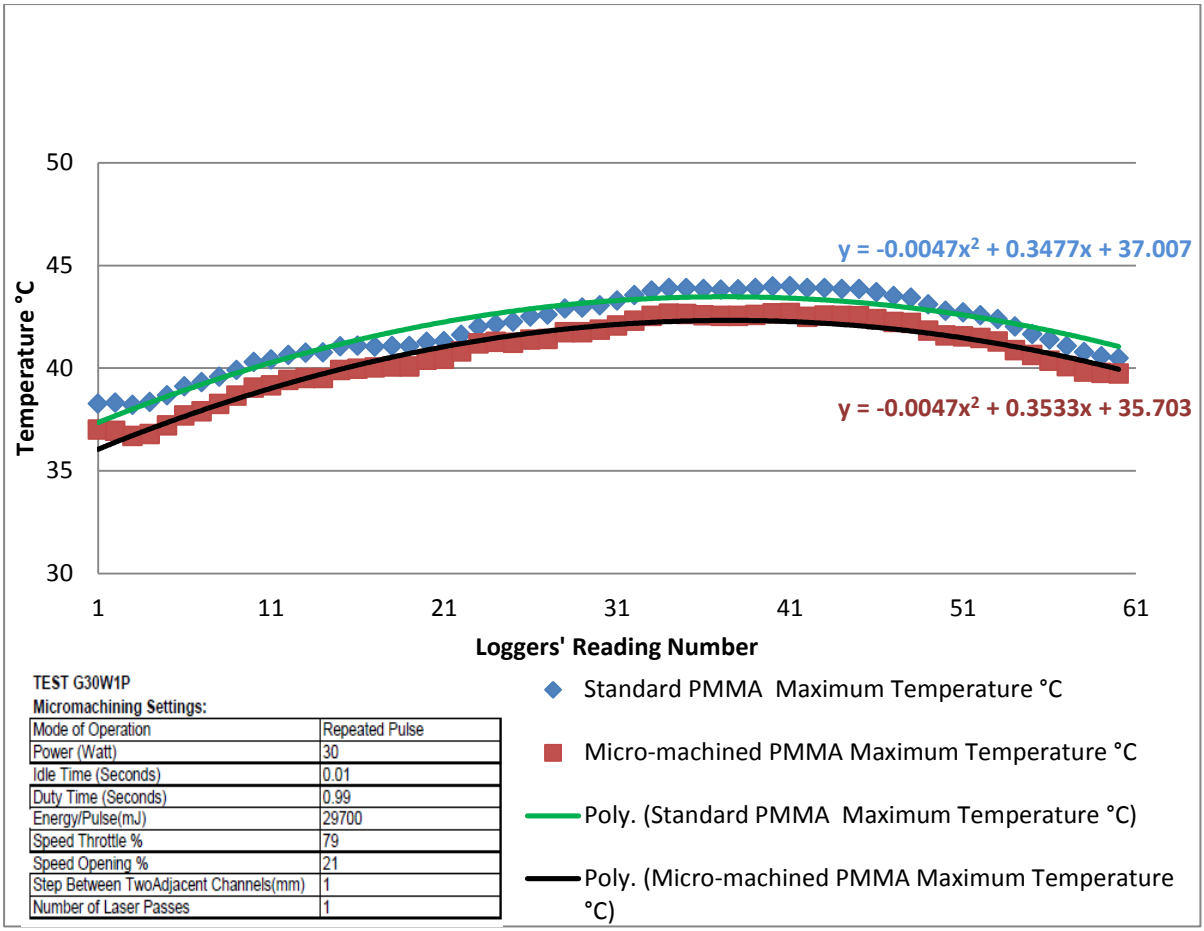

Figure 4.2: Recorded Temperature of Standard and Micro-machined Green PMMA Samples (30W, 1 laser pass)

4.2.3 Temperature difference for blue PMMA samples:

For the blue samples, the same procedure was followed here to determine the difference in temperature between the standard and the micro-machined samples. Results are graphically presented in figure 4.3. The graphical presentation of the recorded data is shown in appendix C.

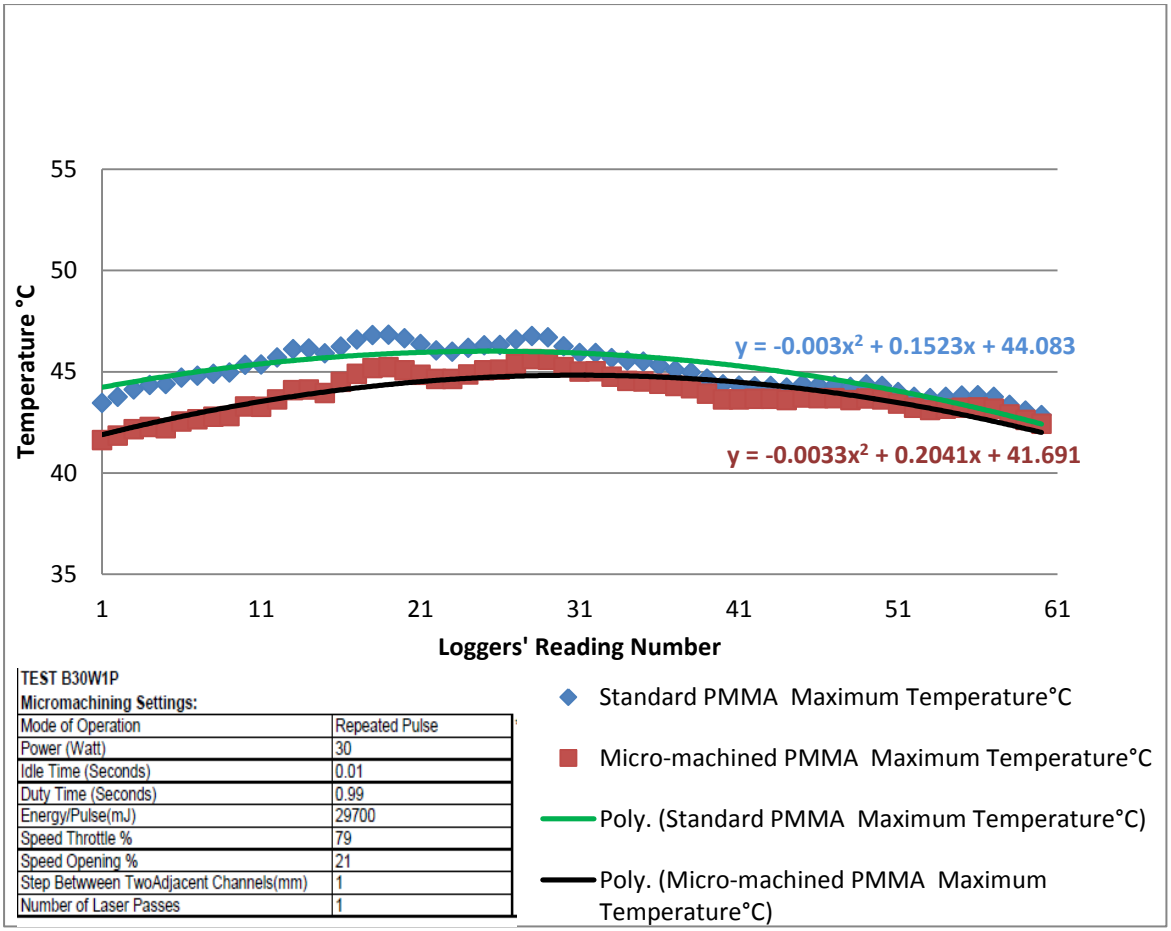

Figure 4.3: Recorded Temperature of Standard and Micro-machined Blue PMMA Samples (30W, 1 laser pass)

4.2.4 Temperature difference for black PMMA samples:

Blue samples showed certain behavior for temperature difference between the standard and micro-machined acrylic samples, following the same experimental procedure for the previous samples. Results are presented in figure 4.4, and the graphical presentation of the recorded data is depicted in appendix D.

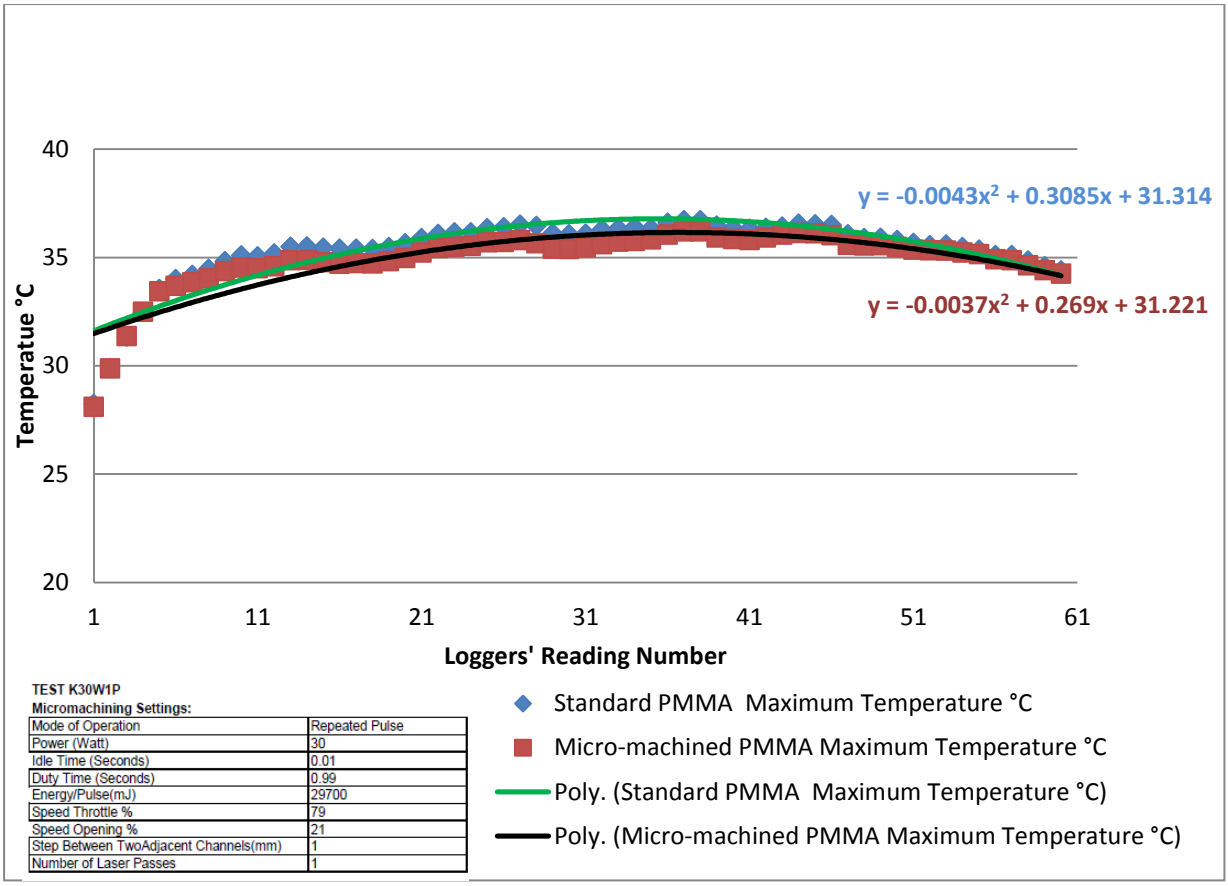

Figure 4.4: Recorded Temperature of Standard and Micro-machined Black PMMA Samples (30W, 1 laser pass)

4.2.5 Temperature difference for white PMMA samples:

Plotted results for temperature difference between the standard and micro-machined white acrylic samples, following the same experimental procedure as the previous samples, are presented in figure 4.5, and the graphs of the recorded data is shown in appendix E.

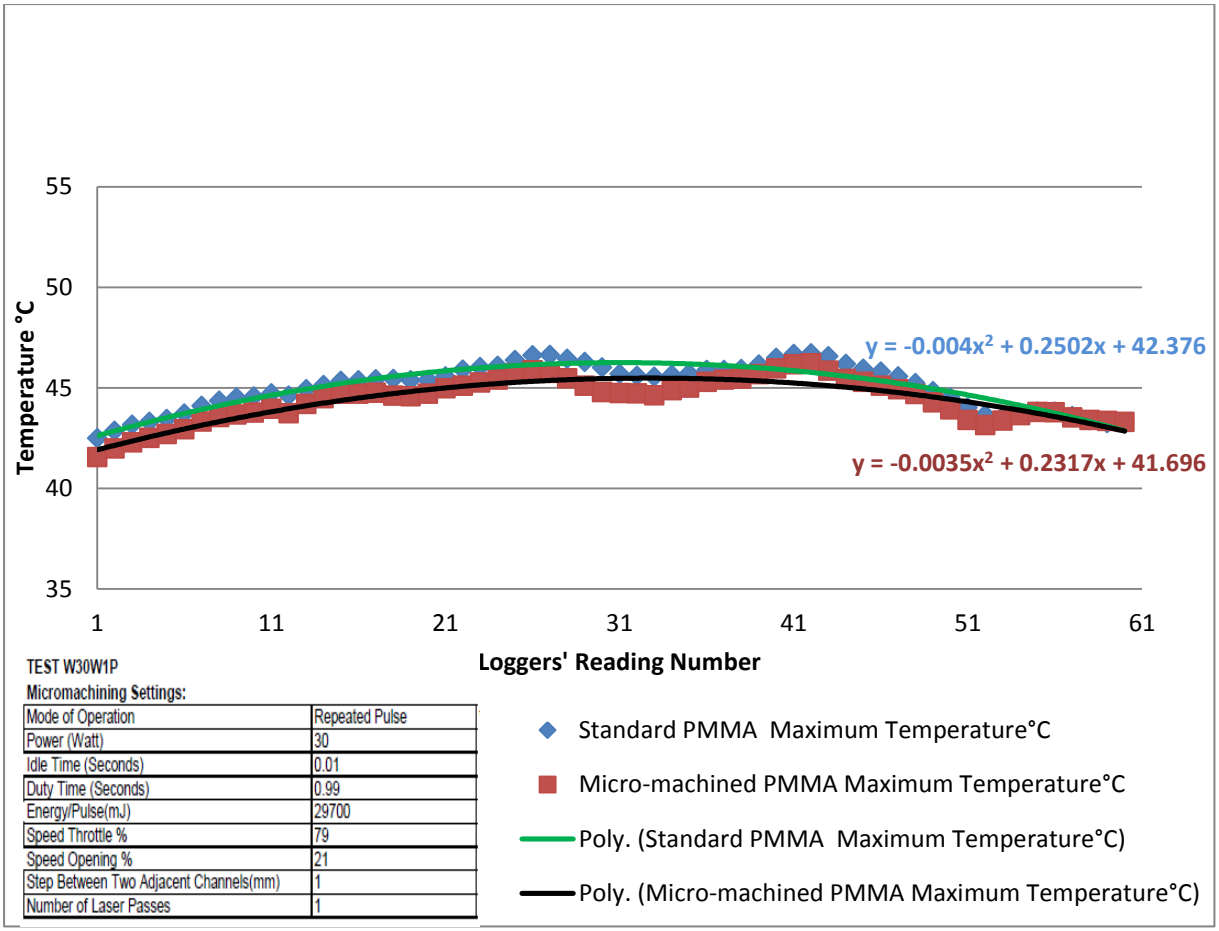

Figure 4.5: Recorded Temperature of Standard and Micro-machined White PMMA Samples (30W, 1 laser pass)

4.2.6 Comparison between the average temperature difference, ΔT, for RGBKW PMMA samples irradiated by 30 Watts and 1 laser pass:

Comparison between the average temperature differences in °C for the recorded 61 reading for each of the different colours of red, green, blue, black, and white PMMA sheets are listed in table 4.1.

Table 4.1: Average Temperature Difference for Different Colours

Colour	**Average $\Delta T, ^\circ C$**
Red	0.7
Green	1.2
Blue	1.2
Black	0.5
White	0.6

4.3 The effect of laser power on the temperature difference:

To investigate the effect of laser power on temperature difference between the micro-machined sheets and the standard sheets, laser micromachining experiments were carried out for different sheets of the same RGBKW model, using different laser powers of 25, 20, and 15 watts. The results are as follows:

4.3.1 ΔT for red PMMA samples:

4.3.1.1 ΔT for red PMMA samples irradiated by 25 Watts and 1 laser pass:

Red sample was laser micro-machined using 25Watt laser power and one laser pass for engraving the channels, the results are graphically presented in figure 4.6.

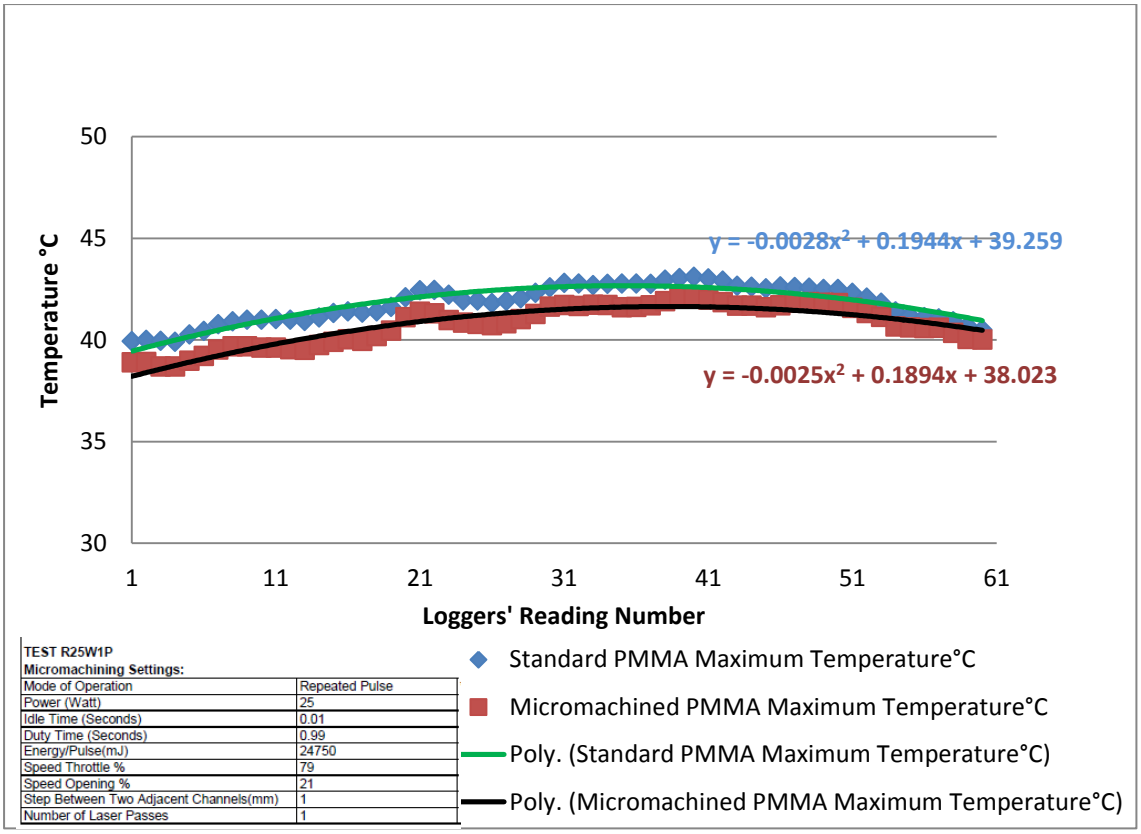

Figure 4.6: Recorded Temperature of Standard and Micro-machined Red PMMA Samples Irradiated by 25Watt and 1Laser Pass

4.3.1.2 ΔT for red PMMA samples irradiated by 20 watts and 1 laser pass: 20Watts of laser power and one laser pass were used to engrave the channels on the red sample, temperature of the standard and micro-machined samples are shown in figure 4.7.

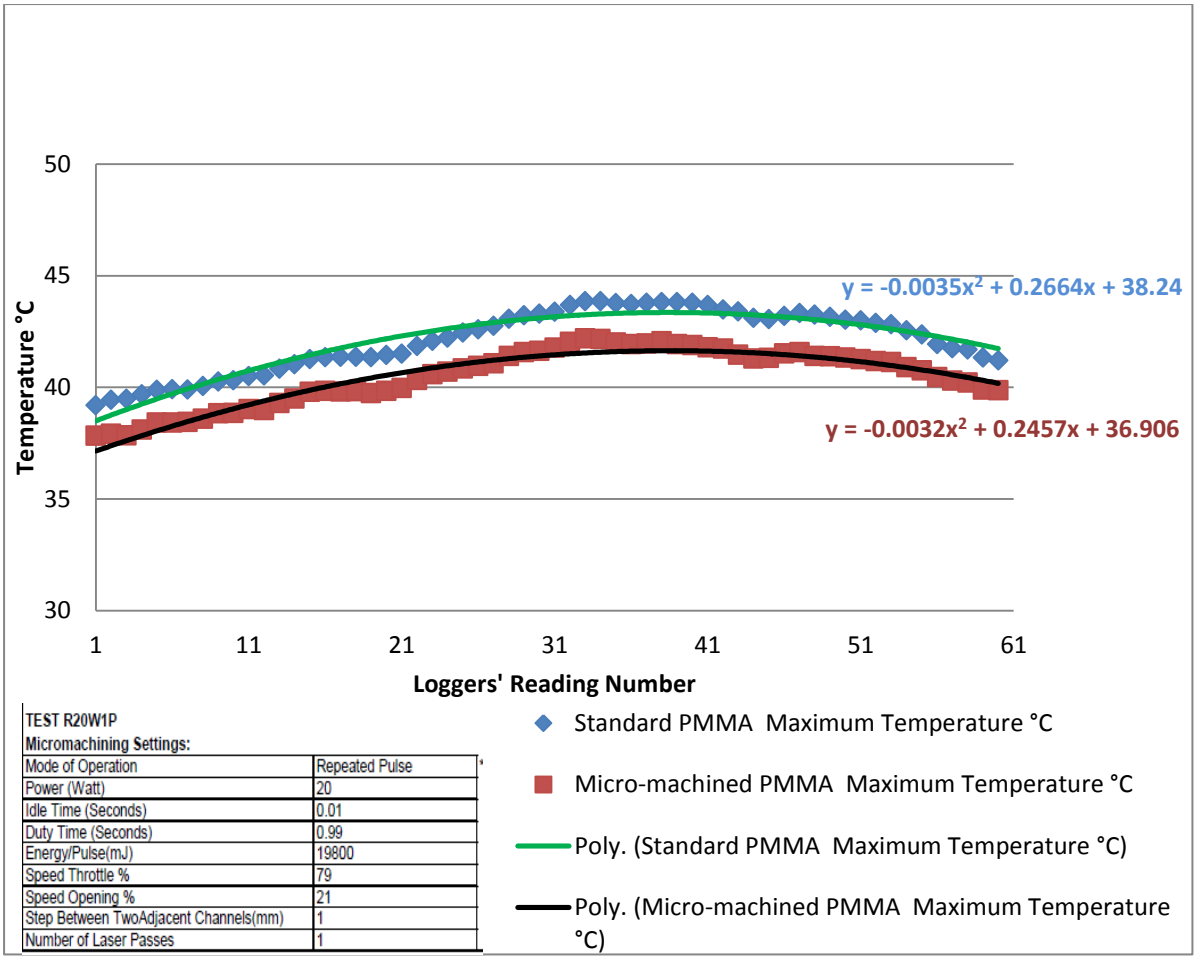

Figure 4.7: Recorded Temperature of Standard and Micro-machined Red PMMA Samples Irradiated by 20Watt and 1Laser Pass

4.3.1.3 ΔT for red PMMA samples irradiated by 15 Watts and 1 laser pass:

Using 15Watts of laser power and one laser pass for engraving each channel, red sample was laser micro-machined .The results are graphically presented in figure 4.8.

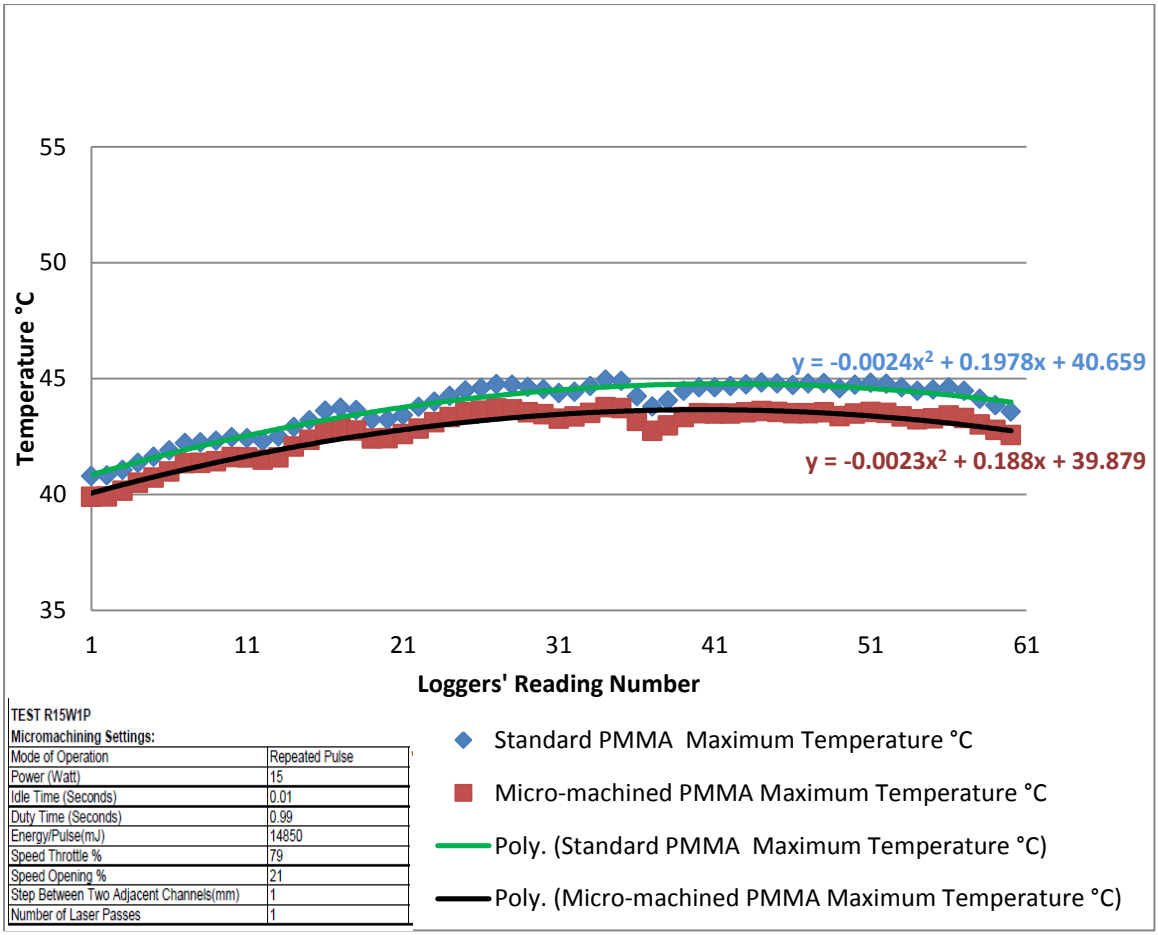

Figure 4.8: Recorded Temperature of Standard and Micro-machined Red PMMA Samples Irradiated by 15 Watt and 1Laser Pass

4.3.1.4 Comparison of temperature difference, ΔT, for red PMMA samples irradiated by 30, 25, 20, 15 Watts and 1 laser pass:

Comparison between temperature differences in degree C for red PMMA samples irradiated by 30,25,20,15 watts and 1 laser pass are graphically represented in figure 4.9.

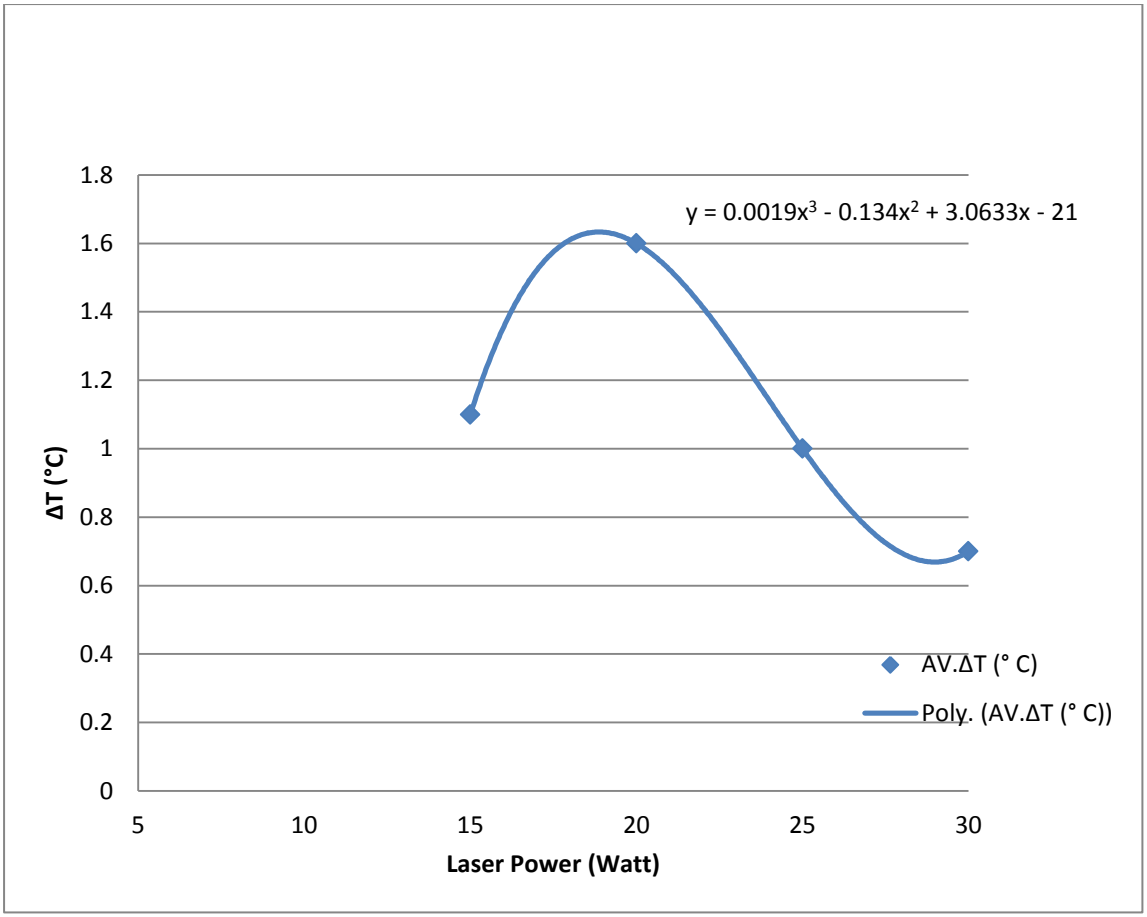

Figure 4.9: The Effect of Varying the Laser Power on the Temperature Difference in Red Samples

4.3.2 ΔT for green PMMA samples:

4.3.2.1 ΔT for green PMMA samples irradiated by 25 Watts and 1 laser pass:

When green sample was laser micro-machined using 25Watt laser power, and one laser pass, for engraving its channels, the following results were obtained and presented graphically in figure 4.10.

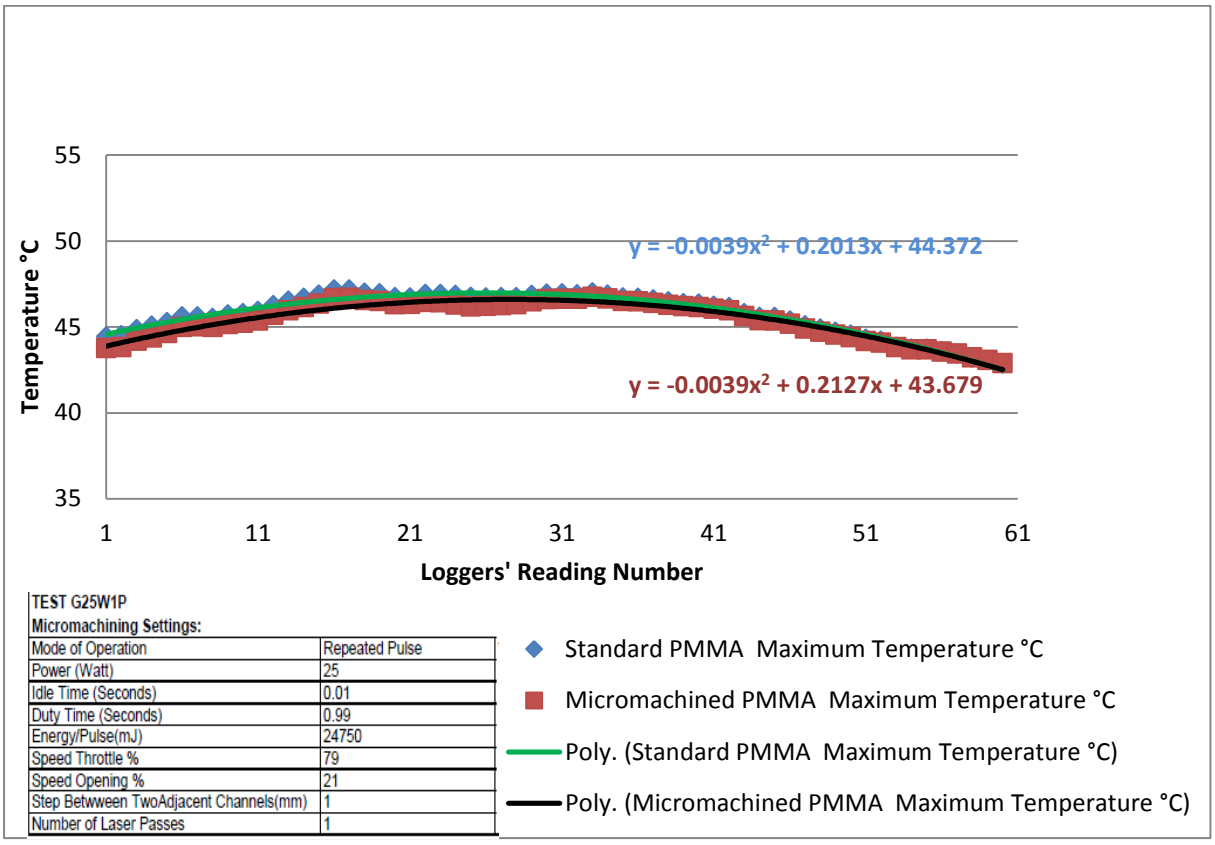

Figure 4.10: Recorded Temperature of Standard and Micro-machined Green PMMA Samples Irradiated by 25 Watt and 1Laser Pass

4.3.2.2 ΔT for green PMMA samples irradiated by 20 Watts and 1 laser pass:

For the green sample to be laser micro-machined, 20 Watt of laser power and 1 laser pass, were used to perform that purpose. The results are graphically presented in figure 4.11.

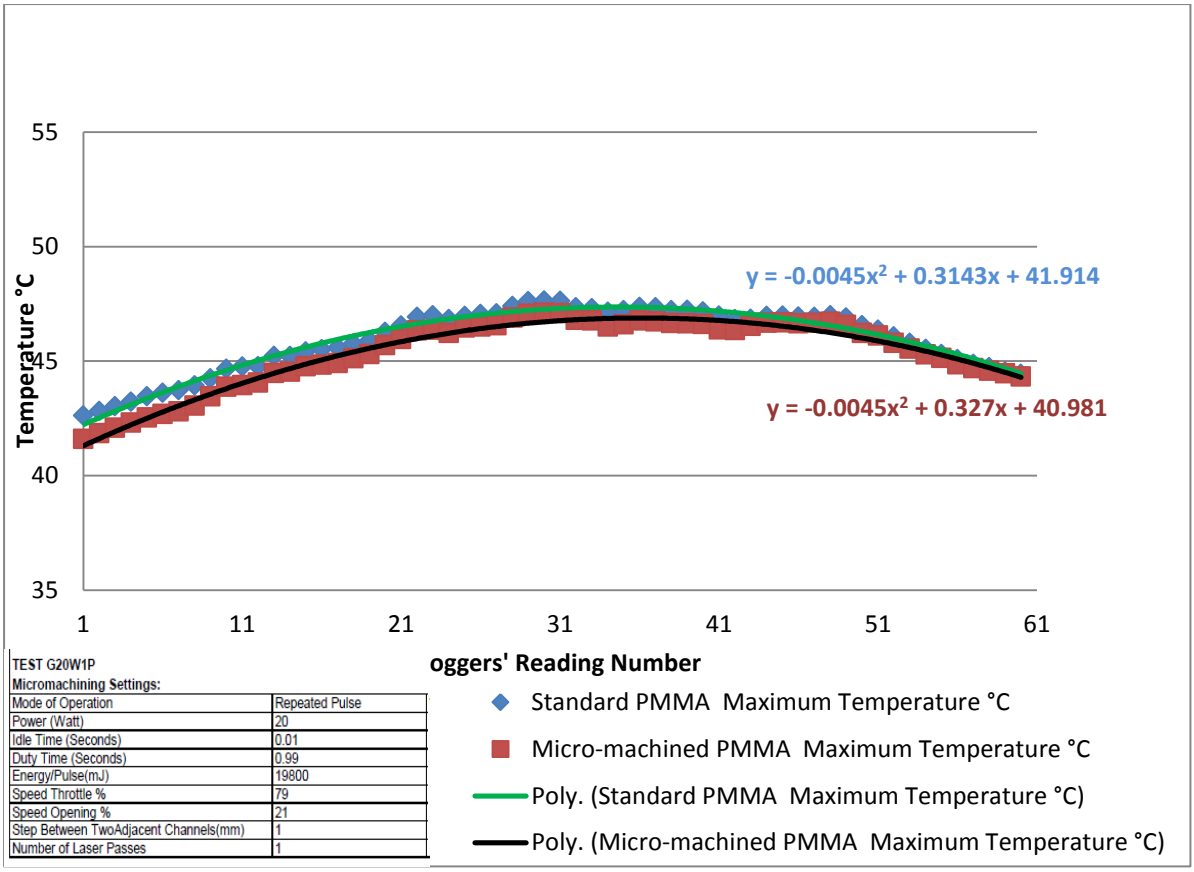

Figure 4.11: Recorded Temperature of Standard and Micro-machined Green PMMA Samples Irradiated by 20 Watt and 1Laser Pass

4.3.2.3 ΔT for green PMMA samples irradiated by 15Watts and 1 laser pass:

Reducing the laser power to 15 Watt, green sample was laser micro-machined using one laser pass for engraving the channels, the results are graphically presented in figure 4.12.

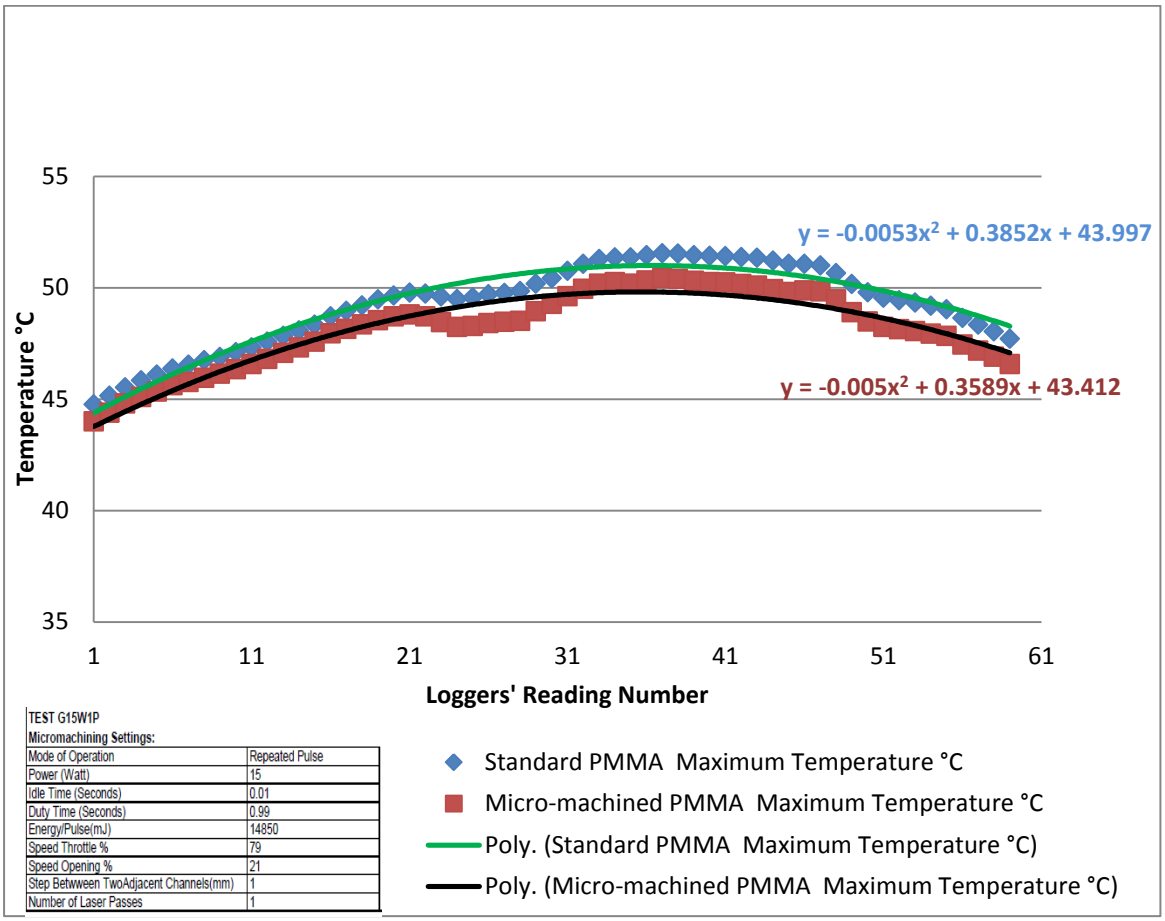

Figure 4.12: Recorded Temperature of Standard and Micro-machined Green PMMA Samples Irradiated by 15 Watt and 1Laser Pass

4.3.2.4 Comparison of temperature difference, ΔT, for green PMMA samples irradiated by 30, 25, 20, 15 Watts and 1 laser pass:

Comparison between temperature differences in degree C, for green PMMA samples irradiated by 30,25,20,15 watts and 1 laser pass are graphically represented in figure 4.13.

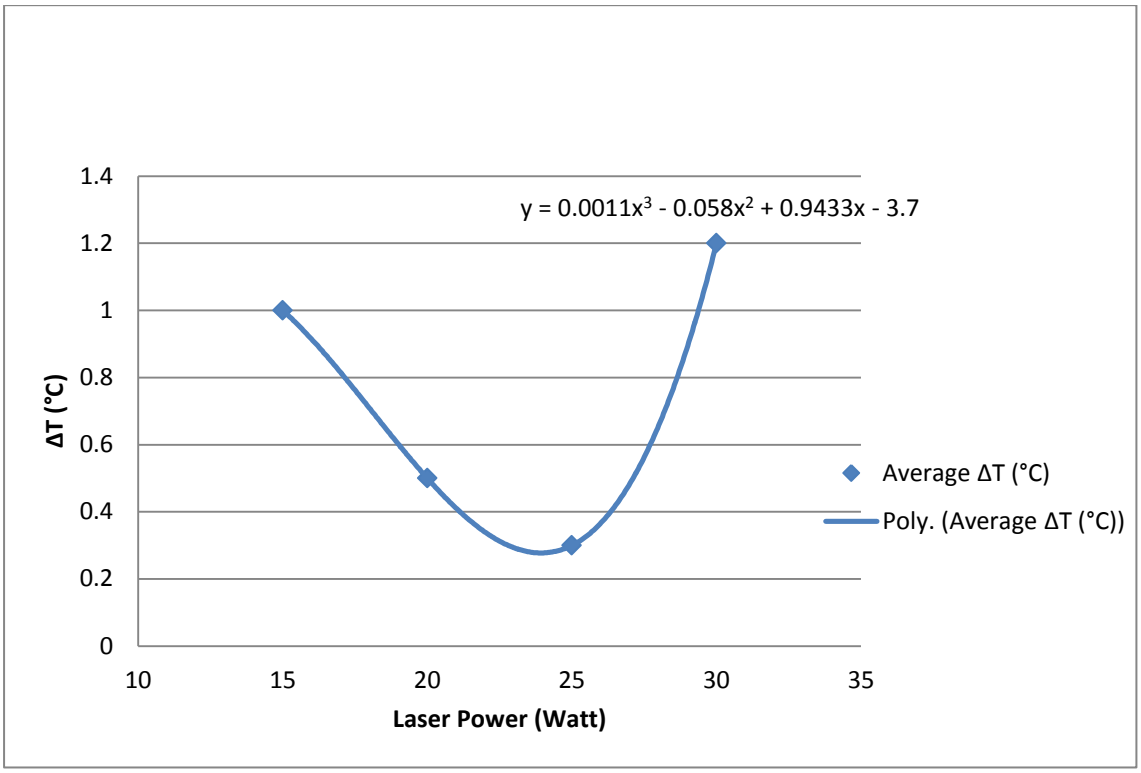

Figure 4.13: ΔT for Green PMMA Samples Irradiated by 30, 25, 20, 15 Watts and 1 Laser pass

4.3.3 ΔT for blue PMMA samples:

4.3.3.1 ΔT for blue PMMA samples irradiated by 25 Watts and 1 laser pass:

laser pass: Blue sample was laser micro-machined using 25Watt of laser power and one laser pass for engraving each channel, the results are and graphically presented in figure 4.14.

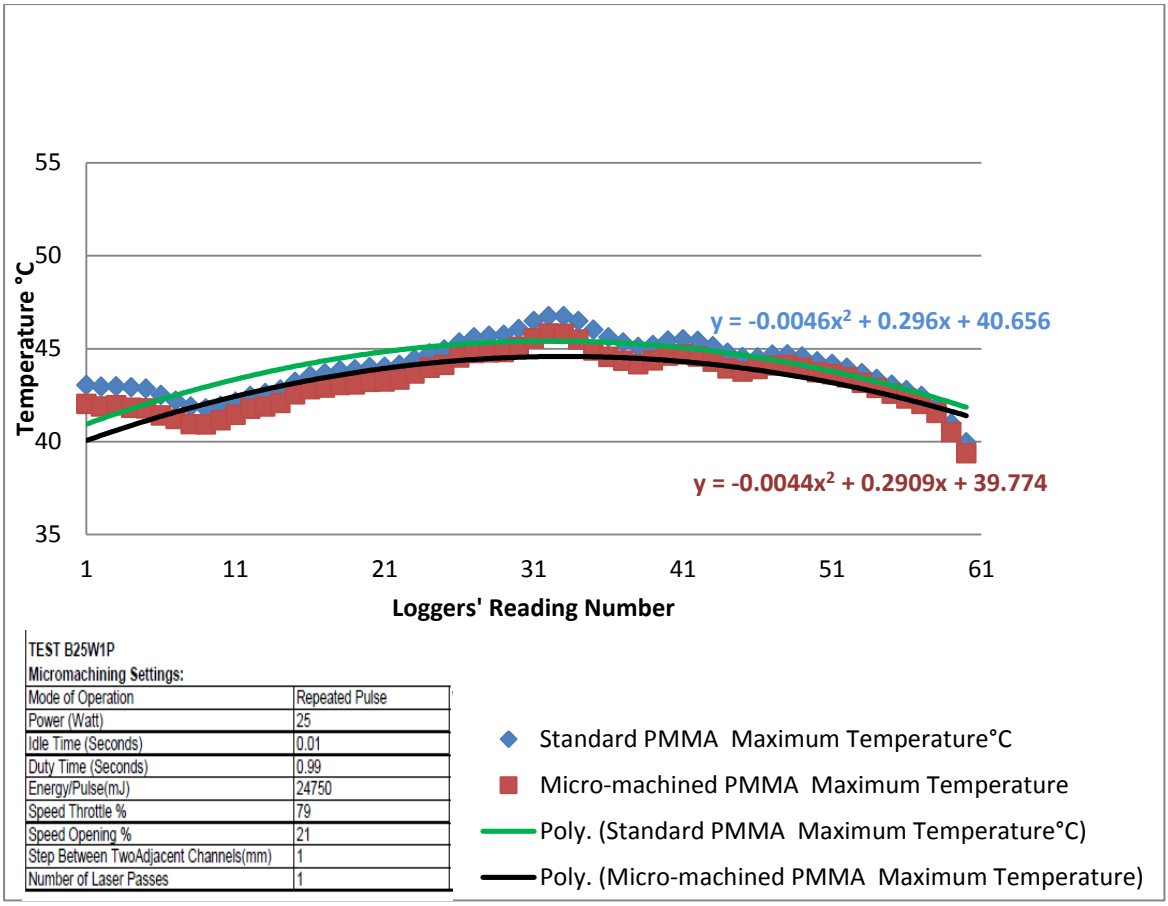

Figure 4.14: Recorded Temperature of Standard and Micro-machined Blue PMMA Samples Irradiated by 25 Watt and 1Laser Pass

4.3.3.2 ΔT for blue PMMA samples irradiated by 20 Watts and 1 laser pass:

Every channel of the blue sample was laser micro-machined using 20 Watt of laser power and one laser pass. The results are graphically shown in figure 4.15.

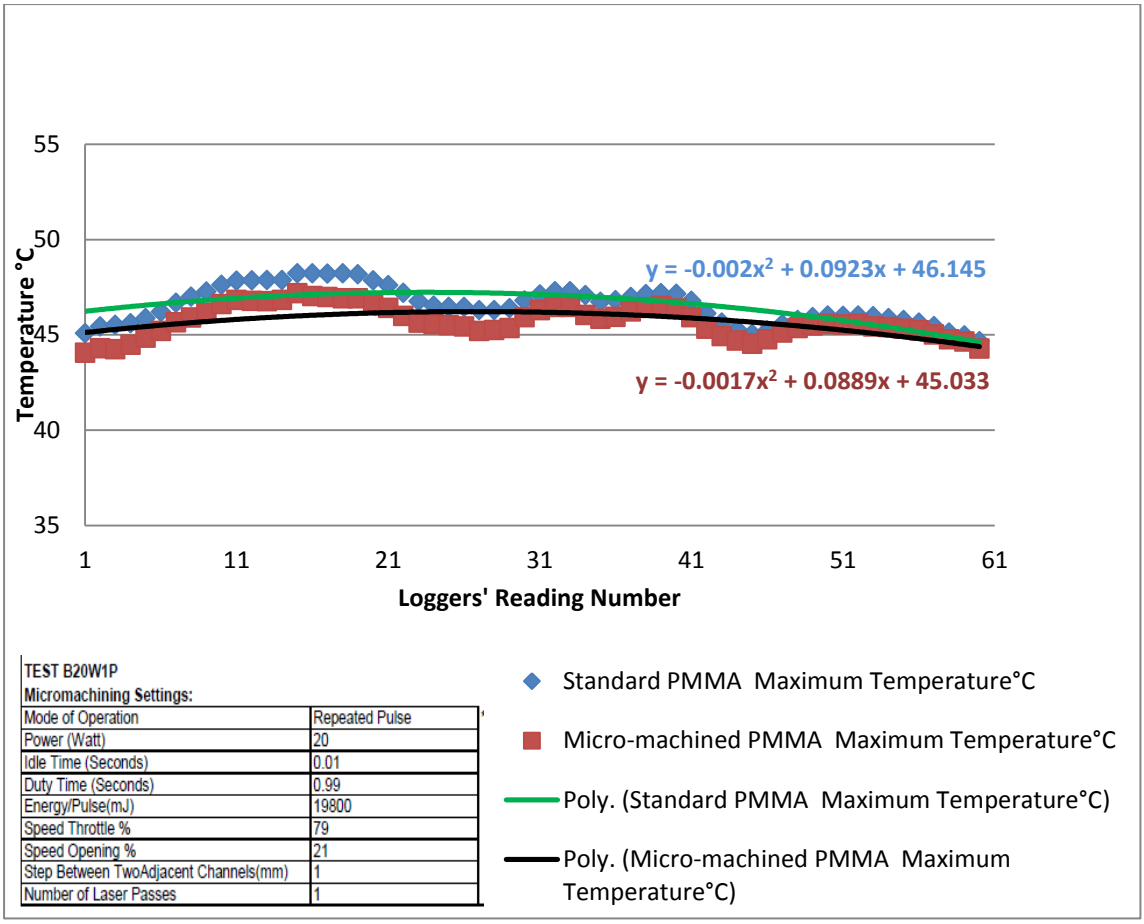

Figure 4.15: Recorded Temperature of Standard and Micro-machined Blue PMMA Samples Irradiated by 20 Watt and 1Laser Pass

4.3.3.3 ΔT for blue PMMA samples irradiated by 15 Watts and 1 laser pass: Blue sample was laser micro-machined using 15Watt laser power and 1 laser pass, the results are graphically presented in figure 4.16.

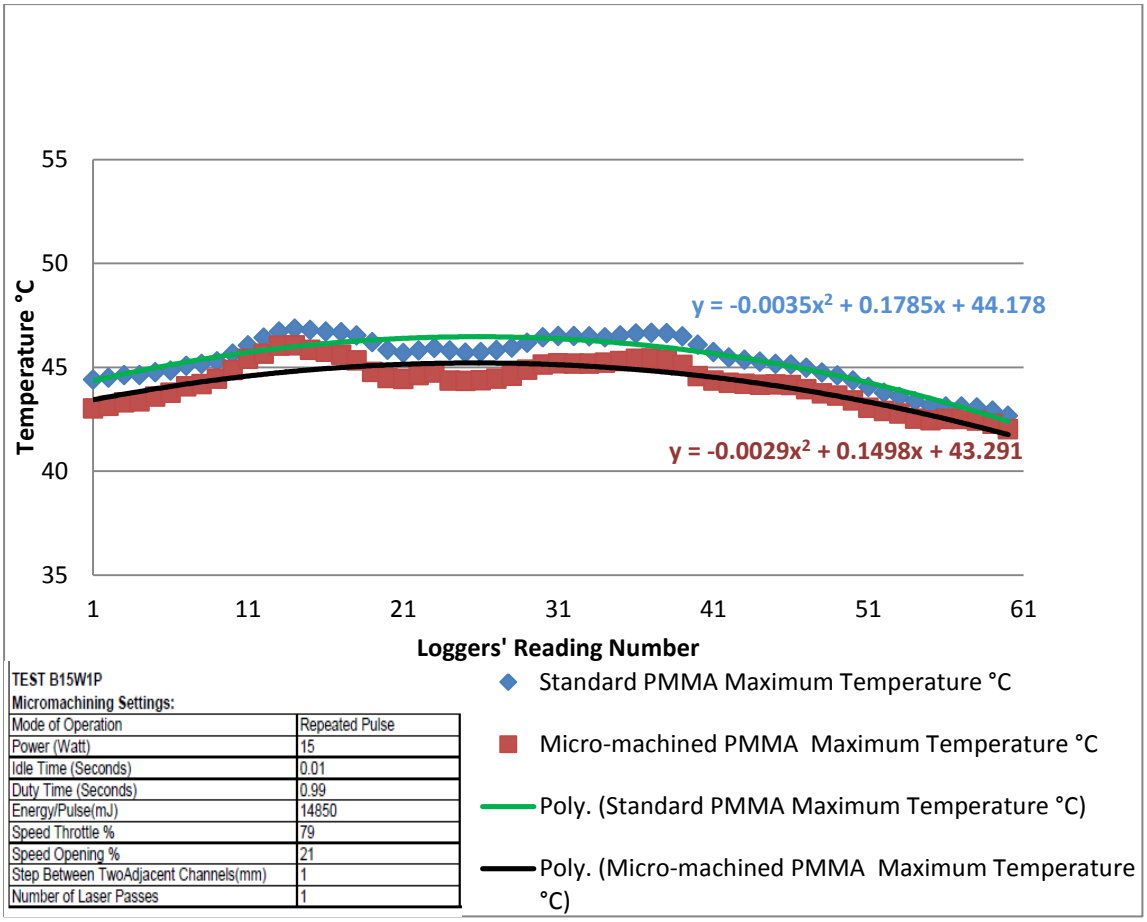

Figure 4.16: Recorded Temperature of Standard and Micro-machined Blue PMMA Samples Irradiated by 15 Watt and 1Laser Pass

4.3.3.4 Comparison of temperature difference, ΔT, for blue PMMA samples irradiated by 30, 25, 20, 15 Watts and 1 laser pass:

For blue PMMA samples irradiated by 30,25,20,15 watts and 1 laser pass ,comparison in ° C was made to know the relationship between laser power and average temperature difference, results are graphically represented in figure 4.17.

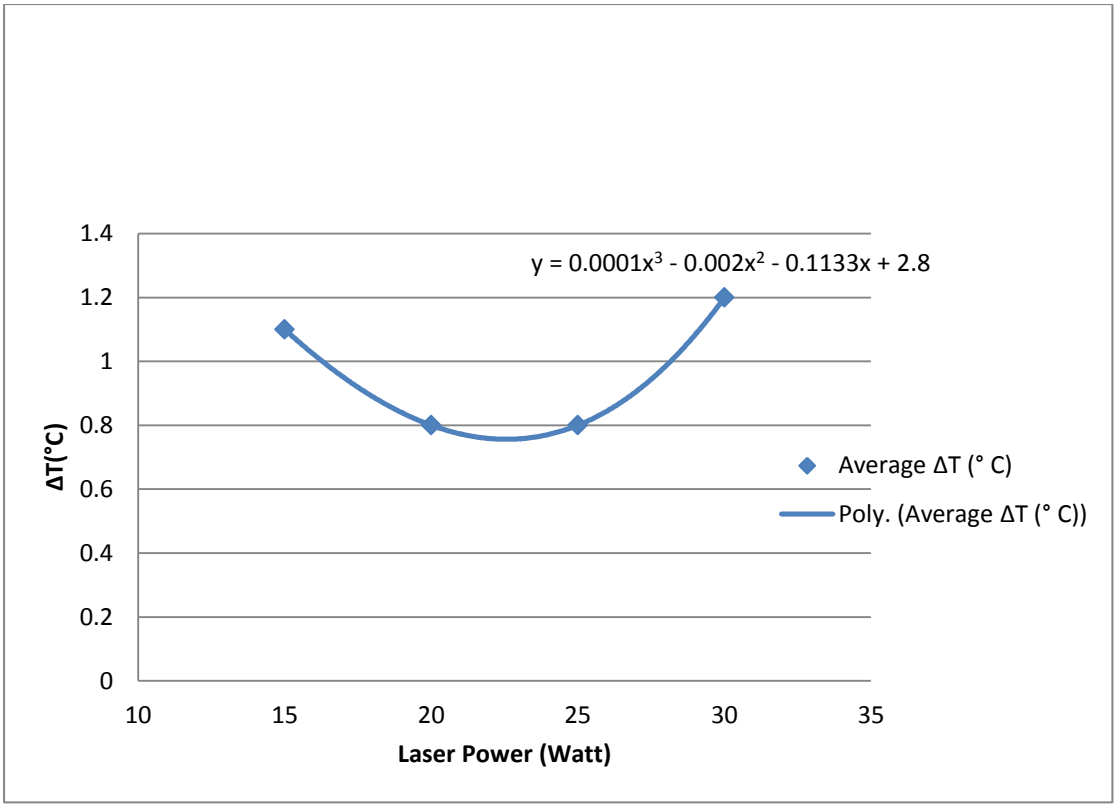

Figure 4.17: ΔT for Blue PMMA Samples Irradiated by 30, 25, 20, 15 Watts and 1 Laser pass

4.3.4 ΔT for black PMMA samples:

4.3.4.1 ΔT for black PMMA samples irradiated by 25 Watts and 1 laser pass:

Black sample was laser micro-machined using 25Watt laser power and one laser pass for engraving each channel, the results are ta graphically presented in figure 4.18.

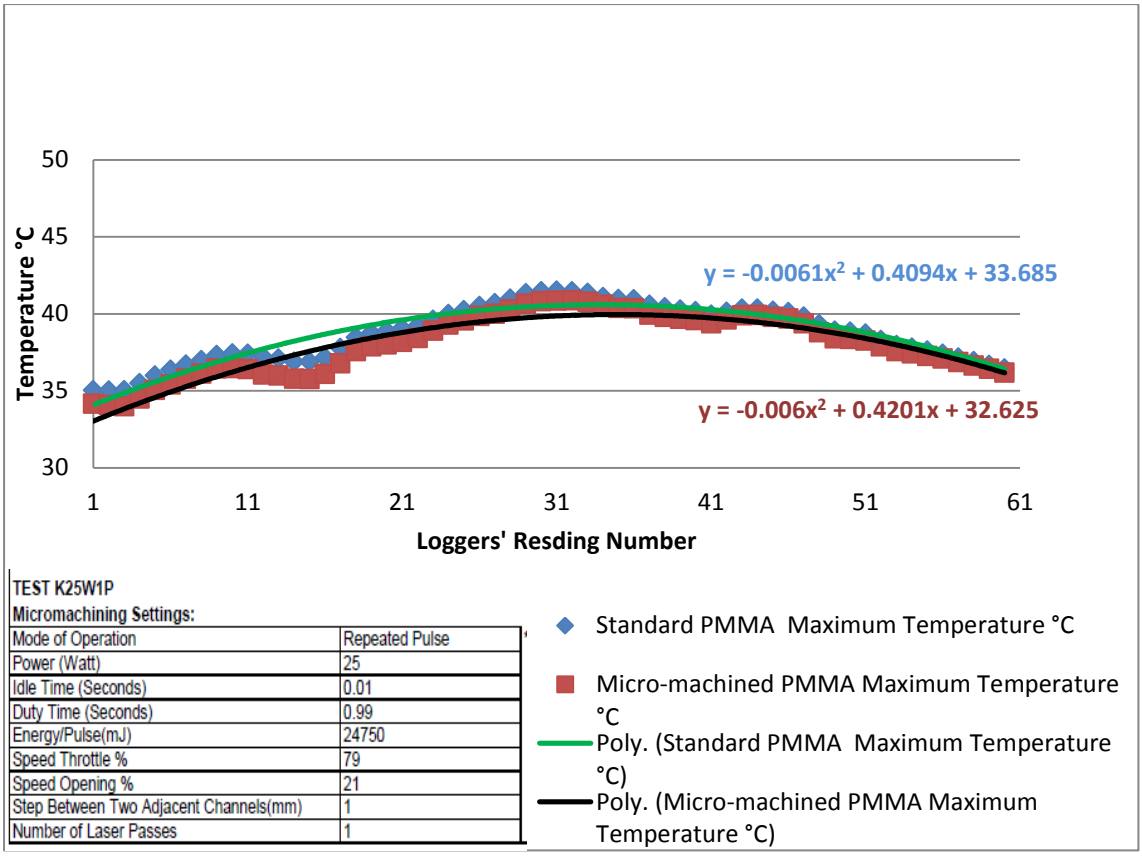

Figure 4.18: Recorded Temperature of Standard and Micro-machined Black PMMA Samples Irradiated by 25 Watt and 1Laser Pass

4.3.4.2 ΔT for black PMMA samples irradiated by 20 Watts and 1 laser pass: Figure 4.19presents the graphical results obtained from the irradiation of black sample using 20 Watts of laser power and one laser pass.

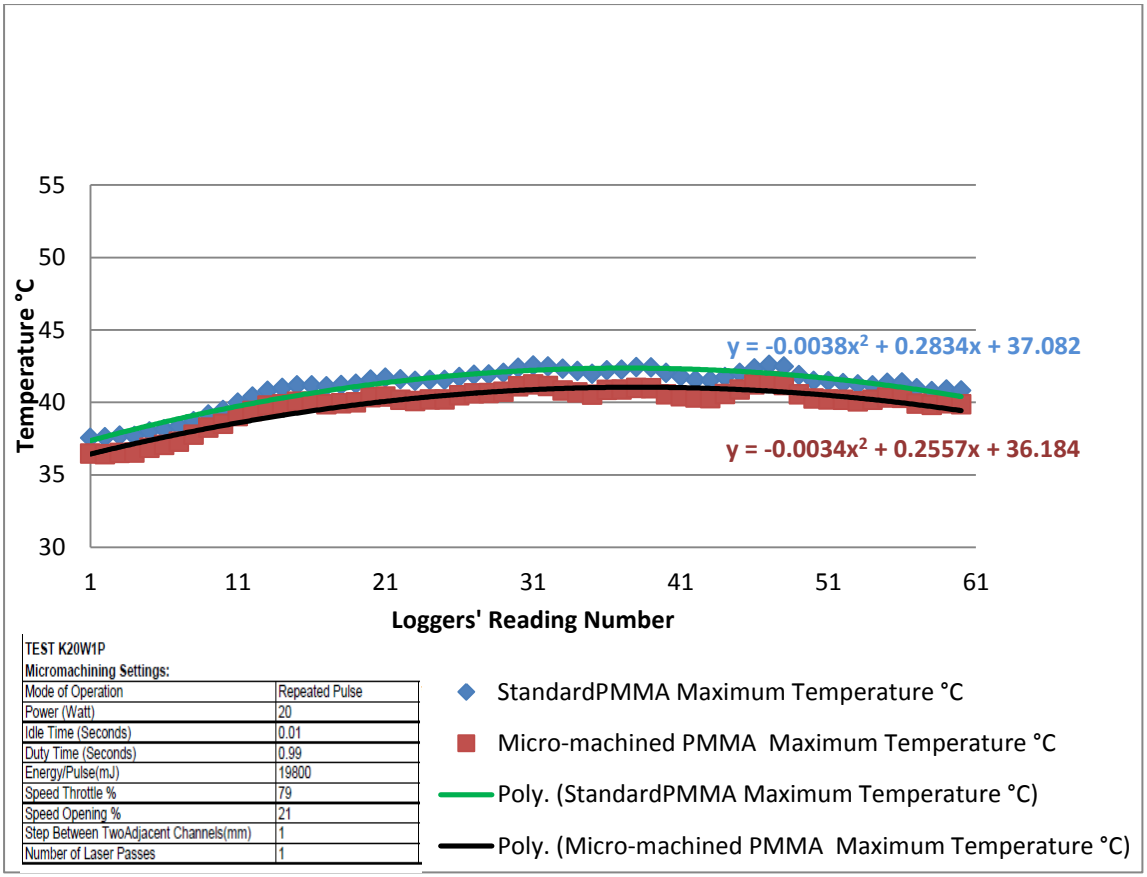

Figure 4.19: Recorded Temperature of Standard and Micro-machined Black PMMA Samples Irradiated by 20 Watt and 1Laser Pass

4.3.4.3 ΔT for black PMMA samples irradiated by 15 Watts and 1 laser pass:

Reducing the laser power to 15 watt, and using one laser pass, the black sample was laser micro-machined by engraving the channels. The results are graphically presented in figure 4.20.

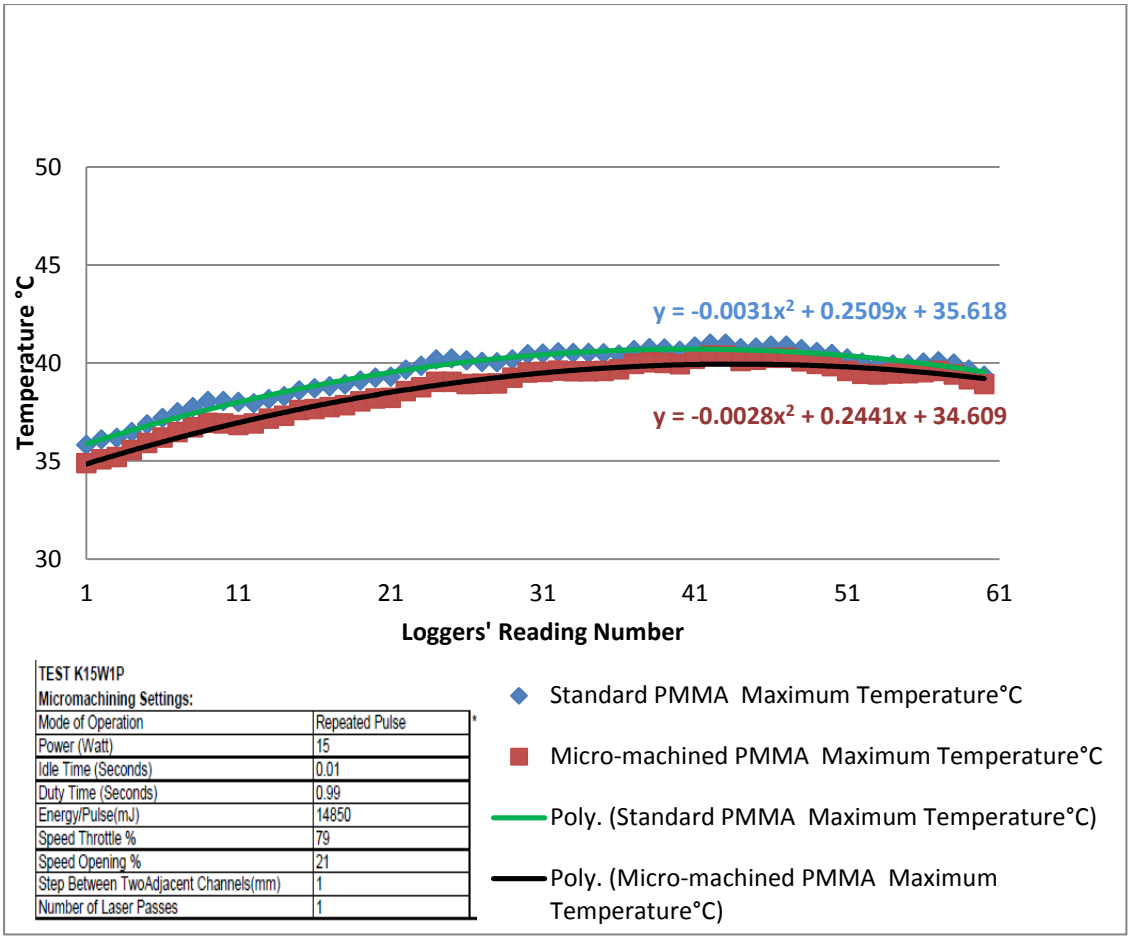

Figure 4.20: Recorded Temperature of Standard and Micro-machined Black PMMA Samples Irradiated by 15 Watt and 1Laser Pass

4.3.4.4 Comparison of temperature difference, ΔT, for black PMMA samples irradiated by 30, 25, 20, 15 Watts and 1 laser pass:

Comparison between temperature differences in °C for black PMMA samples irradiated by 30,25,20,15 watts and 1 laser pass are graphically represented in figure 4.21.

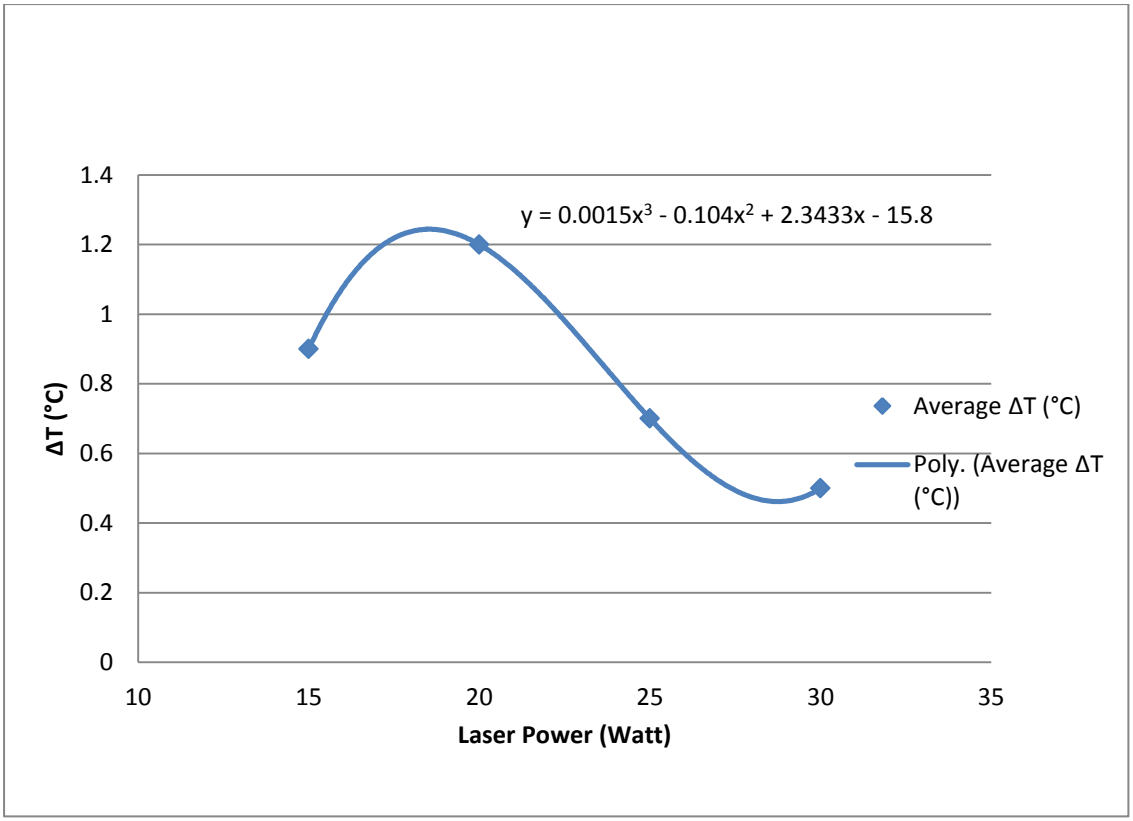

Figure 4.21: ΔT for Black PMMA Samples Irradiated by 30, 25, 20, 15 Watts and 1 Laser pass

4.3.5 ΔT for white PMMA samples:

4.3.5.1 ΔT for white PMMA samples irradiated by 25 Watts and 1 laser pass:

To investigate the effect of laser power on the temperature difference, white sample was laser micro-machined using 25Watt laser power and one laser pass for engraving the channels, the results are presented in figure 4.22.

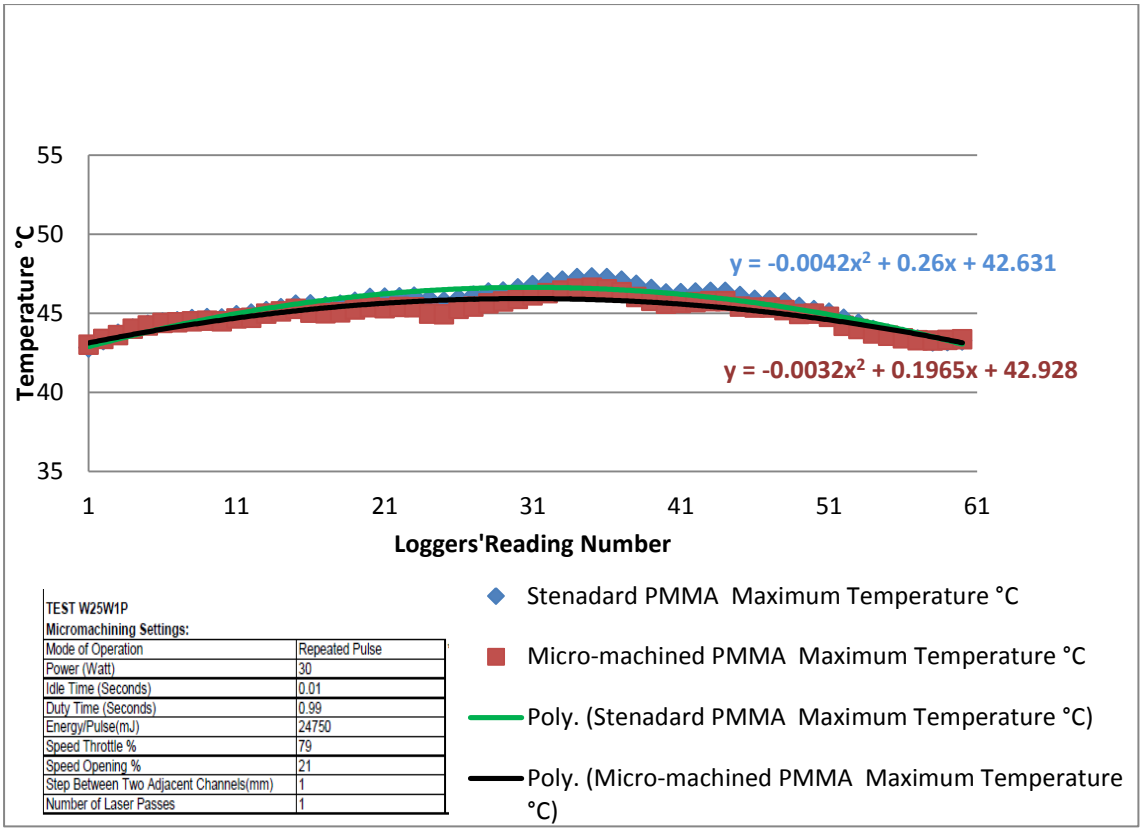

Figure 4.22: Recorded Temperature of Standard and Micro-machined White PMMA Samples Irradiated by 25 Watt and 1Laser Pass

4.3.5.2 ΔT for white PMMA samples irradiated by 20 Watts and 1 laser pass: White sample was laser micro-machined using 20Watt laser power and 1 laser pass for engraving the channels, the results are graphically shown in figure 4.23.

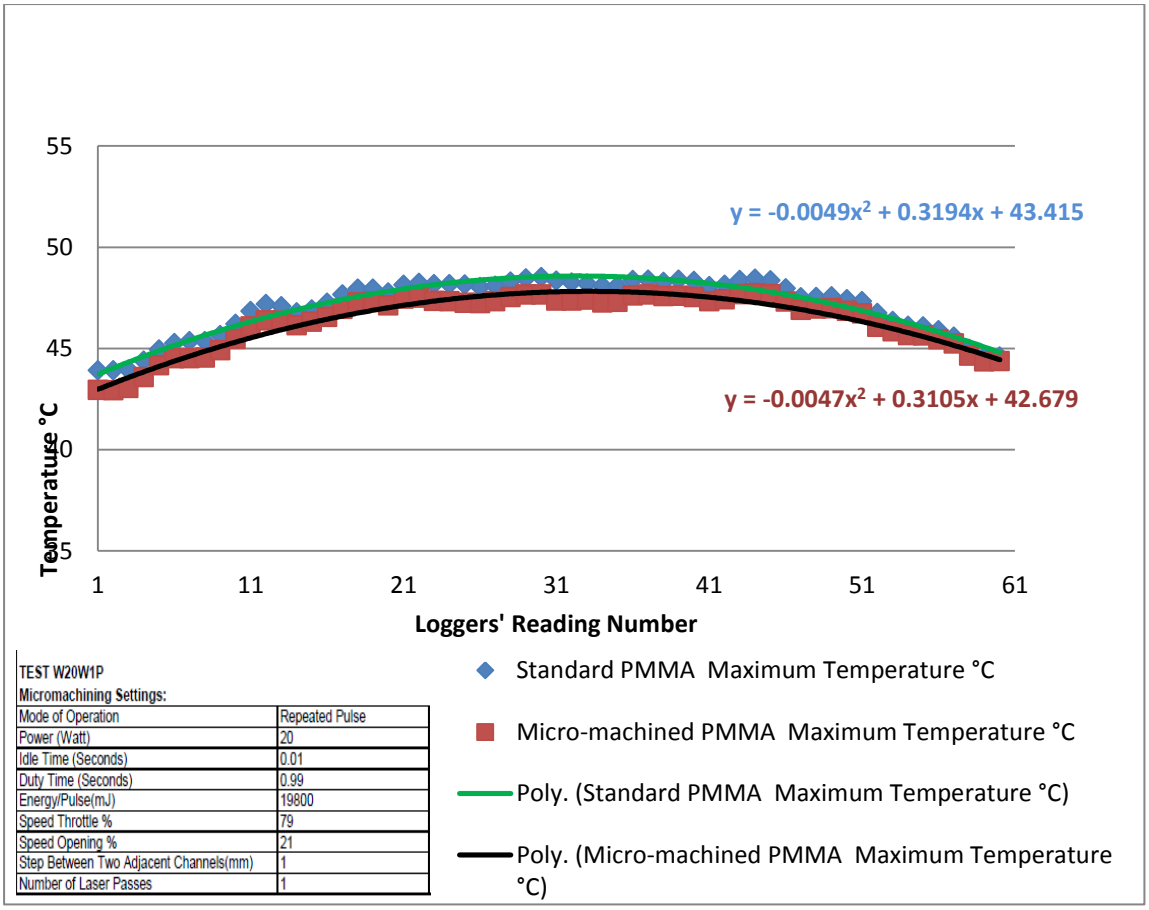

Figure 4.23: Recorded Temperature of Standard and Micro-machined White PMMA Samples Irradiated by 20Watt and 1Laser Pass

4.3.5.3 ΔT for white PMMA samples irradiated by 15 Watts and 1 laser pass:

15 watts of laser power and one laser pass were used to micro-channel the white sample in order to know the effect of this reduced power on the temperature difference between the standard and the micro-machined samples. The results are graphically presented in figure 4.24.

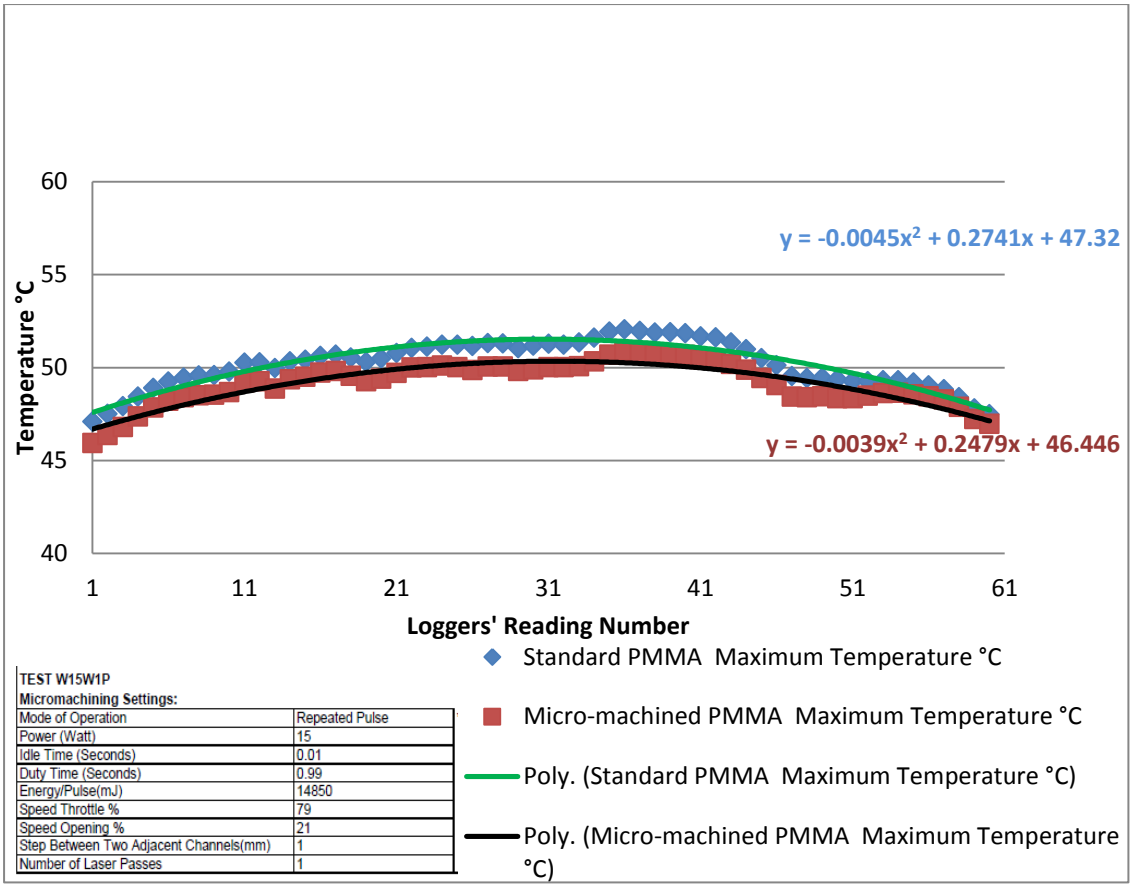

Figure 4.24: Recorded Temperature of Standard and Micro-machined White PMMA Samples Irradiated by 15Watt and 1Laser Pass

4.3.5.4 Comparison of Temperature Difference, ΔT, for White PMMA Samples Irradiated by 30, 25, 20, 15 Watts and 1 Laser pass:

To investigate the effect of different laser powers on the temperature difference of the white PMMA samples, the graph in figure 4.25 is presented to show the comparison.

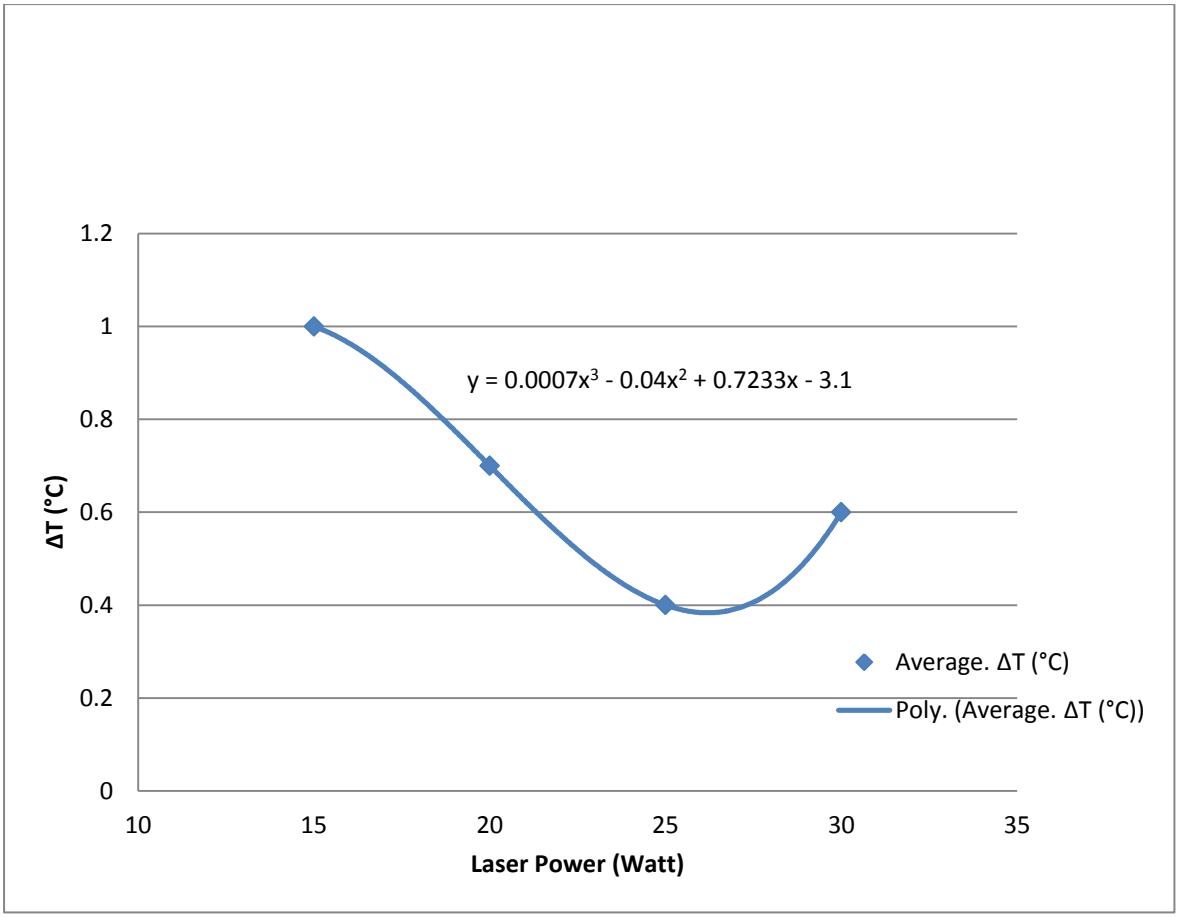

Figure 4.25: ΔT for White PMMA Samples Irradiated by 30, 25, 20, 15 Watts and 1 Laser pass

4.4 The effect of different laser passes on the temperature difference:

To investigate the effect of laser passes on temperature reduction between micro-machined samples and standard samples, laser micromachining experiments were carried out for different samples of the same RGBKW model, using different laser passes of 2, 3, and4 passes, the results of which are shown in the graphs mentioned below.

4.4.1 ΔT for Red PMMA Samples:

4.4.1.1 ΔT for Red PMMA Samples Irradiated by 30 Watts and 2 Laser passes:

Laser passes: Red sample was laser micro-machined using 30 watt laser power and 2 laser passes for engraving each channel, the results are graphically presented in figure 4.26.

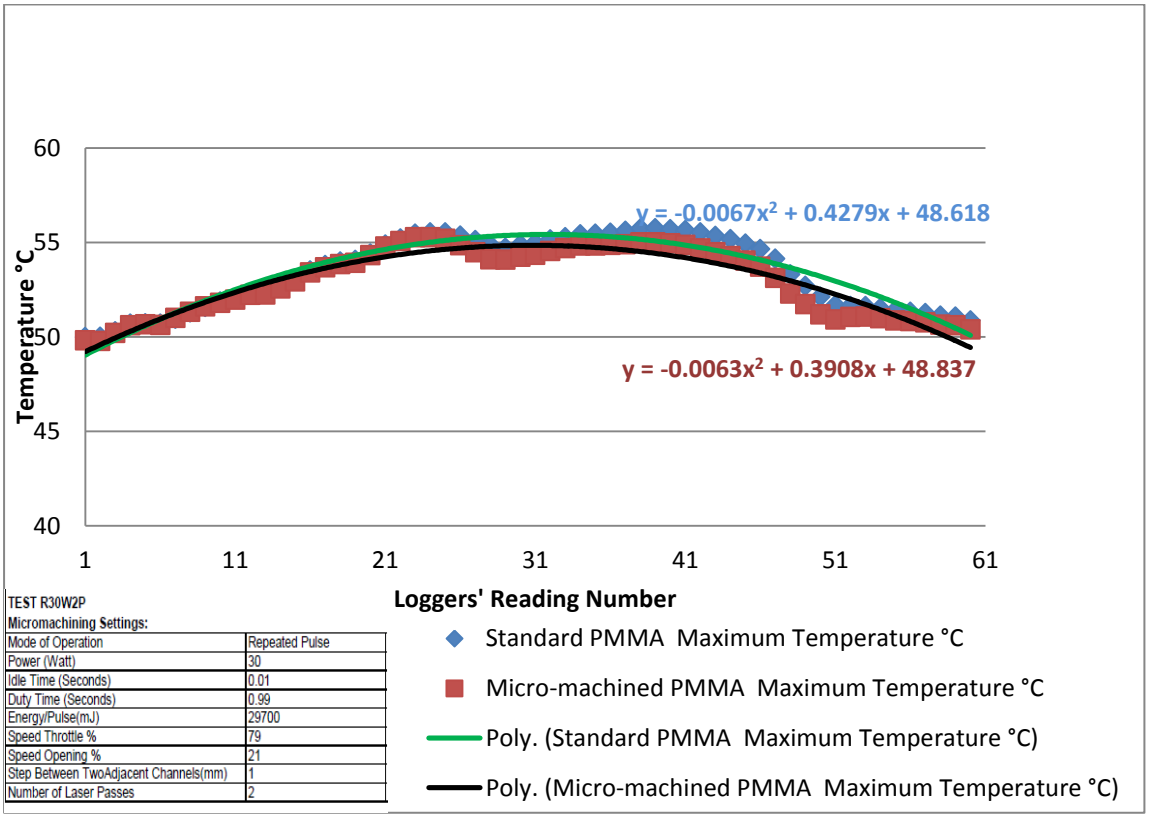

Figure 4.26: Recorded Temperature of Standard and Micro-machined Red PMMA Samples Irradiated by 30Watt and 2Laser Passes

4.4.1.2 ΔT for red PMMA samples irradiated by 30 Watts and 3 laser passes:

laser passes: Laser micromachining of red samples using 30 Watt laser power and 3 laser passes for engraving each channel was performed. The results are graphically presented in figure 4.27.

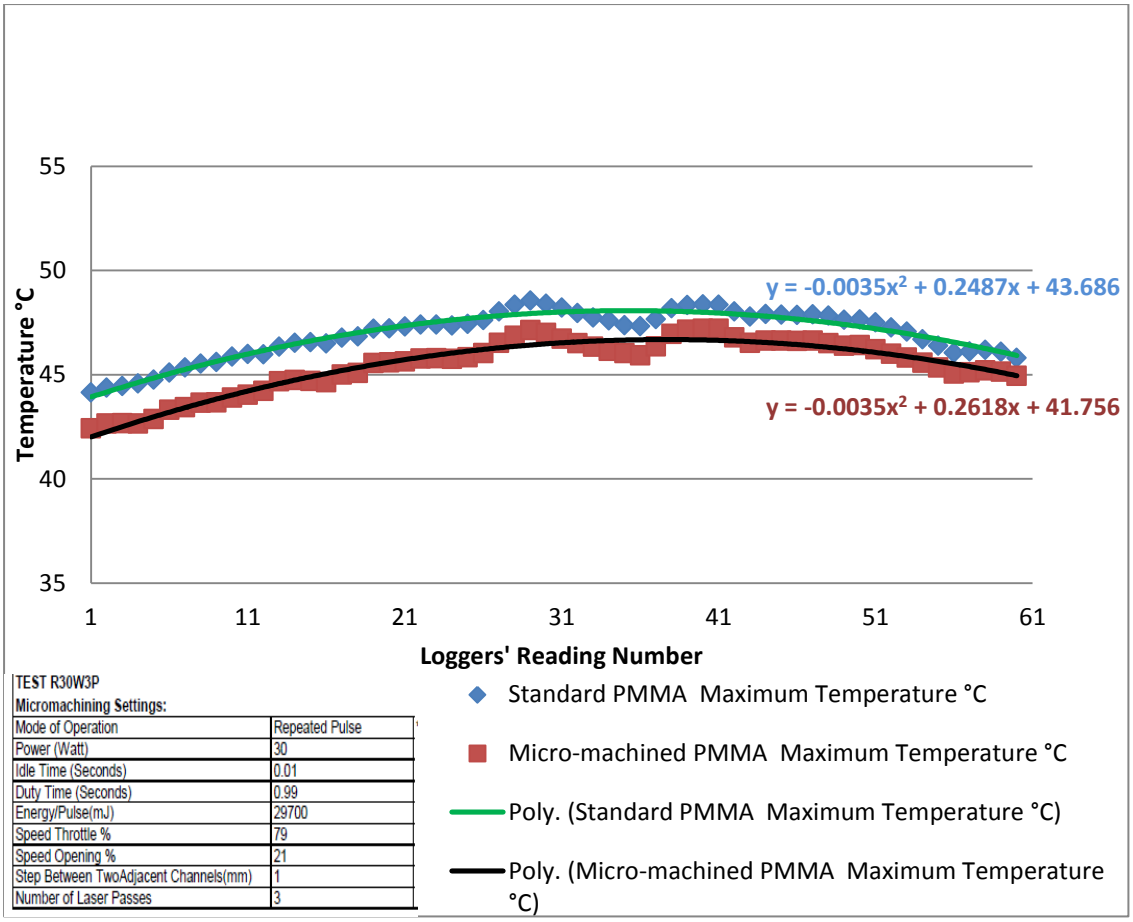

Figure 4.27: Recorded Temperature of Standard and Micro-machined Red PMMA Samples Irradiated by 30Watt and 3 Laser Passes

4.4.1.3 ΔT for Red PMMA Samples Irradiated by 30 Watts and 4

Laser passes: Increasing the number of laser passes to four, using the same 30 Watt of laser power, has an effect on the temperature difference between red micro-machined samples and standard ones. This effect is shown graphically in figure 4.28.

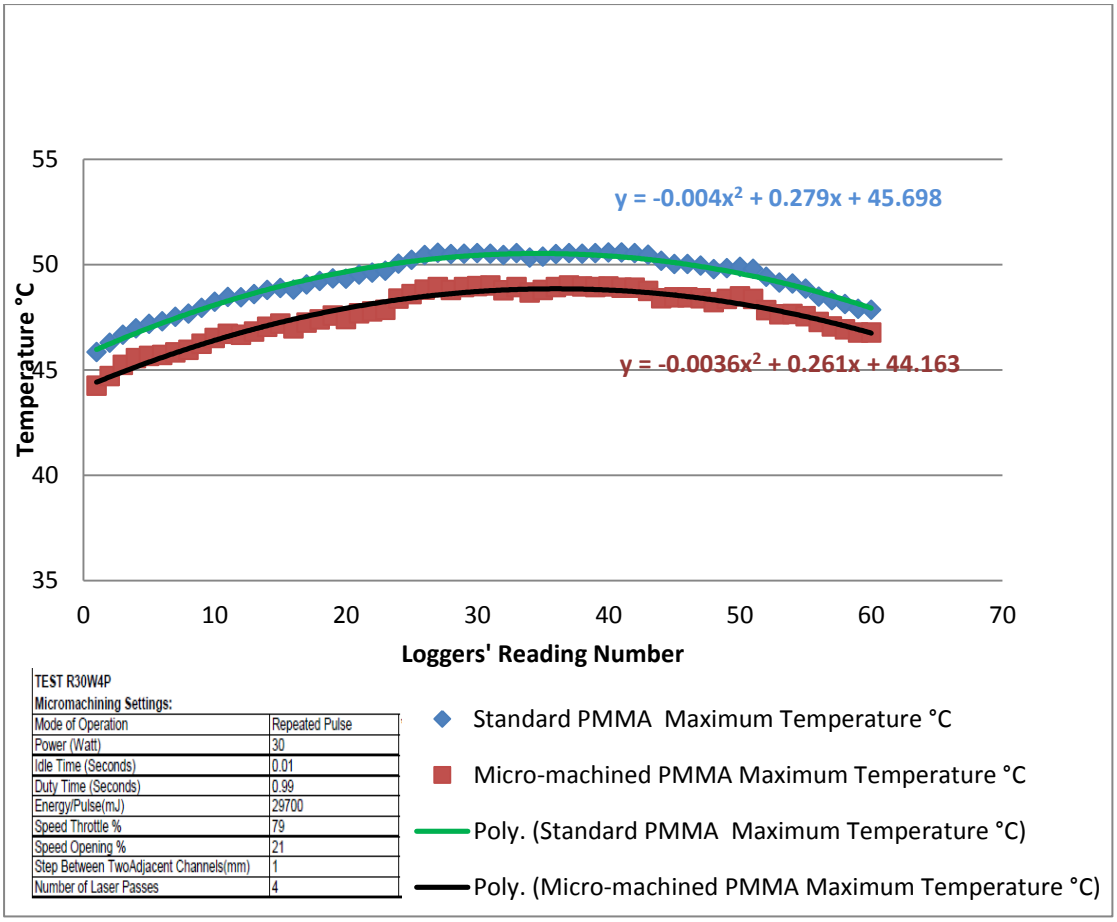

Figure 4.28: Recorded Temperature of Standard and Micro-machined Red PMMA Samples Irradiated by 30Watt and 4Laser Passes

4.4.1.4 Comparison of temperature difference, ΔT, for red PMMA samples irradiated by 30Watt and 1, 2, 3 and4 laser passes respectively:

Comparison between temperature differences in degree C, and for red PMMA samples irradiated by 30watt and 1,2,3,4 laser passes respectively are graphically represented in figure 4.29.

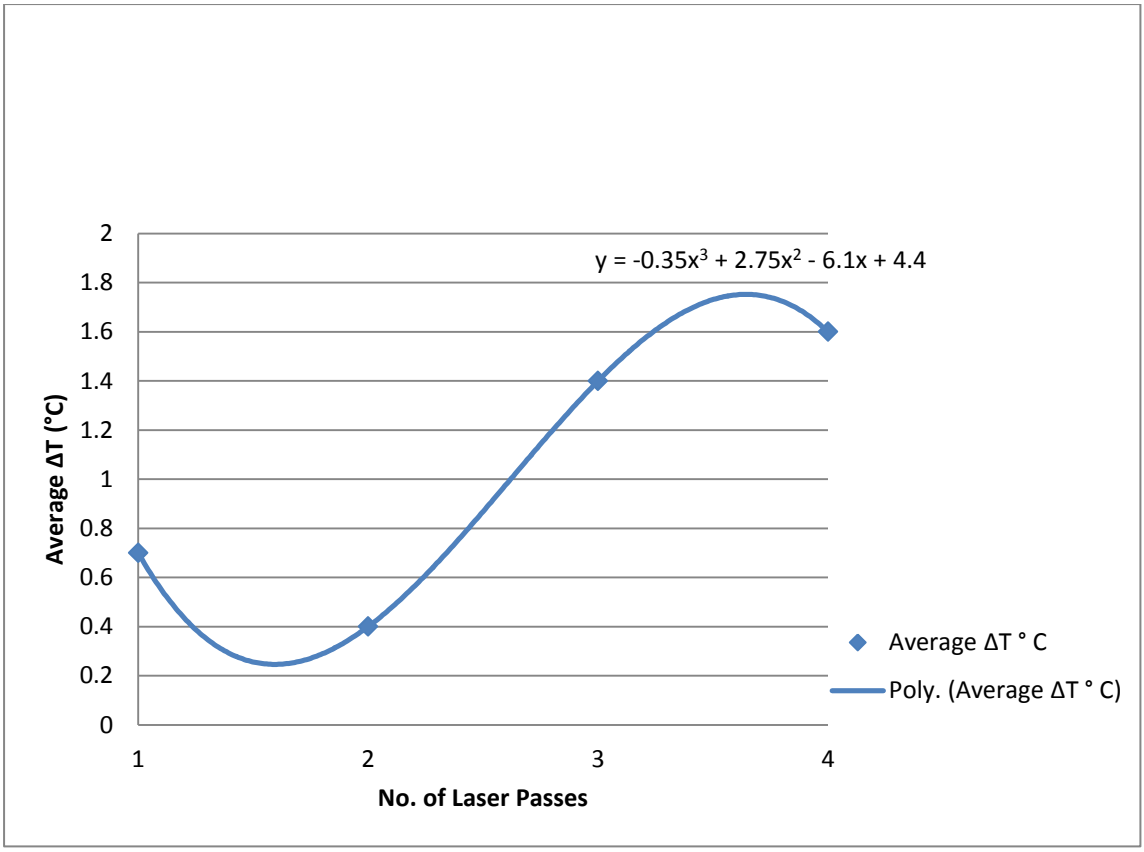

Figure 4.29: ΔT for Red PMMA Samples Irradiated by 30Watts and 1, 2, 3 and4 Laser passes

4.4.2 ΔT for Green PMMA Samples:

4.4.2.1 ΔT for Green PMMA Samples Irradiated by 30 Watts and 2 Laser passes:

Using 30 Watt laser power and two laser passes, green sample was micro-machined to identify the results of the laser passes on the temperature difference between the standard and the micro-machined samples. The results are presented in the graph shown in figure 4.30.

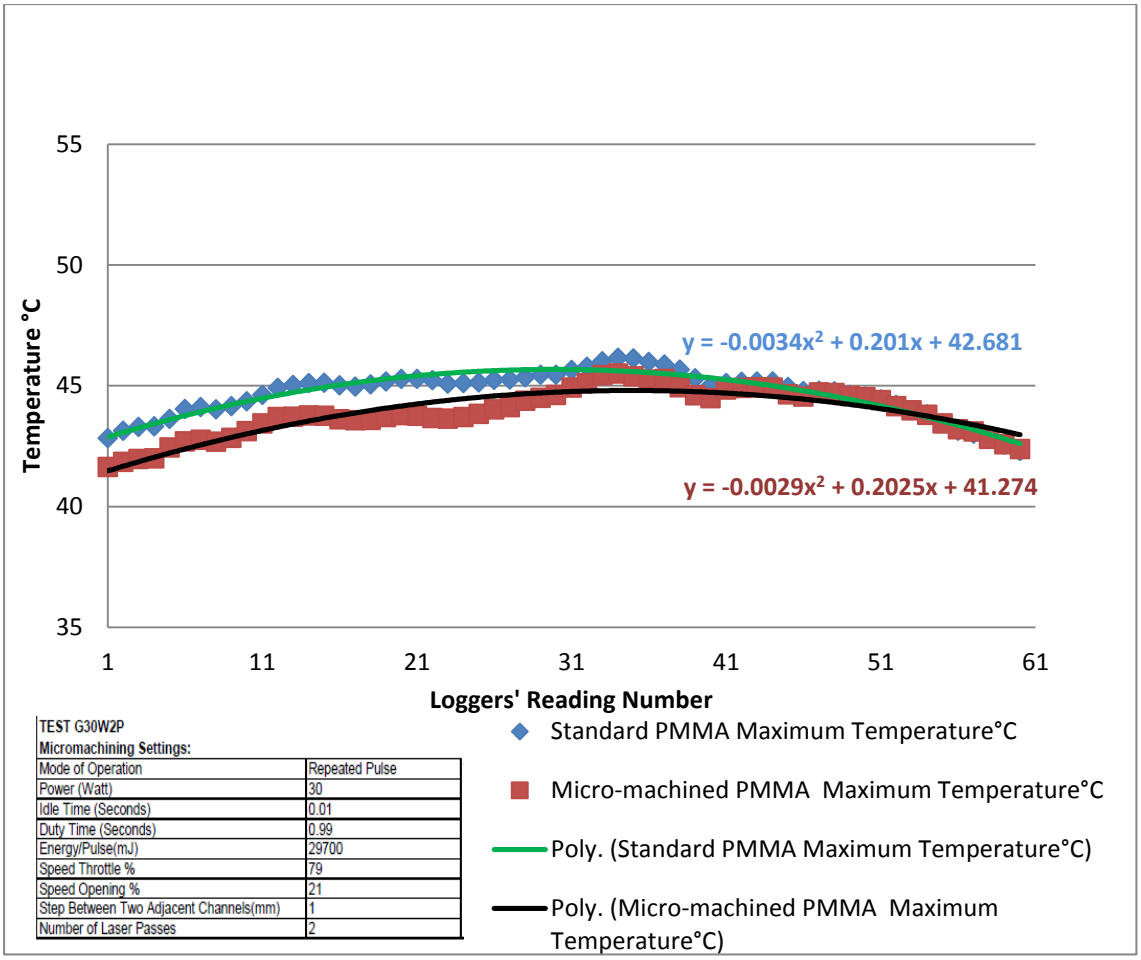

Figure 4.30: Recorded Temperature of Standard and Micro-machined Green PMMA Samples Irradiated by 30Watt and 2Laser Passes

4.4.2.2 ΔT for green PMMA samples irradiated by 30 Watts and 3 laser passes:

Green sample was laser micro-machined using 30 Watt laser power and 3 laser passes for engraving the channels, the results are graphically presented in figure 4.31.

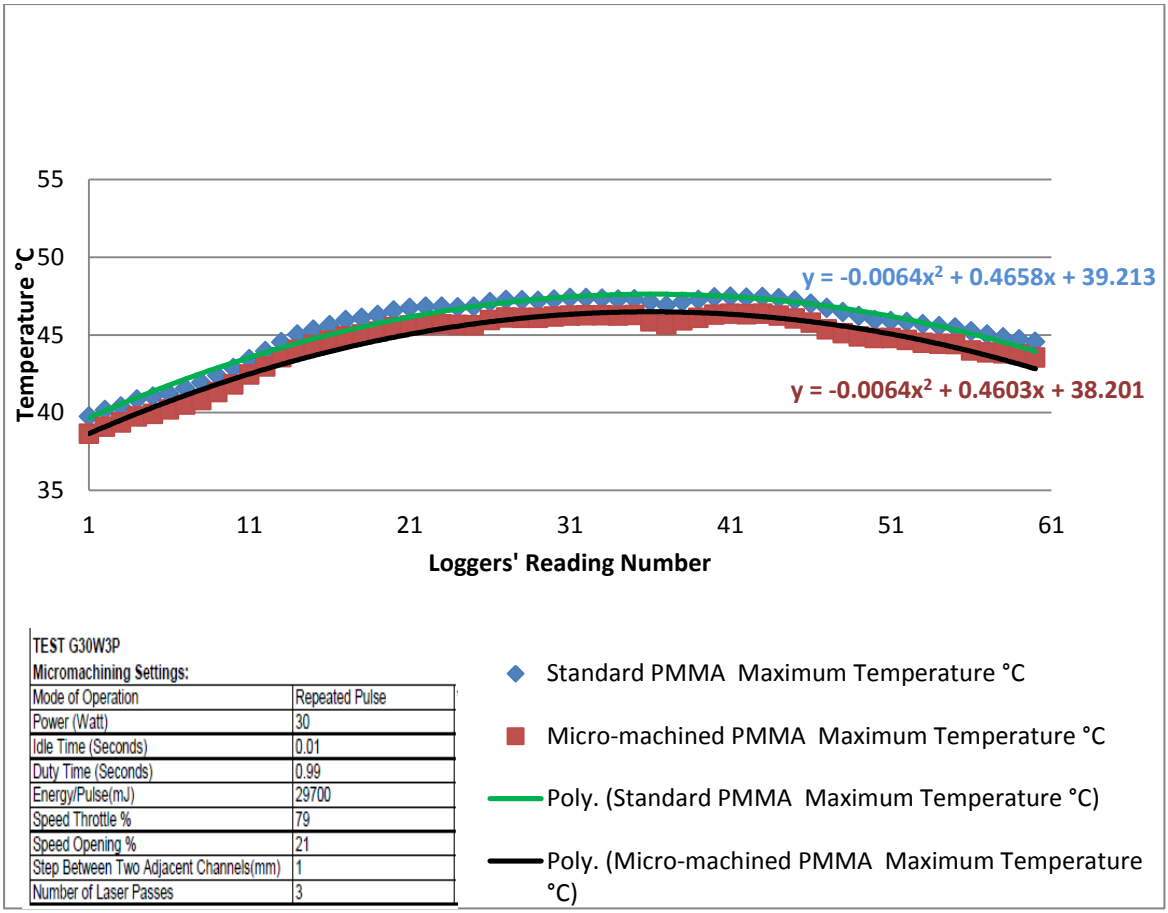

Figure 4.31: Recorded Temperature of Standard and Micro-machined Green PMMA Samples Irradiated by 30Watt and 3Laser Passes

4.4.2.3 ΔT for green PMMA samples irradiated by 30 Watts and 4 laser passes: Increasing the number of laser passes to four, green sample was laser micro-machined using 30 watt laser power, for engraving each channel, the results are presented in figure 4.32.

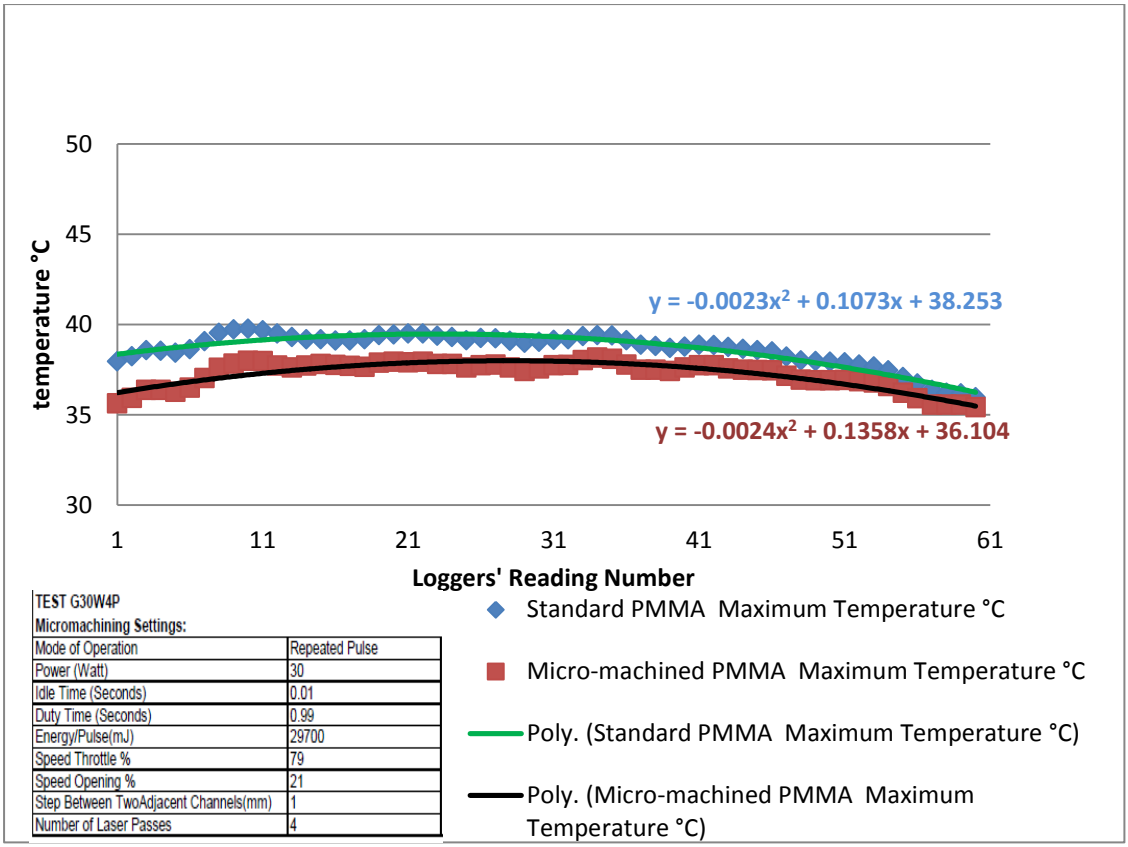

TEST G30W4P

Micromachining Settings:

Mode of Operation	Repeated Pulse
Power (Watt)	30
Idle Time (Seconds)	0.01
Duty Time (Seconds)	0.99
Energy/Pulse(mJ)	29700
Speed Throttle %	79
Speed Opening %	21
Step Between TwoAdjacent Channels(mm)	1
Number of Laser Passes	4

Figure 4.32: Recorded Temperature of Standard and Micro-machined Green PMMA Samples Irradiated by 30Watt and 4Laser Passes

4.4.2.4 Comparison of temperature difference, ΔT, for green PMMA samples irradiated by 30Watt and 1, 2, 3 and 4 laser passes respectively:

In figure 4.33, the comparison between temperature differences in degree C, for green PMMA samples irradiated by 30watt and 1, 2, 3and 4 laser passes respectively are graphically represented.

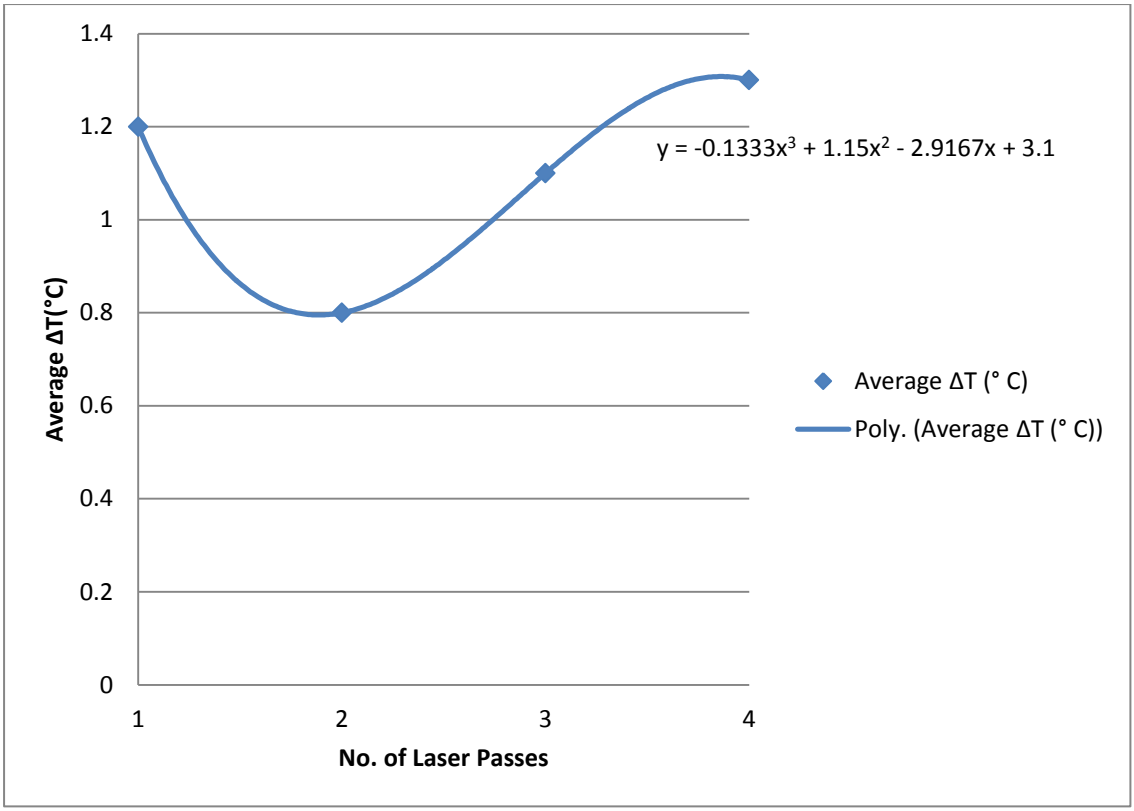

Figure 4.33: ΔT for Green PMMA Samples Irradiated by 30Watts and 1, 2, 3 and4 Laser passes

4.4.3 ΔT for Blue PMMA Samples:

4.4.3.1 ΔT for blue PMMA samples irradiated by 30 Watts and 2 laser passes:

Blue sample showed certain behavior when laser micro-machined using 30 watt laser power and 2 laser passes to scribe the channels, this is graphically presented in figure 4.34.

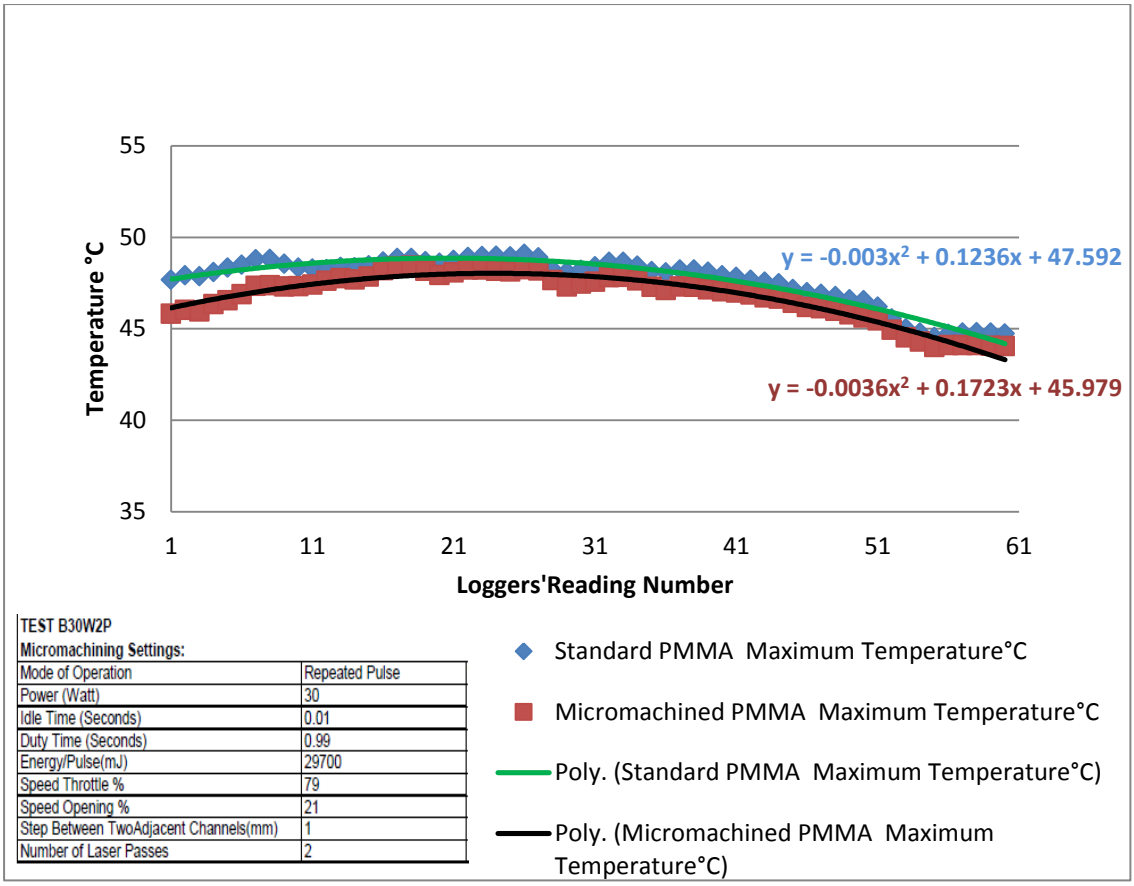

Figure 4.34: Recorded Temperature of Standard and Micro-machined Blue PMMA Samples Irradiated by 30Watt and 2 Laser Passes

4.4.3.2 ΔT for blue PMMA samples irradiated by 30 Watts and 3 laser passes: 30 watts of laser power and 3 laser passes were used to engrave the micro- channel of the blue sample. The results are presented graphically in figure 4.35.

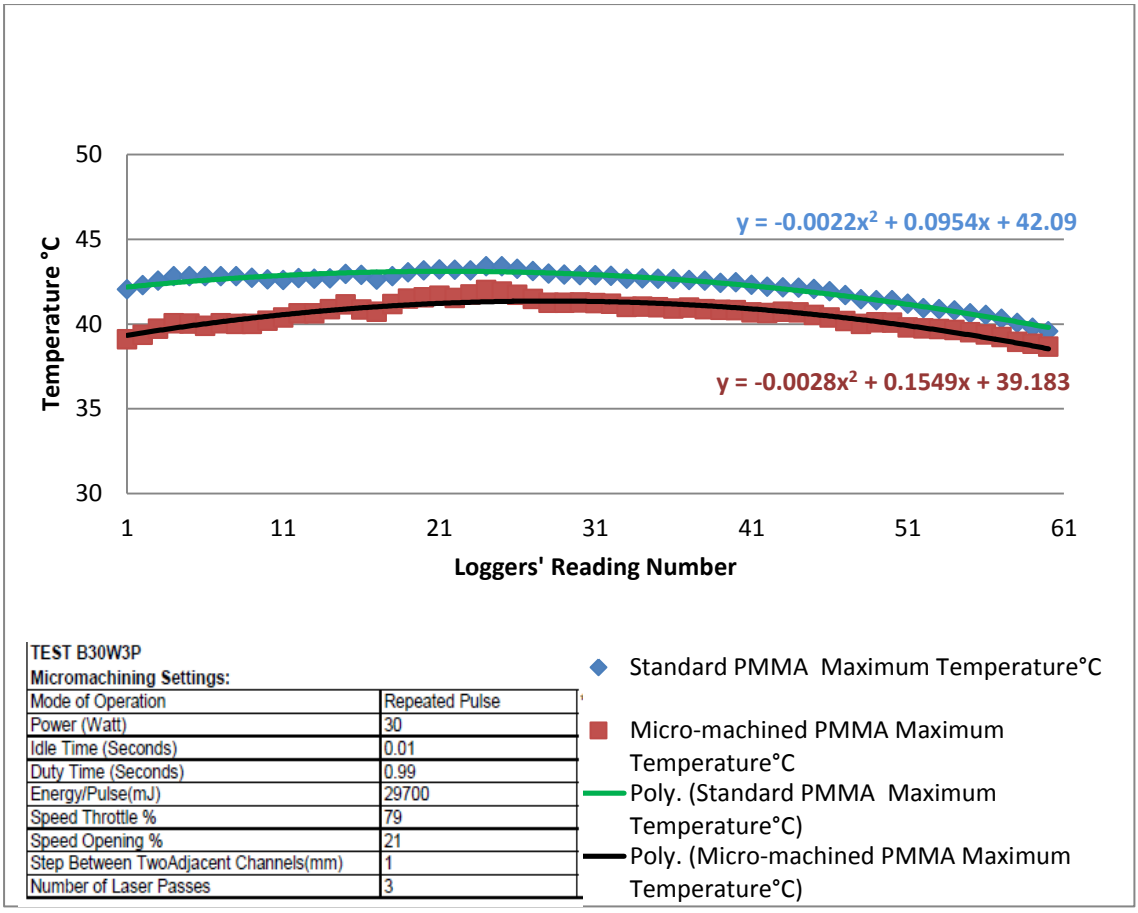

Figure 4.35: Recorded Temperature of Standard and Micro-machined Blue PMMA Samples Irradiated by 30Watt and 3Laser Passes

4.4.3.3 ΔT for blue PMMA samples irradiated by 30 Watts and 4 laser passes:

Using the same 30 watt laser power , and increasing the laser passes to 4, for micromachining the channels, blue sample was laser processed, the results of this process is shown in a graph in figure 4.36.

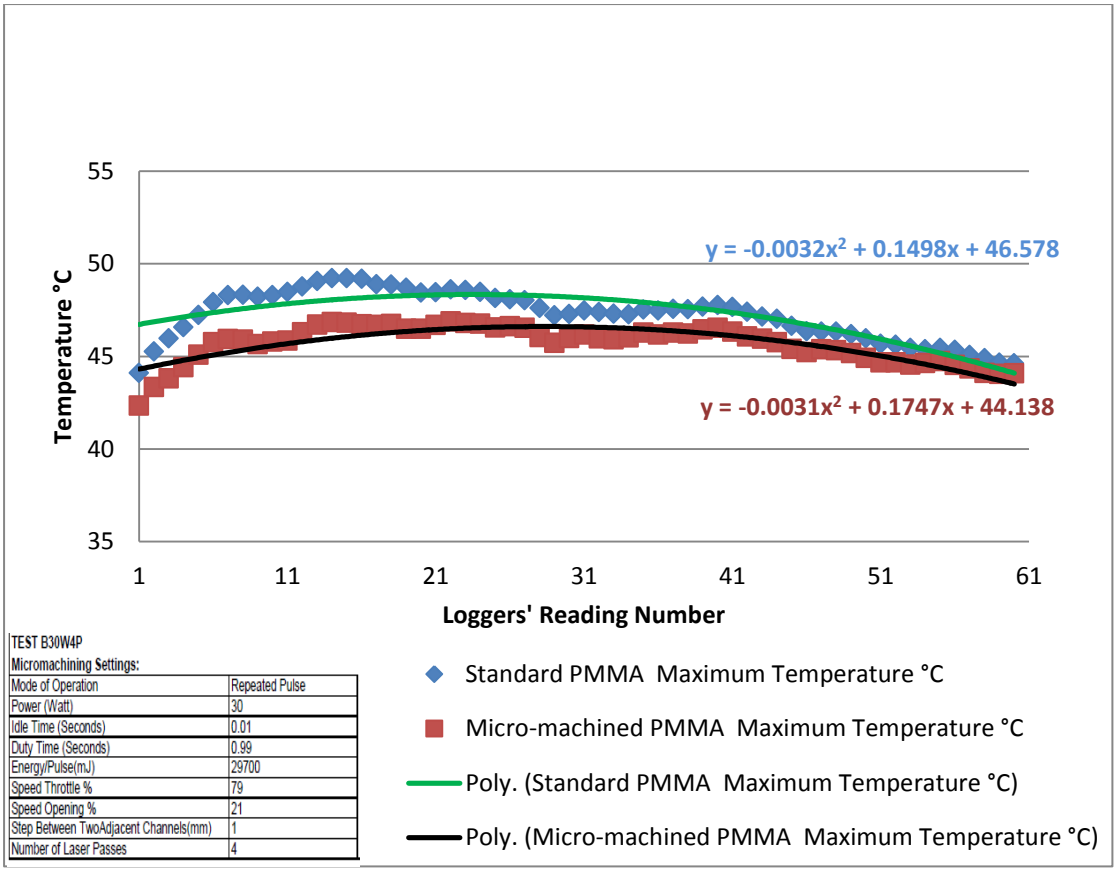

Figure 4.36: Recorded Temperature of Standard and Micro-machined Blue PMMA Samples Irradiated by 30Watt and4 Passes

4.4.3.4 Comparison of temperature difference, ΔT, for blue PMMA samples irradiated by 30Watt and 1, 2, 3 and 4 laser passes respectively:

The effect of different laser passes on the average temperature difference between the standard and the laser micro-machined blue samples using 30 Watt laser power and 1, 2, 3 and 4 laser passes is presented graphically in figure 4.37.

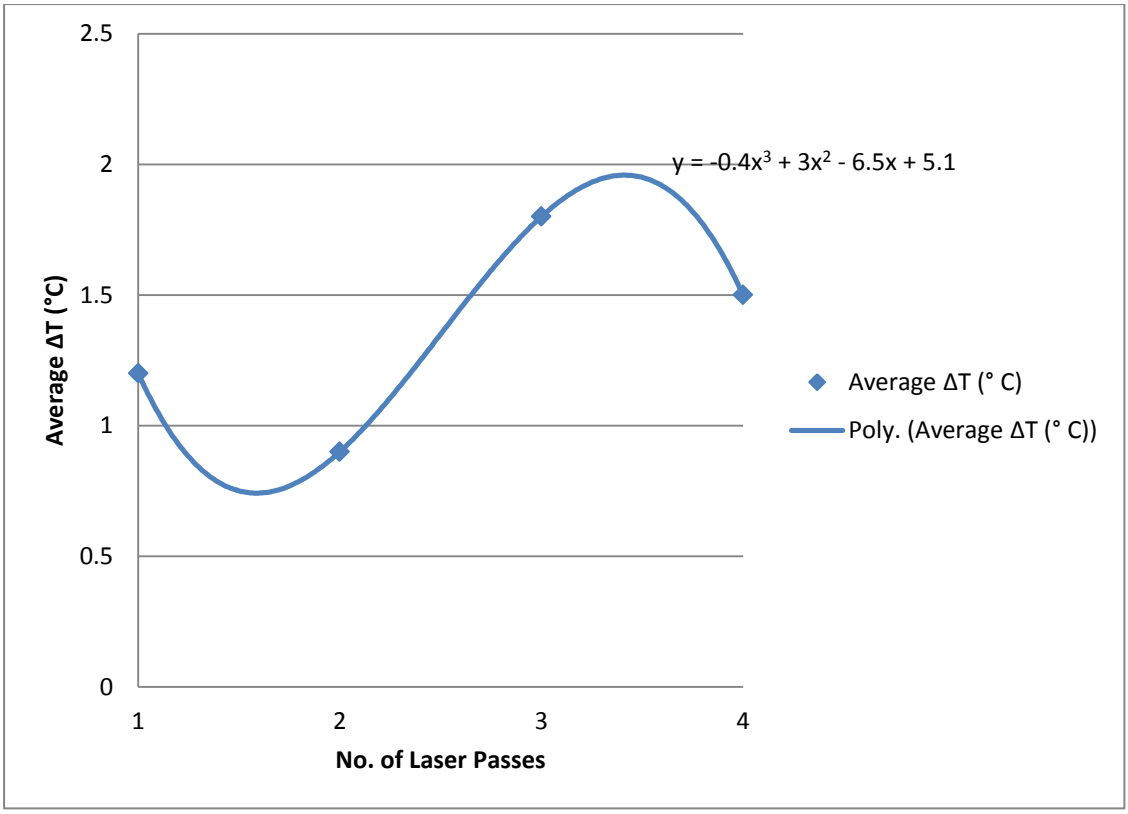

Figure 4.37: ΔT for Blue PMMA Samples Irradiated by 30Watts and 1, 2, 3 and4 Laser passes

4.4.4 ΔT for black PMMA samples:

4.4.4.1 ΔT for black PMMA samples irradiated by 30 Watts and 2 laser passes:

Black sample was laser micro-machined using 30 watt laser power and 2 laser passes for scribing the channels in order to increase their solar thermal insulation ,as for all the channels mentioned before, the results are graphically presented in figure 4.38.

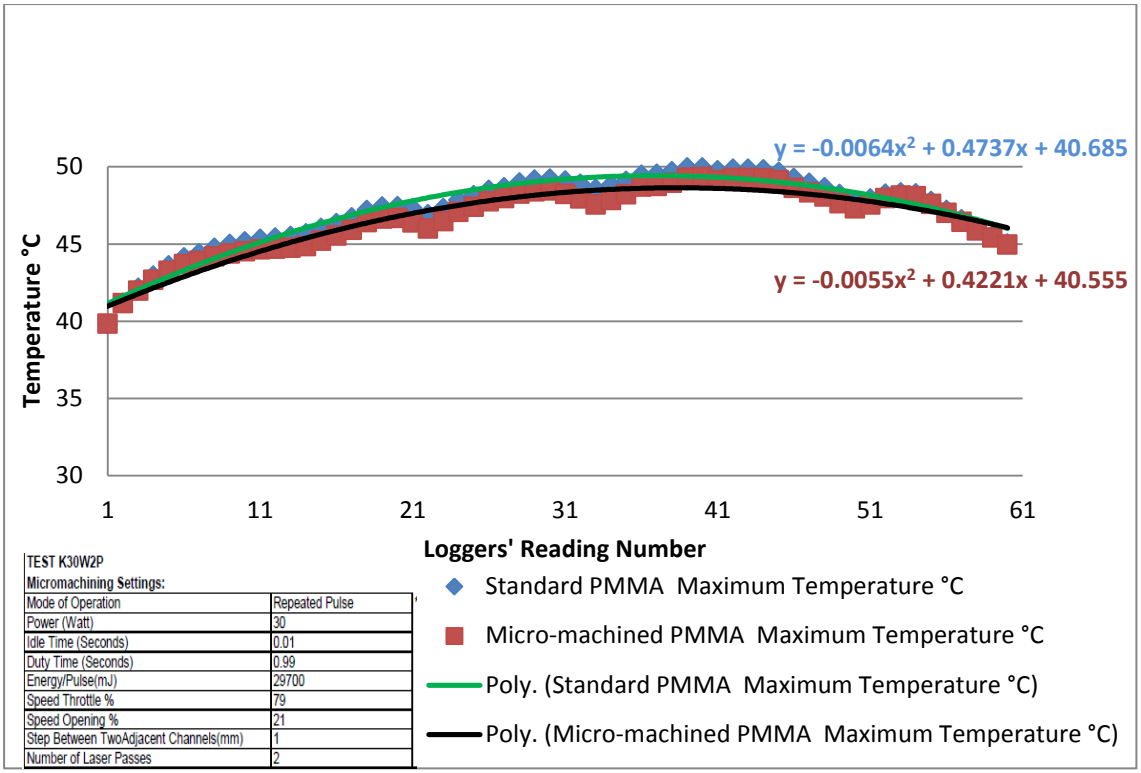

Figure 4.38: Recorded Temperature of Standard and Micro-machined Black PMMA Samples Irradiated by 30Watt and 2 Passes

4.4.4.2 ΔT for black PMMA samples irradiated by 30 Watts and 3 laser passes: The results of the micromachining of channels on black sheets using 30 Watts of laser power and 3 laser passes are shown in a graph in figure 4.39.

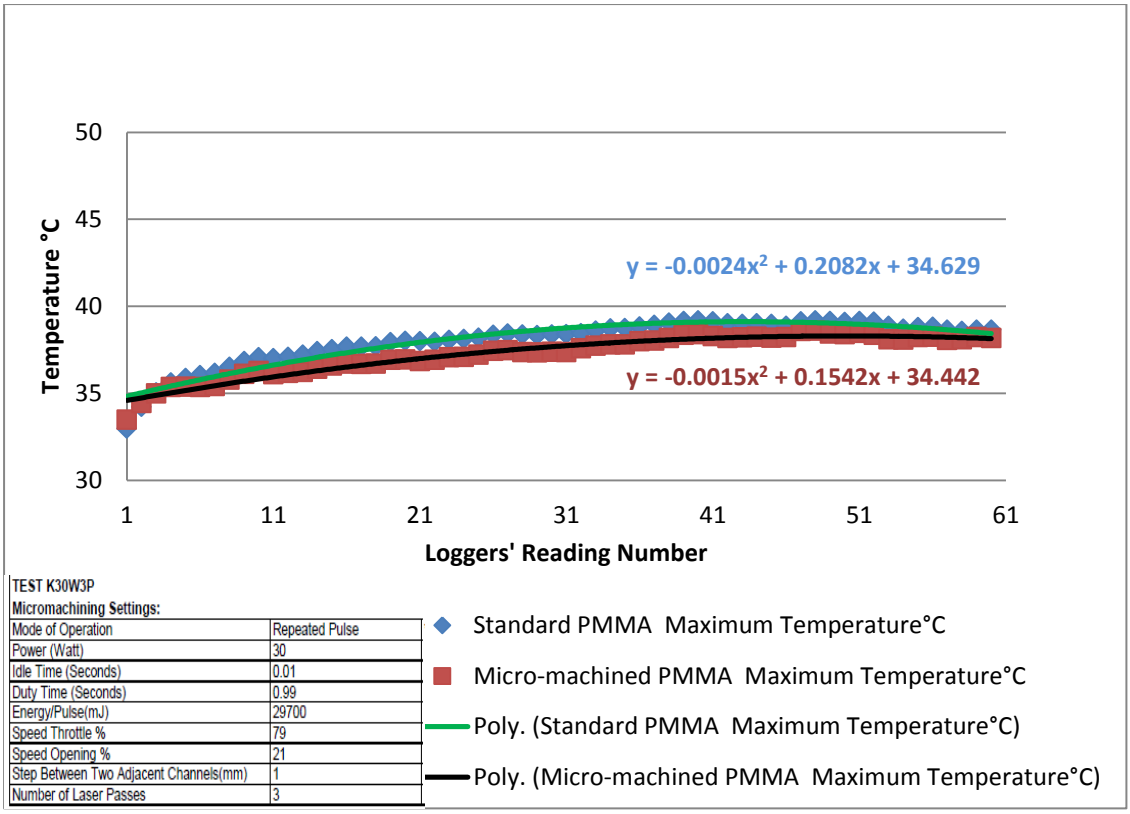

Figure 4.39: Recorded Temperature of Standard and Micro-machined Black PMMA Samples Irradiated by 30Watt and 3 Passes

4.4.4.3 ΔT for black PMMA samples irradiated by 30 Watts and 4 laser passes:

Black sample was laser micro-machined using 30 Watt laser power and increasing the laser passes to 4.The purpose is to scribe micro-channel in the sheets using bulk micromachining technique. The results are presented in figure 4.40.

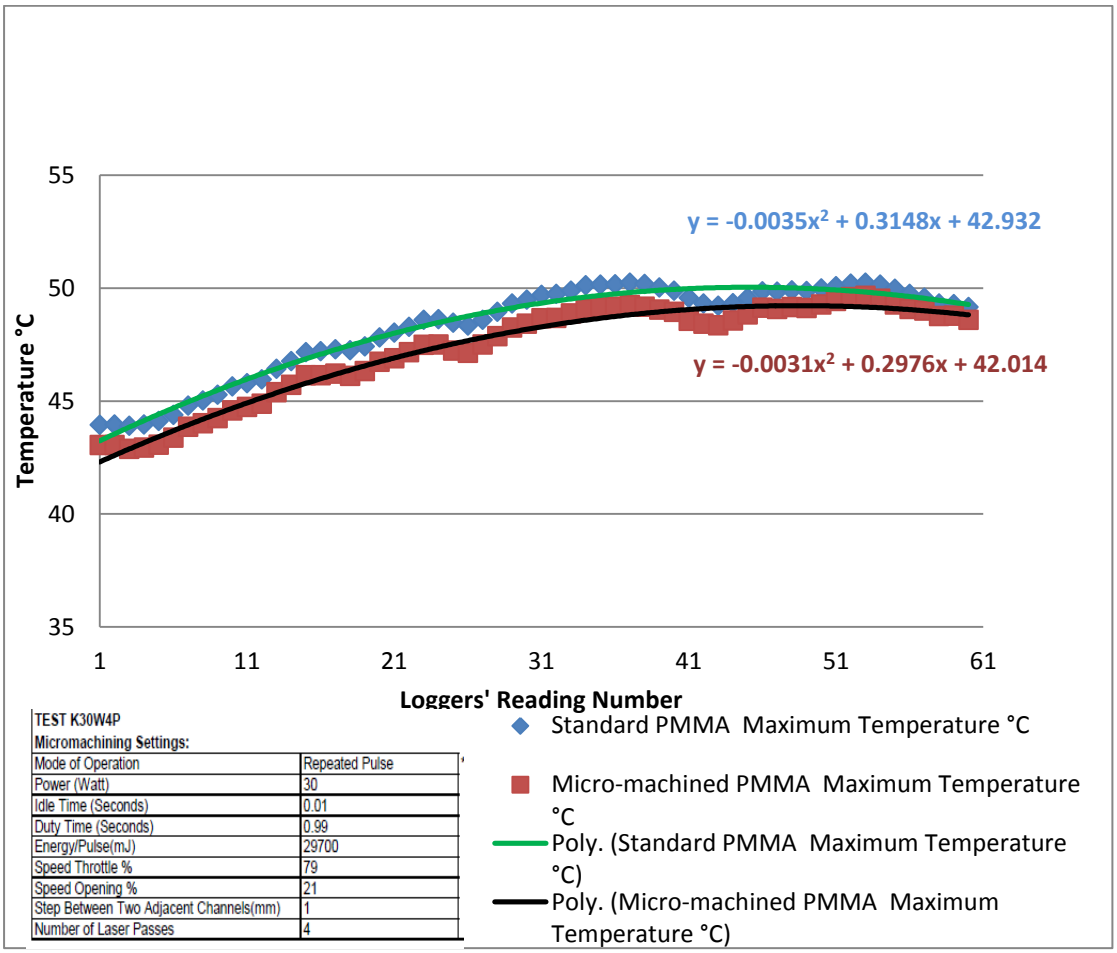

Figure 4.40: Recorded Temperature of Standard and Micro-machined Black PMMA Samples Irradiated by 30Watt and 4 Passes

4.4.4.4 Comparison of temperature difference, ΔT, for black PMMA samples irradiated by 30Watt and 1, 2, 3and 4 laser passes respectively:

Irradiating the black samples by laser power of 30 Watts of operation, all samples, and using different laser passes of 1, 2, 3 and 4 pass resulted in difference in temperature reduction between the standard and micro-machined black samples, the results are shown in figure 4.41.

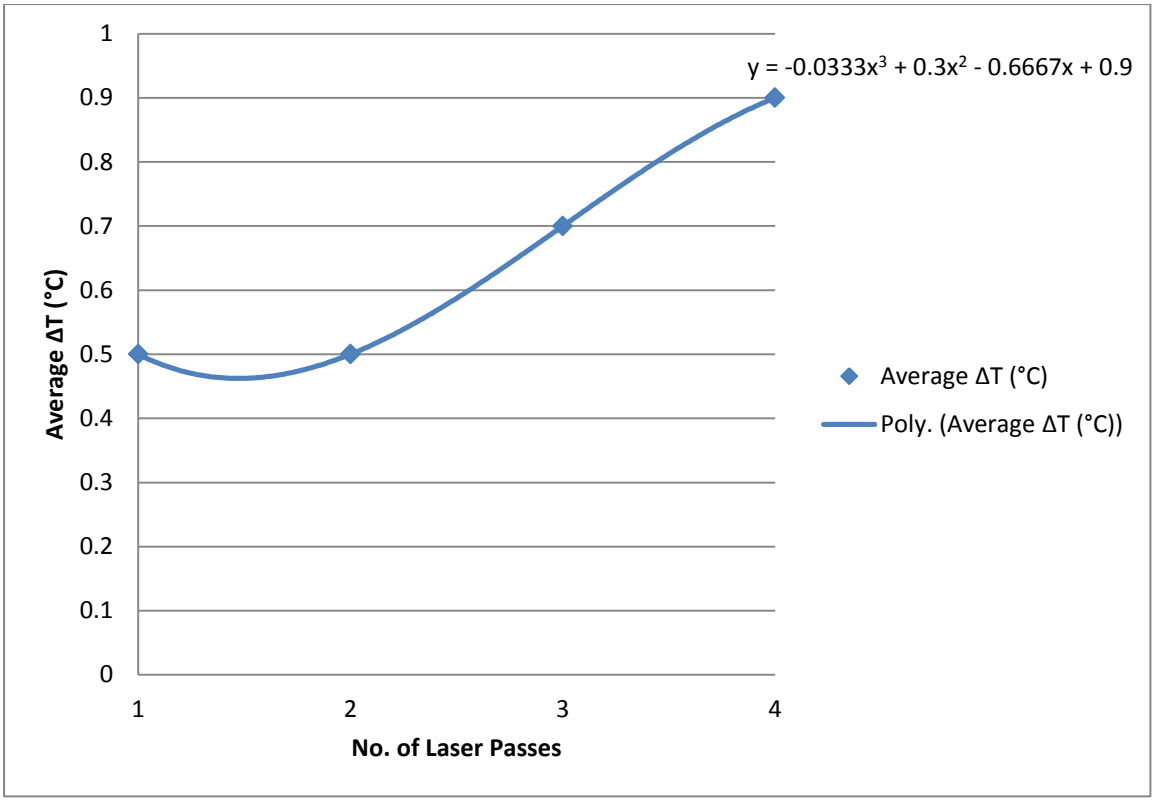

Figure 4.41: ΔT for Black PMMA Samples Irradiated by 30Watts and 1, 2, 3 and4 Laser passes

4.4.5 ΔT for white PMMA samples:

4.4.5.1 ΔT for white PMMA samples irradiated by 30 Watts and 2 laser passes:

White sample was micro-machined by laser using 30 Watt laser power, and 2 laser passes .The micro-machined channels have reduced the solar temperature compared to the standard channels. The obtained results are graphically presented in figure 4.42.

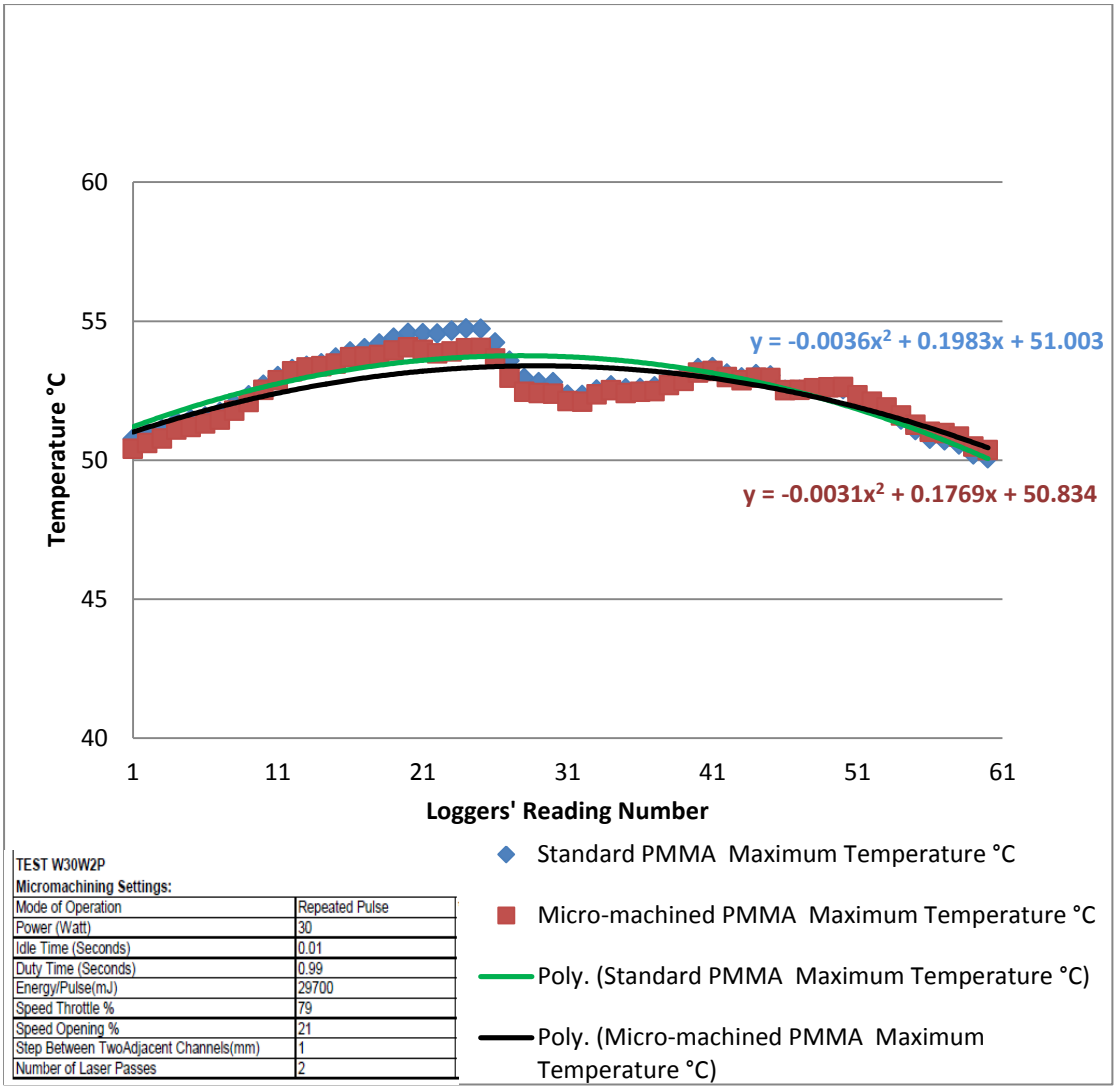

Figure 4.42: Recorded Temperature of Standard and Micro-machined White PMMA Samples Irradiated by 30Watt and 2 Passes

4.4.5.2 ΔT for white PMMA samples irradiated by 30 Watts and 3 laser passes: White sample was laser micro-machined using 30 watt laser power and 3 laser passes for engraving each channel, the results are graphically presented in figure 4.43.

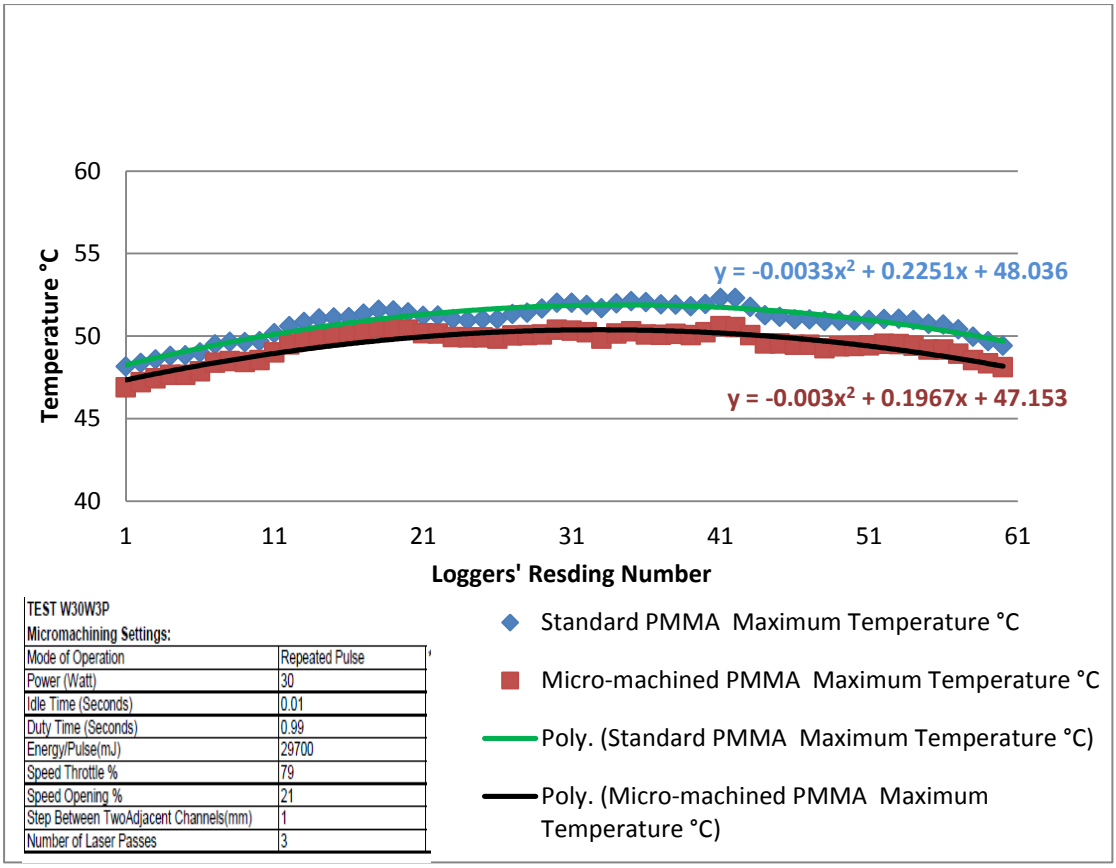

Figure 4.43: Recorded Temperature of Standard and Micro-machined White PMMA Samples Irradiated by 30Watt and 3 Passes

4.4.5.3 ΔT for White PMMA Samples Irradiated by 30 Watts and 4Laser Passes:

The final white sample was laser micro-machined by using 4 laser passes and 30 watt laser power for scribing its channels. The results are presented in a graph shown figure 4.44.

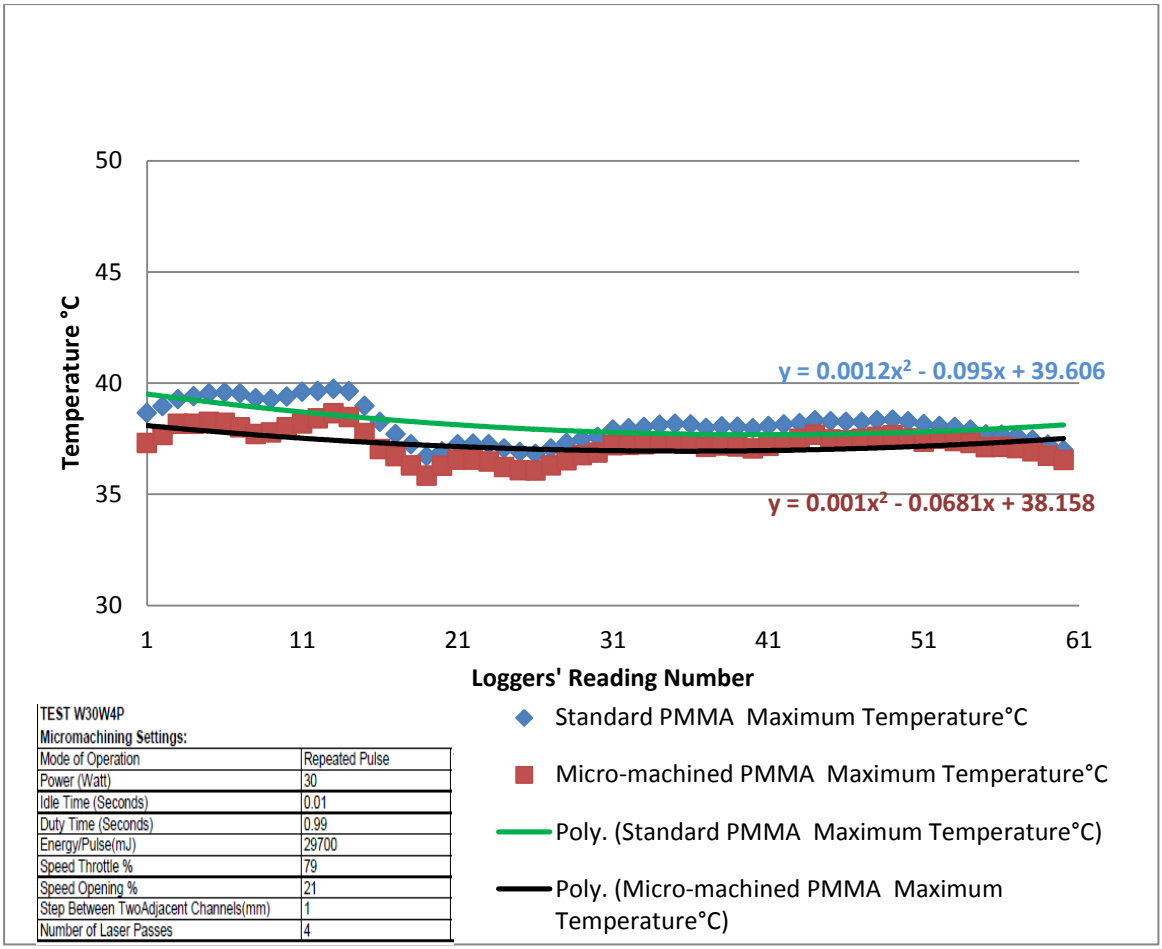

Figure 4.44: Recorded Temperature of Standard and Micro-machined White PMMA Samples Irradiated by 30Watt and 4 Passes

4.4.5.4 Comparison of temperature difference, ΔT, for white PMMA samples irradiated by 30Watt and 1, 2, 3and 4 laser passes respectively:

The last comparison is between temperature differences in ° C, for white PMMA samples irradiated by 30Watt and 1, 2, 3and 4 laser passes respectively, in order to identify the effect of different laser passes on temperature difference. The results are graphically presented in figure 4.45.

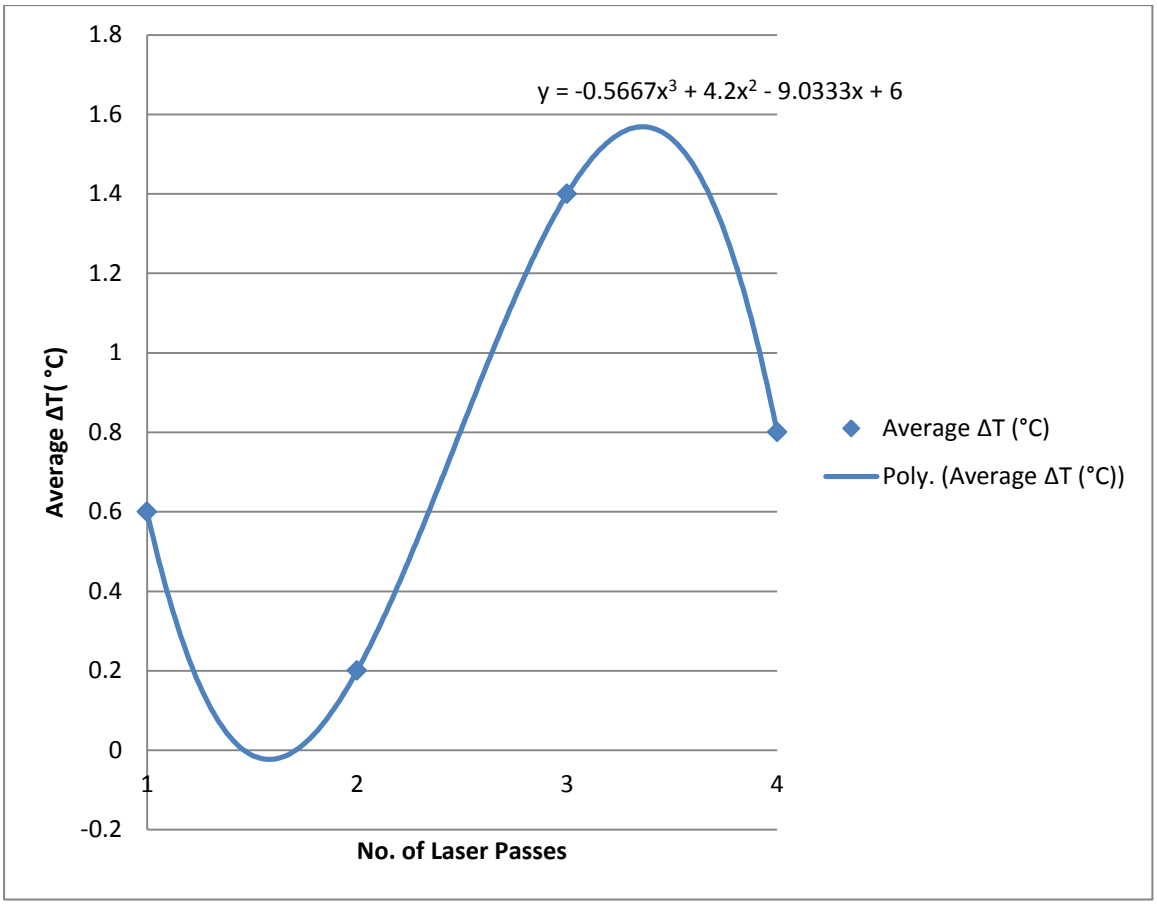

Figure 4.45: ΔT for White PMMA Samples Irradiated by 30Watts and 1, 2, 3 and4 Laser passes

4.5 Discussion:

It is clear from the experimental results that PMMA samples of different colours red, green, blue, black and white were very well micro-machined by CO_2 laser and gave good results in terms of minimal burned areas and damaged areas around the heat affected zone. The good results of micromachining PMMA with CO_2 laser supports the results obtained by Martin F. Jensen, 2004, of getting good machinability of PMMA using laser.

All the mentioned micro-machined samples showed increased thermal insulation to solar heat compared to the standard samples. The reduction in temperature was clearly indicated after laser micromachining which is positively backup the theory of increasing thermal insulation of PMMA by laser micromachining.

When comparing the thermal insulation for PMMA of different colours, the green and the blue samples micro-machined by 30 watt and one pass showed the highest value of 1.2°C, followed by red, black and finally white. Some of the reasons for that can be explained as a red colour filter absorbs all colours except red and transmits only red light. Green sheets absorb red and blue light and reflect the green component of the incident white light. The fractional transmittance of a commercial blue glass colour filter indicates that the filter absorbs red light strongly and transmits violet and blue-green light (Richard Tilley 2000).

From the experimental results, the highest value of thermal insulation was deduced using 30 watts and 1 laser pass, and that could be achieved by using colours lie in between the green and blue colours by the help of the RAL colour code.

Extrapolation of the fitting curve formula obtained from the graph shown in figure (4.9), $y = 0.0019x^3 - 0.134x^2 + 3.0633x - 21,$ using different laser powers resulted the curve shown in figure (4.46).The curve shows the fluctuating effect of laser power on temperature difference below 35 Watts; However the extrapolated curve shows a considerable increment in temperature difference when increasing the laser power to above 35 Watts, and compete solar thermal insulation could be achieved for red sheets when increasing the laser power to 57 Watts.
These interesting results gained from the extrapolation need to be

checked experimentally, when they come true an amazing result of entire thermal insulation could be achieved.

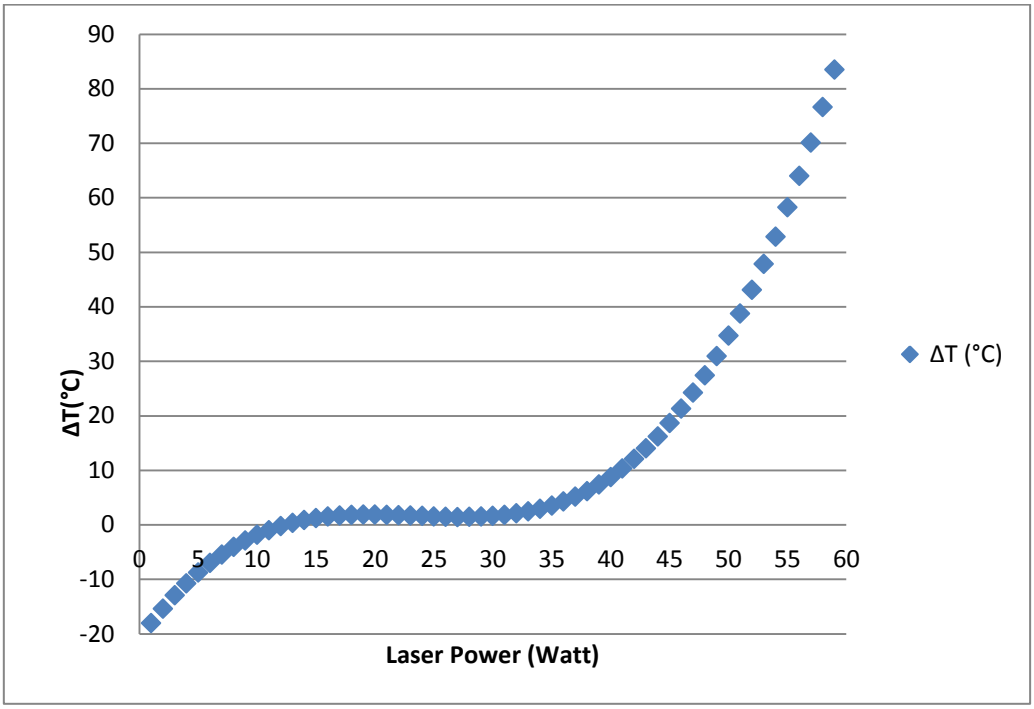

Figure 4.46: Extrapolation curve of the formula $y = 0.0019x^3 - 0.134x^2 + 3.0633x - 21$ for Red sheets

On the other hand, the fitting formula obtained from the graph shown in figure (4.13) using different laser powers also lead to the fact of inrcreased temperature reduction by increasing laser powers,

which is shown in figure (4.47).

This curve indicates the rapid increase of temperature difference by laser irradiation with more than 35 Watts. For the green sheets and at around 58 Watt, complete thermal insulation could be achieved.

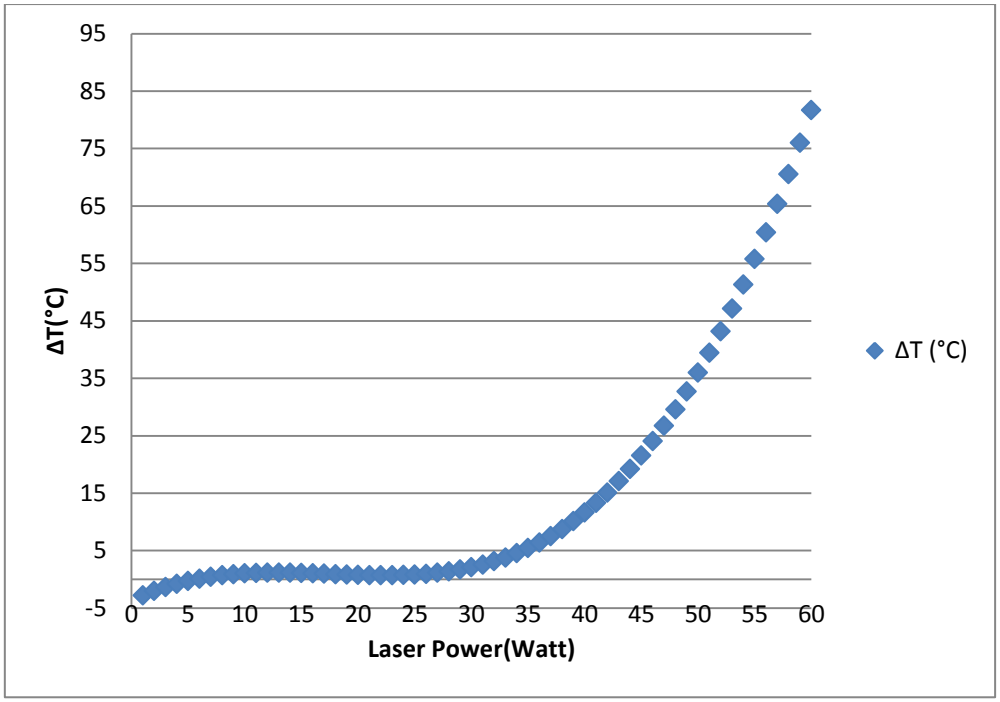

Figure 4.47: Extrapolation curve of the formula $y = 0.0011x^3 - 0.058x^2 + 0.9433x - 3.7$ for Green sheets

Extrapolating the equation of $y = 0.0001x^3 - 0.002x^2 - 0.1133x + 2.8$ for the blue sheets resulted in the curve shown in figure 4.48 below.

A direct linear relationship between laser power and temperature reduction was achieved when irradiating the sheets with more than 35 Watts. Complete thermal insulation would take place at laser power of around 99 Watts, the value which is higher than that of red and green sheets, the reason of that could be the degree of transparency of the blue sheets used experimentally which is higher than all the other sheets.

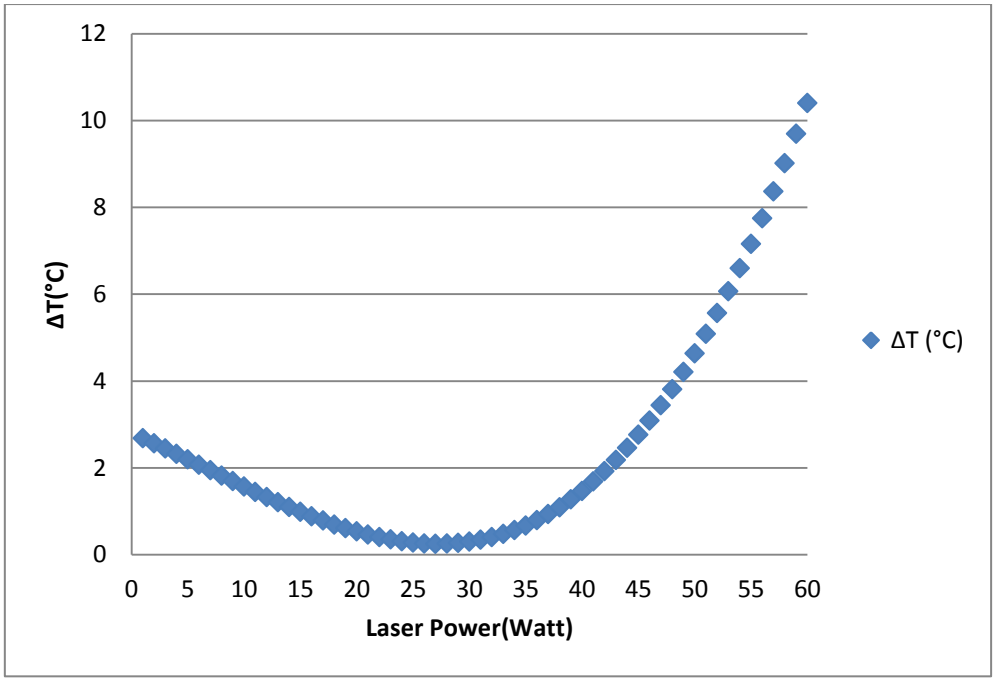

Figure 4.48: Extrapolation curve of the formula $y = 0.0001x^3 - 0.002x^2 - 0.1133x + 2.8$ for Blue sheets

For the black sheets, the extrapolation curve also shows a rapid increase in linear direct relationship between the laser power more than 35 watts and the temperature difference between the micro-machined and the standard samples. Complete thermal insulation could be achieved at around 59Watts of laser power. See figure (4.49).

Finally, extrapolating the formula of $y = 0.0007x^3 - 0.04x^2 + 0.7233x - 3.1$ for the white samples resulted in the curve shown in figure (4.50), which also indicate the rapid increase in temperature difference when irradiating the sheets with more than 35 watts. Complete thermal insulation can be achieved at 64 Watts laser power.

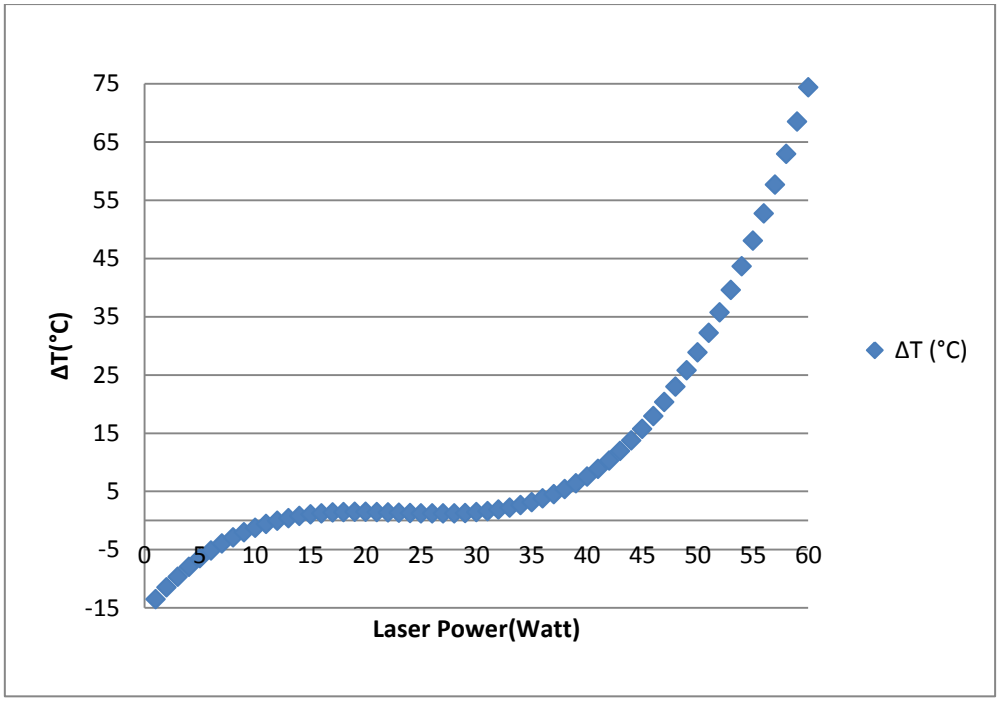

Figure 4.49: Extrapolation curve of the formula $y = 0.0015x^3 - 0.104x^2 + 2.3433x - 15.8$ for Black sheets

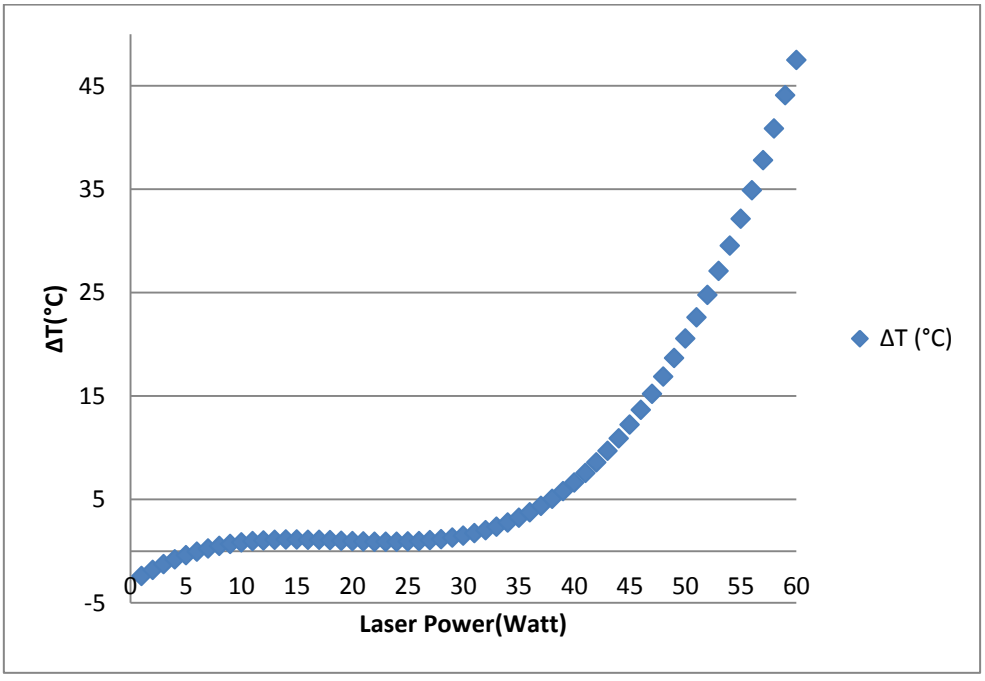

Figure 4.50: Extrapolation curve of the formula $y = 0.0007x^3 - 0.04x^2 + 0.72333x - 3.1$ for White sheets

Sample R20W1P gave the highest average value of temperature difference of 1.6 °C using different laser powers compared to its counterpart samples.

In this respect, the results go in the same direction of what Wilhelm Pfleging *et al* .mentioned for the ablation of polymers which can be described by the ablation depth (d) as a function of laser power (P) and feed rate (*v*) of the laser beam. The ablation depth d is directly proportional to the laser power, and inversely proportional to the feed rate. Depending on the laser power and the feed rate, the energy input and therefore the ablation depth varies (Wilhelm Pfleging, 2009).

The effect of increasing the number of laser passes on the temperature difference between the standard and micro-machined samples, experimentally, showed the direct positive relationship, to some extend, for the red, green, blue, black and white samples irradiated by 30 Watts. The highest result of 1.8°C was achieved using sample B30W3P. Increasing the number of laser passes lead to an increase in the channels depths and consequently lead to deeper channels, then high aspect ratio; however some samples showed decrease between the two successive laser passes, this may be due to the re-condensation of material in the walls of the channel, which may affect the geometry of the channel. By increasing the aspect ratio, the number of internal multiple reflections of the infrared radiation may be increase and their energy will be attenuated resulting in an increment in thermal insulation of the micro-machined acrylics.

4.6 Conclusions:

From the obtained results, the followings can be concluded:

1- PMMA with colours red, green, blue, black and white can be well micro-machined using CO_2 laser with 15 to30 Watts.
2- Increasing the laser power lead to an increase in the temperature difference to some extend between the standard and the micro-machined samples and consequently to an increase in thermal insulation of the micro-machined PMMA sheets.
3- Increasing the laser passes, to around four passes, lead to an increase in the temperature difference to some extend between the standard and the micro-machined samples and consequently to an increase in the thermal insulation of PMMA sheets.
4- A blend of green and blue colours for PMMA sheets, or using greenish-blue colour of PMMA may give better results in thermal insulation than that of other RGBKW colours.
5- Increasing the CO_2 laser power to around 58 Watt, or more, may give complete solar thermal insulation for red and green PMMA sheets.
6- Increasing the CO_2laser power to around 60Watt, or more, may give complete solar thermal insulation for black and white PMMA sheets.
7- Increasing the CO_2 laser power to around 99 Watt, or more, may give complete solar thermal insulation for blue PMMA sheets.

5.7 Future Work:

For the future work, the followings are suggested:

1- Sheets other than acrylic could also be micro-machined using the table, trying different laser sources in comparison with the CO_2 laser. The x-y electro-pneumatic table can be supplied with suction fan for better ventilation and evacuation of smoke resulted from the irradiation of acrylic sheets by laser.

2- Focusing of the CO_2 laser beam by optics to minimize its spot diameter and consequently the channel width, to increase the aspect ratio of the micro-machined channel.

3- Investigation of other parameters, like laser scanning speed to give higher aspect ratio and better temperature difference, then higher thermal insulation of the micro-machined PMMA samples.

4-Investigation of increasing the number of micro-machined channels using step distances of 750µm, 500µm and 300µm.

5- Usage of a noble gas flow (like N_2) to clean the channels from any residuals during laser operation.

6- Investigation of the effect of using CO_2 laser with 58 Watts for red and green sheets, 60 Watts for black and white sheets and 99 Watts for blue sheets in order to compare the results with the extrapolated curves.

References:

*Allison Suggs, Kr-F Laser Surface Treatment of Poly(methyl methacrylate, Glycol-modified Poly(Ethyleneterephthalate),and Polytetrafluorethylene for Enhanced Adhesion of Escherichia Coli K-12,Thesis submitted to the faculty of Virginia Polytechnic Institute and State University for the partial fulfillment of Master of Science in Materials Science and Engineering, September 13,2002.

*Anis Malik Al-Rawi, Nidhal Rashad Hatim, ABC Infrared, Baghdad University, Iraq, Dar Al-Hikma Printing Press 1992.

Arvi Kruusing, Underwater and Water-assisted Laser Processing:Part2-Etching, Cutting and Rarely used Methods, Tallinn Technical University, Department of Mechatronics, Ehitajate tee 5,EE-19086V Tallinn, Estonia, Optics and Laser Engineering 41(2004)329-352.Published by Elsevier Science Ltd,©2002.

*A.S.C.M.d'Oliveira,R.S.C.Paredes,F.P.Weber,R.Vilar, Microstructural Changes Due to Laser Surface Melting of an AISI 304 Stainless Steel, Materials Research, Vol. 4,no.2,93-96,2001©2001.

Beijing Innobri Technology Co.Ltd, Operation and Service Manual, IB-601B 30W CO_2 Surgical System. www.innobri-beauty.en.alibaba.com.2014.

*C. Emmelman, and Different Authors, Introduction to Laser Material Processing, ROFIN SINAR LASER, Hamburg, 2000.

Colin H. Simmons and Dennis E. Maguire, Manual of Engineering Drawing, ELSEVIER, Copyright© Colin H. Simmons and Dennis E. Maguire, 2004.

*Daniel Day and Min Gu, Microchannel Fabrication in PMMA Based on Localized Heating by Nanojoule High Repetition rate

Femtosecond Pulses, Centre of Micro-Photonics, Faculty of Engineering and Industrial Science, Swinburne Universityof Technology, Hawthorn, Victoria 3122,Australia,©2005 Optical Society of America.

*Detlef Snakenborg, Henning Klank and Jörg P. Kutter, Microstructure Fabrication with CO2 Laser System, MIC – Mikroelektronic Center, µTAS project, Technical University of Denmark, 2800 Kgs. Lyngby, Denmark, Journal of Micromechanics and Microengineering©2004 IOP Publishing Ltd.

*Deyao Ren, Laser Micromachining and Its Applications in Manufacturing of Micro Medical Devices, Ph.D. Thesis, Industrial Engineering, North Carolina State University, 2009.

*Duke Pointer et al, Case Study, Natural Stone Solar Reflectance Index and the Urban Heat Island Effect, University of Tennessee Center for Clean Products, July ,17,2009,© Copyright 2008 Natural Stone Council.

* Evgueni Bordatchev and Suwas Nikumb, Fabrication of Moulds and Dies Using Precision Laser Micromachining and Micromilling Technologies, Industrial Materials Institute, National Research Institute of Canada, JLMN-Journal of Lase Micro/Nanoengineering Vol.3, No.3, 2008.

*E. Gentili, L. Tabaglio, F.Aggogri, Review on Micromachining Techinques, Department of Mechanical engineering, University of Brescia, Italy.

*FESTO, Learning Systems, the Current Range of . Products from FESTO Didactic. 2011/2012

*FluidSIM®, 3.5, Pneumatics, FESTO, © Festo Didactic GmbH &Co., D-73770Denkendorf1996- 2001,Internet:www.festo.com/didactic. ©Art systems software GmbH, D-33102Paderbom1995-200, Internet:

www.art-systems.com,www.fluidsim.com

*Hao Liu,Jae-Cheon Lee and Bao-Ren Li,High Precission Pressure Control of a Pneumatic Chamber using a Hybrid Fuzzy PID Controller; International Journal of Precission Engineering and Manufacturing;Vol.8,No.3,July2007.Copyright©2007 by KSPE.

*H. G. Rubahn , Laser Applications in Surface Science and Technology, English translation copyright©1999by John Wiley& Sons Ltd.

*Harald Keller, Uwe Erb, Dictionary of Engineering Materials,

Copyright©2004 by John Wiley &Sons, Inc.

*Hitoshi Sai and Hiroo Yugami,Thermophotovoltaic Generation with Selective Radiators Based on Tungsten Surface Gratings, Applied Physics Letters, Volume 85, Number 16,18 October 2004© 2004 American Institute of Physics.

*Jens Holtkamp, Stephan Eifel and Joachim Ryll, Mterial Processing with Ultrashort- pulsed Lasers, Laser Techinik Journal, © 2014 WILEY-VCH Verlag GmbH &Co.KGaA,Weinheim.

*John C. Ion Eur. Ing., CEng., FIMMM, Laser Processing of Engineering Materials, Elsevier Butterworth-Heinemann, Copyright © 2005, John C. Ion.

*J. Chae, S. S. Park, T. Freiheit, Investigation of micro-cutting operations, International Journal of Machine Tools & Manufacture 46 (2006) 313-332, ©2005Elsevier Ltd.

*John F. Ready, Industrial Applications of Lasers 2nd edition.

Copyright © 1997, 1978 by Academic Press.

*John H. Lienhard IV and John H. Lienhard, heat Transfer Handbook, Third Edition, Copyright© 2008 by John H. Lienhard IV and John H. Lienhard, Phlogiston Press, Cambridge, Massachusetts.

*Johns Manville, Energy, Environment and Roofing Engineering, R S-7651 6-10 (Replaced 7-07), www.jm.com/roofing.

Joseph Mc. Geough, Micromachining of Engineering Material Copyright © 2002 by Marcel Dekker, Inc.

*K. S. Tiaw, S. W. Goh, M. Hong, Z. Wang, B. Lan, S. H. Teoh, Laser Surface Modification of Poly(ε- caprolactone) (PCL) membrane for Tissue Engineering Applications, Biomaterials 26 (2005) 763-769 ©2004Elsevier Ltd.

*Mark J. Jackson, Micro-and Nano-manufacturing, © 2007 Springer Science+ Business Media, LLC.

*Martin F. Jensen, Laser Micromachining of Ploymers, Ph.D. Thesis, Department of Micro and Nanotechnology(MIC),Technical university of Denmark(DTU),October 2004.

*M. Bart, P. Saunders and D.R. White, May, Technical Guide 2 Infrared Thermometry Ice Point,m2004, Measurements Standard Laboratory of New Zeland, www.irl.cri.nz/msl/.

*Muammer Koç and Tugrul Özel, Editors, Micro-Manufacturing: Design and Manufacturing of Micro-Products, First Edition. ©2011 John Wiley &Sons, Inc. Published 2011 by John Wiley &Sons, Inc.

*Medgar L. Marceau and Martha G. Van Geem, Solar Reflectance of Concretes for LEED Sustainable Sites Credit: Heat Island Effect, SN2982, ©Portland Cement Association, Skokie, Illinois, USA, 2007.

*M. Richardson, A. Zoubir, C. Rivero, C. Lopez, L. Petit and K. Richardson, Femtosecond Laser Micro-structuring and Refractive Index Modification Applied to Laser and Photonic Devices, School of Optics and CREOL, University of Central Florida, Micromachining Technology for Micro-Optics and Nano-Optics II, edited by Eric G. Johnson, Gregory P. Nordin, Proceedings of SPIE Vol.5347(SPIE, Bellingham, WA,2004).

*M. G. Papoutsidakis, G. Chamiloothoris, F. Dailami, N. Larsen and A. Pipe, Accurate Control of a Pneumatic System using an Innovative Fuzzy Gain-Scheduling Pattern, Proceedings of World Academy of Science, Engineering and Technology,Volume 8 October 2005 ISSN1307-6884, ©2005WASET.ORG.

*M. Muthukkaruppan and K. Manjo, Low Cost Automation using Electro-pneumatic System-an Online Case Study in Multi-station Part Transfer, Drilling and Tapping Machine,24th.International Symposium on Automation and Robotics in Construction (ISARC2007) . Minimum Specifications, Tinytag® Explorer, www.tinytag.info, 2010.

McGraw-Hill (www.digitalengineeringlibrary.com),Variations on the Laser Theme: A Classification of Major Types, Copyright©2004 The McGraw-Hill Companies.

*M. M. Noor, K. Kadirgama and M.M. Rahman, Particle swarm optimization prediction model for surface roughness, International Journal of Physical Science Vol.6 (13), ISSN 1992-1950©2011 Academic Journals.

Nam-Trung Nguyen, Zhigang Wu, Yien-Chian Kwok, Modelling, Fabrication and Microfluidic Applications of Laser -Machined Microchannel in PMMA, School of Mechanical and Production Engineering,*Natural Institute of Education, Nanyang Technological University, Singapore.

*Narendra B. Dahotre, Sandip P. Harimkar, Laser Fabrication and Machining of Materials. © 2008 Springer Science+ Business Media, LLC.

*Richard Tilley, Colour and the Optical Properties of Materials. Copyright © 2000 by John Wiley and Sons Ltd.

*Stefan Böhm, Klaus Dilger, Elisabeth Stammen, Laser Based Surface Treatment of aluminum Alloys for Adhesive Bonding, IFS-Institute of Joining and Welding, Technical University Braunschweig, Langer Kamp8, 38106 Braunschweig, Germany, s.boehm@tu-bs.de.

*Sunil Ranganath Belligundu, Experimental Characterization of Femtosecond Laser Micromachining for Silicon Mold Fabrication and Hot Embossing for Polymer Microreplication, Ph.D. Thesis, The University of Texas at Arlington, December 2005.

*Subbah Chandra Singh, Haibo Zeng, Chuneli Guo, and Weiping Cai, Nanomaterials: Processing and Characterization with Lasers, First Edition, © 2012 Wiley-VCH Verlag GmbH & Co.KGaA.

*Thomas Klotzbücher, Torsten Braune, Susanne Sigloch, Jens Hoßfeld, Michel Neumeier, Han-Dieter Bauer, Wolfgang Ehrefeld, Polymer Microsystems by Excimer Laser Ablation: From Rapid Prototyping to Large Number Fabrication, Institut für Mikrotechnik Mainz GmbH,Carl-Zeiss-Str.18-20, D-55129 Mainz, Germany,©2001SPIE.

*Thomas Lippert, Interaction of Photons with Polymers: From Surface Modification to Ablation, Paul Scherrer Institut, 5232 Villigen PSI, Switzerland, © WILEY-VCH Verlag GmbH &Co.KGaA,Weinheim.

*Thomas Lippert, Laser Application of Polymers, Paul Scherrer Institute, 5232 Villigen-PSI, Switzerland, ©Springer-Verlag Berlin Heidelberg 2004.

*Wenwu Zhang, Y Lawrence Yao, Laser Materials Processing , Manufacturing Engineering Handbook, Digital Engineering Library@ McGraw- Hill (www.digitalengineeringlibrary.com) Copyright©2004 The McGraw-Hill Companies.

*William M. Steen, PhD, MA, CEng., Laser Material Processing, Third Edition,© Springer-Verlag London Limited 2003.

*Wilhelm Pfleging, Robert Kohler, Phillip Schierjott and Werner Hoffmann, Laser patterning and packaging of CCD-CE-Chips made of PMMA, ©2009 Elsevier B.V. All rights reserved.

*Y. Zhang, R. M. Lowe, E. Harvey, P. Hannaford, A. Endo, High Aspect-ratio Micromachining of Polymers with an Ultrafast Laser, © Elsevier Science B.A.

APPENDICES

APPENDIX A: Temperature for Red Samples, RSDT and R30W1P.

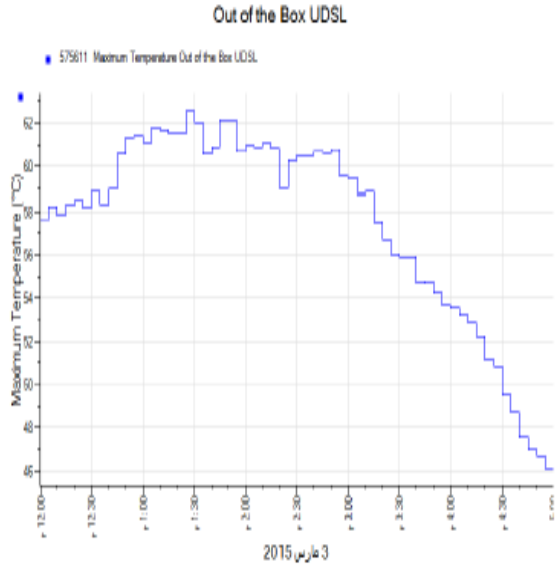

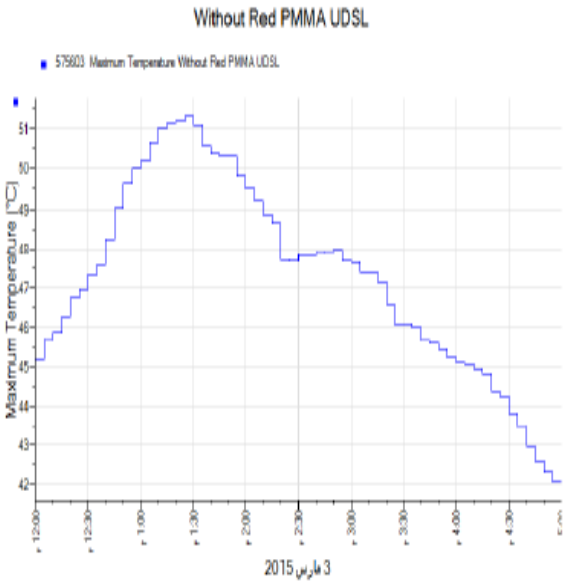

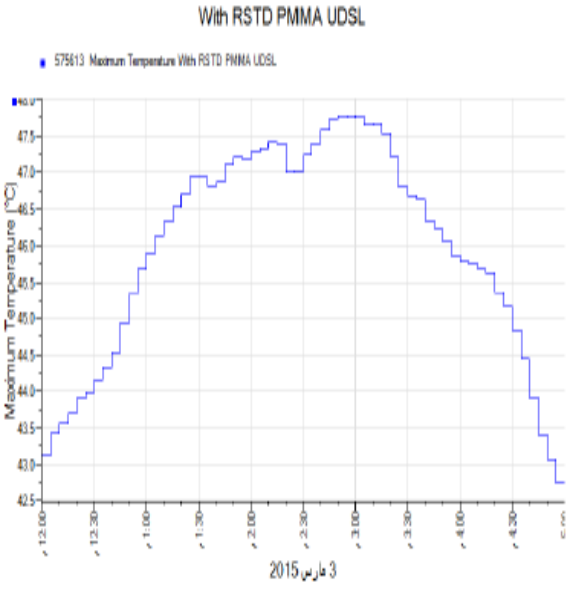

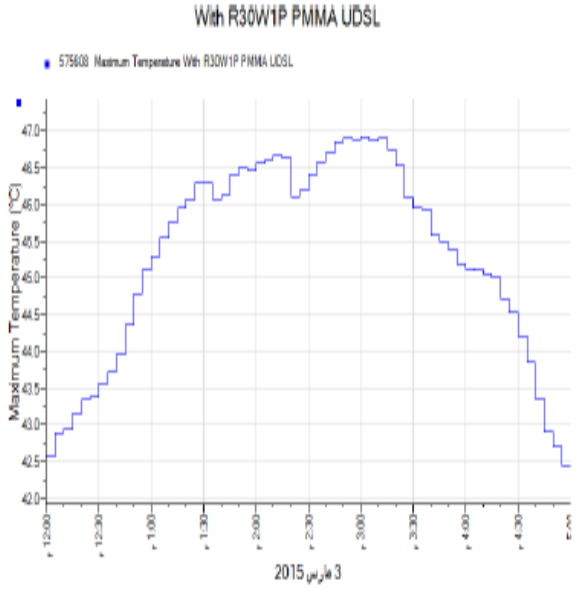

APPENDIX B: Temperature for Green Samples, GSDT and G30W1P.

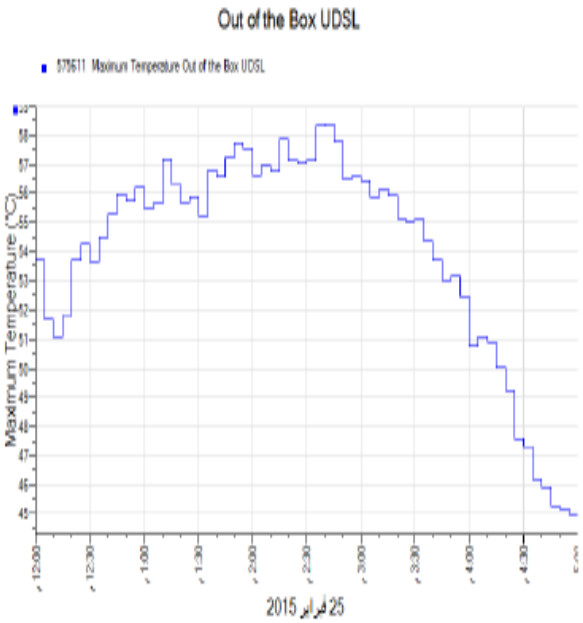

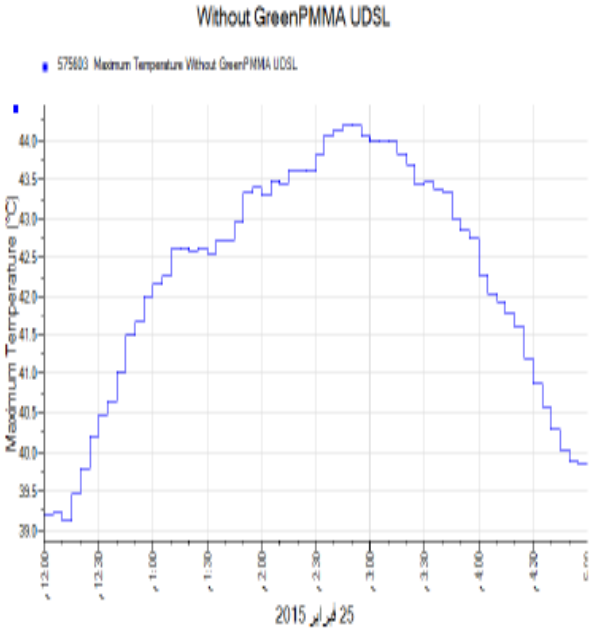

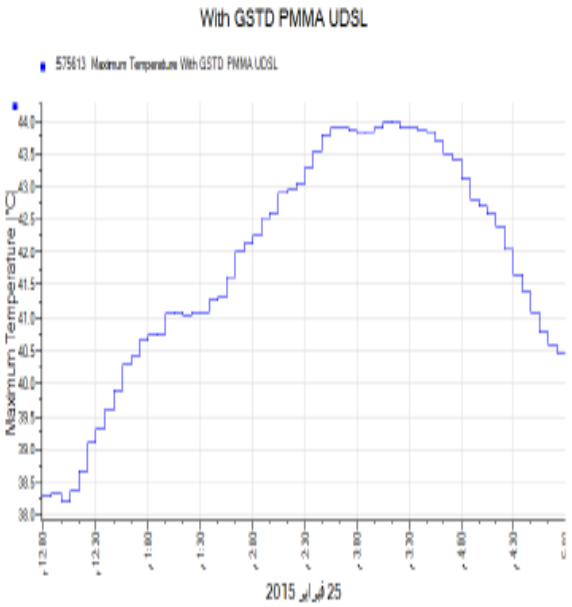

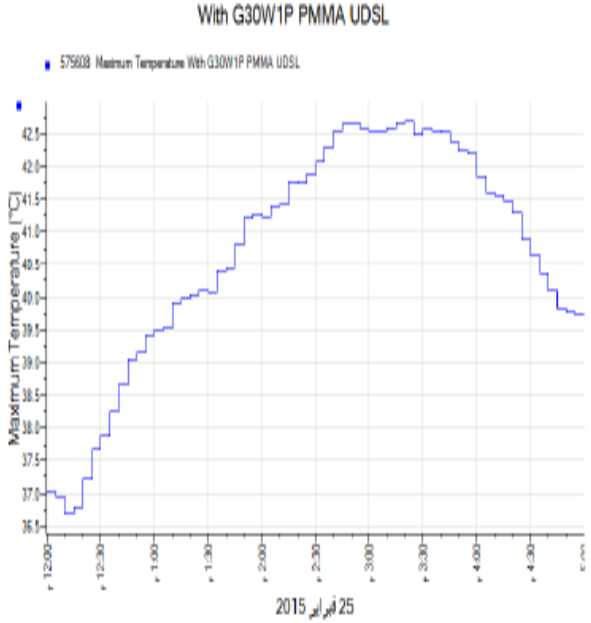

APPENDIX C: Temperature for Blue Samples, BSDT and B30W1P

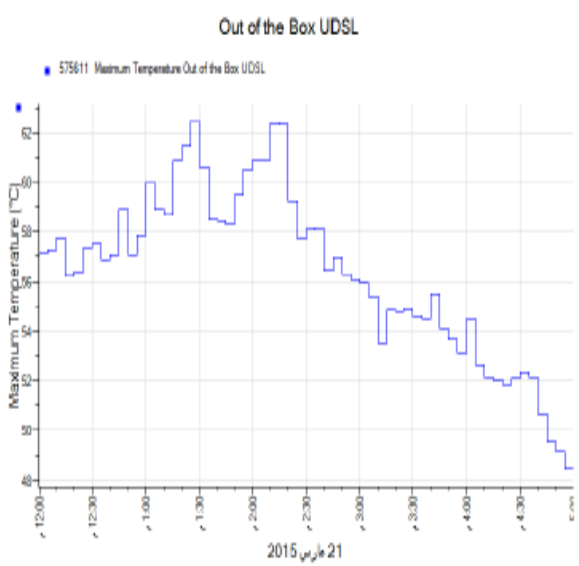

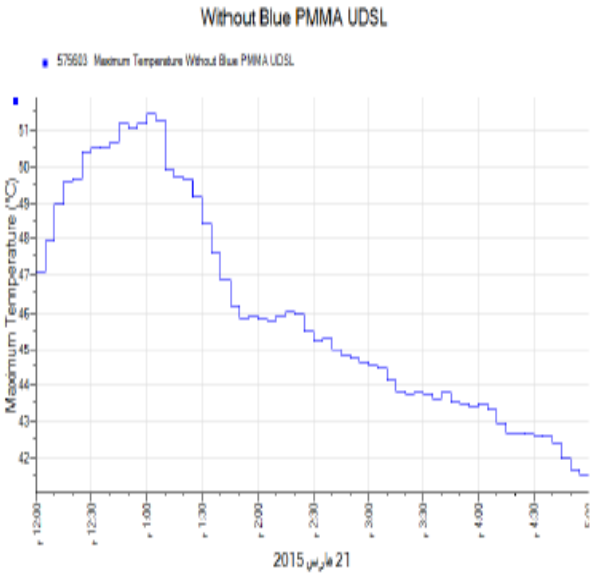

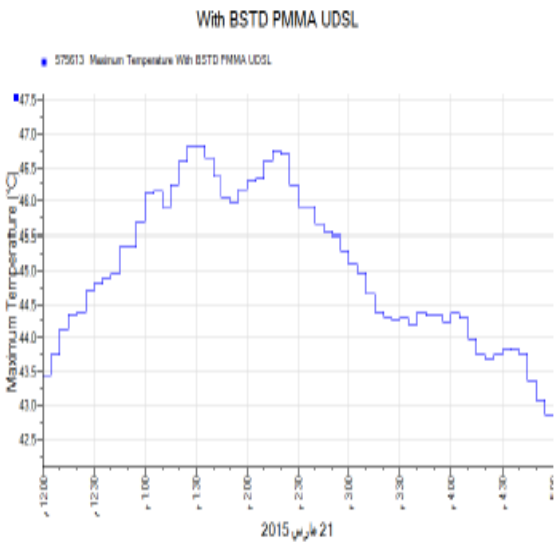

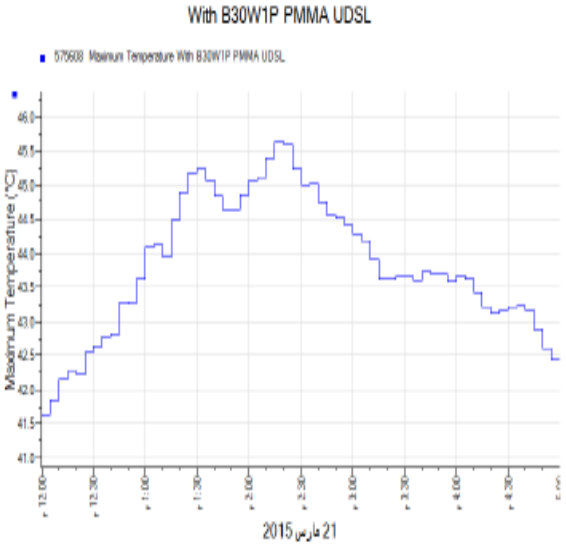

APPENDIX D: Temperature for Black Samples, KSDT and K30W1P

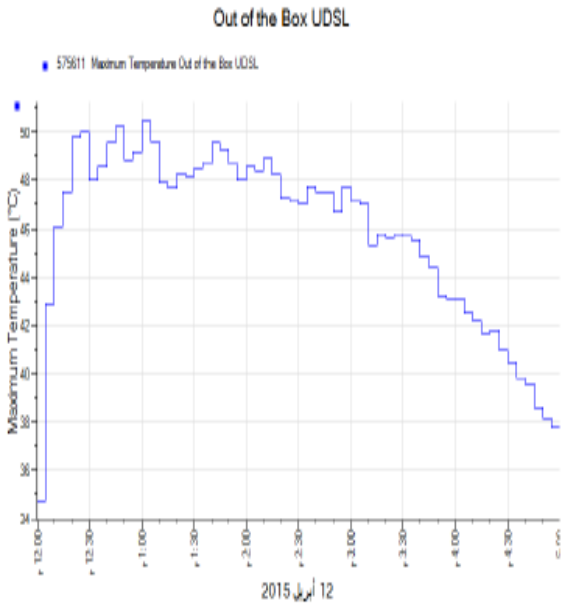

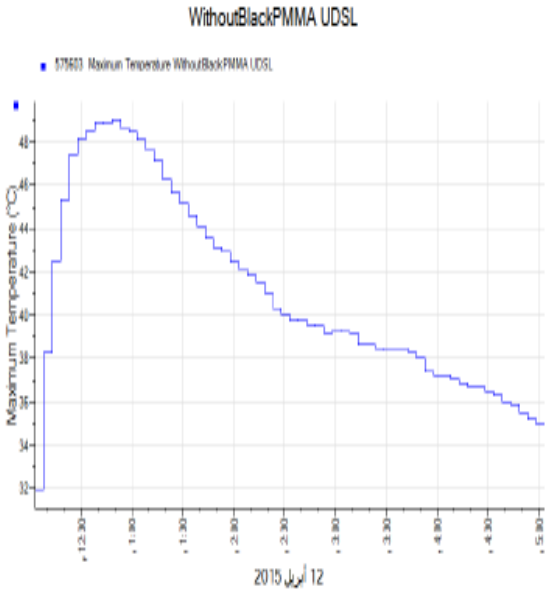

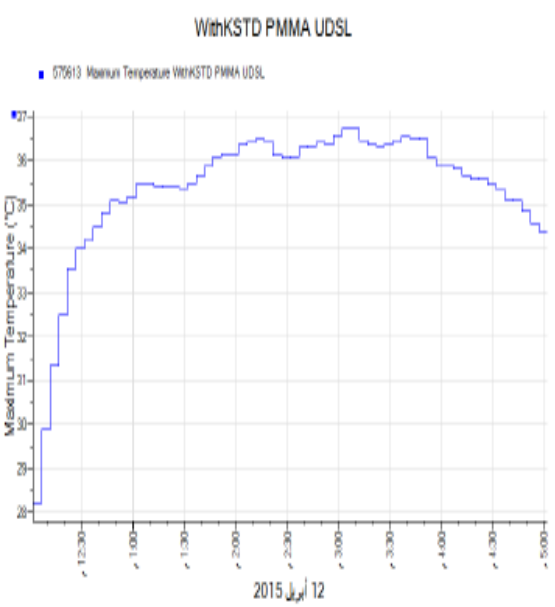

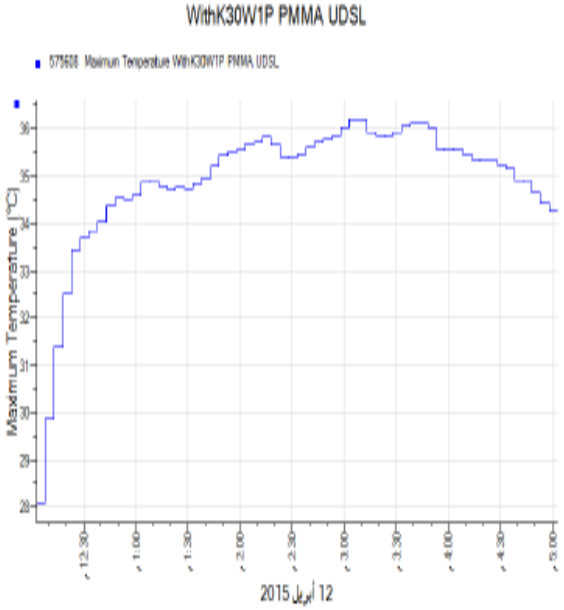

APPENDIX E: Temperature for White Samples, WSDT and W30W1P